



NATIONAL CONFERENCE ON PHYSICS-2021

06 – 07 August 2021

Theme
PHYSICS FOR NATIONAL DEVELOPMENT

PROGRAMME & ABSTRACTS

Venue
Zoom Online Platform



Organized by
Bangladesh Physical Society



NATIONAL CONFERENCE ON PHYSICS-2021

06 – 07 August 2021

Theme
PHYSICS FOR NATIONAL DEVELOPMENT

PROGRAMME & ABSTRACTS

Venue
Zoom Online Platform



Organized by
Bangladesh Physical Society

Message from President

It gives me great pleasure to say a few words on the National Conference on Physics 2021 during 6-7 August 2021 through the online platform. The theme of the conference is “Physics for National Development”. Bangladesh Physical Society is an association of researchers, academicians, and professionals, working in the field of Physics. The theme of the conference indicates the dedication of society to the research and development of the nation.

Since Bangladesh is a densely populated country with a strong demographic dividend, we must grab this comparative advantage of it and transform this huge young population into capable human resources for national development through appropriate technical and vocational education training and various other skill development programs.

A large number of research papers have been submitted for the conference by researchers from academic, research and other organizations. The two days event would be a feast and delight for researchers. The conference will provide an excellent platform for developing new ideas and technologies.

On behalf of the Bangladesh Physical Society, I welcome the invited speakers, authors, presenters, session chairs, co-chairs, students and participants of the conference. Without their participants, the conference would not have been possible.

I wish all the success of this conference.

(Professor Dr. Mesbahuddin Ahmed)
President
Bangladesh Physical Society

Foreword

It is my pleasure to share that Bangladesh Physical Society (BPS) is going to organize a National Conference on Physics-2021 to be held through online platform during 06-07 August 2021. The theme of the conference is “Physics for National Development”. On the eve of this grand event, I would like to take this opportunity to convey my sincere gratitude and warm congratulations to all the academicians, scientists, researchers and professionals who are tirelessly working to bring the fruits of Physics research and education for socio-economic development of the country.

The aim of the conference is to share knowledge and ideas on the state-of-the-art technology through mutual interactions among the academicians, scientists, researchers and professionals to create inspiration and to encourage for creative innovation to contribute to realization of developed Bangladesh.

A large number of research papers have been submitted for the conference by the scientists and researchers. After careful reviewing, 48 papers were selected for technical presentations in the technical sessions of the conference and 75 papers have been selected for poster presentation. A number of invited papers will be presented by experienced researchers and professionals from home and abroad in the technical sessions.

On behalf of Bangladesh Physical Society, I would like to thank the invited speakers, authors, presenters, session chairs, co-chairs, students and participants of the conference. Without their participations, the conference would not have been possible. We believe that this conference will encourage and create enthusiasm among young scientists, researchers and professionals engaged in the field.

I take this opportunity to thank the advisors, members of the organizing committee and sub-committees and the reviewers of papers for support and encouragement. We believe that the conference will contribute significantly to the socio-economic development of the country.

We hope that with your participation and cooperation, this conference will be lively and enjoyable in these two days. Thank you all very much and I invite you to this conference of the Bangladesh Physical Society with best wishes to all.

Dr. Mohammed Nazrul Islam Khan
General Secretary
Bangladesh Physical Society

CONTENTS

SL.	Topics	Page Number
1.	Organizing Committee	05
2.	Sub Committees	06
3.	Executive Board	07
4.	Honorable President and Secretary list of BPS	08
5.	Sessions List	09
6.	Invited Speakers List	09
8.	Sessions Chair and Co-Chair List	10
9.	Inaugural Programme	11
10.	Technical Sessions	11
11.	Abstracts for Oral Presentation	22
12.	Abstracts for Poster Presentation	60

NATIONAL CONFERENCE ON PHYSICS-2021

ORGANIZING COMMITTEE

CONVENER	:	Prof. Dr. Mesbahuddin Ahmed
MEMBER-SECRETARY	:	Dr. Mohammed Nazrul Islam Khan
MEMBERS	:	Prof. Dr. Md. Abu Hashan Bhuiyan (BUET) Prof. Dr. Golam Mohammed Bhuiyan (DU) Dr. A. K. M. Abdul Hakim (BUET) Prof. Dr. Shibendra Shekher Sikder (KUET) Prof. Dr. M. Khalilur Rahman Khan (RU) Prof. Dr. Md. Rafiqul Islam (CU) Prof. Dr. Syed Jamal Ahmed (DUET) Prof. Dr. Md. Manjurul Haque (IU) Prof. Dr. Ishtiaque M. Syed (DU) Prof. Dr. A K M Moinul Haque Meaze (CU) Prof. Dr. Abdullah Shams Bin Tareq (RU) Prof. Dr. Suranjan Kumar Das (JnU) Prof. Dr. Md. Mizanur Rahman (DU) Prof. Dr. Md. Hamidur Rahman Khan (AUST) Dr. Mohammad Amirul Islam (BAEC) Prof. Dr. Jahirul Islam Khandaker (JU) Dr. Mohammad Khurshed Alam (BUET) Dr. Harinarayan Das (BAEC) Dr. Mohammad Abdur Rashid (JUST) Dr. Mohammed Kamrul Haque Bhuiyan (NCTB) Prof. Dr. Faruque-Uz-Zaman Chowdhury (CUET) Prof. Dr. Abdul Hannan (SUST) Prof. Dr. Md. Abu Taher (CoU) Prof. Dr. Md. Khairul Islam (PUST) Prof. Dr. Gaji Mazharul Anowar (BRU) Prof. Dr. Md. Rashedur Rahman (KU) Dr. M. A. Gafur (BCSIR)

ADVISORY COMMITTEE

Prof. Dr. A. M. Harun-Ar-Rashid (Fellow, BAS)
 Prof. Dr. H. M. Sen Gupta (DU)
 Prof. Dr. M. Shamsher Ali (Fellow, BAS)
 Prof. Dr. Arun K. Basak (Emeritus Professor, RU)
 Prof. Dr. Giasuddin Ahmad (BUET)
 Prof. Dr. Tofazzal Hossain (AIUB)
 Prof. Dr. R. I. M. A. Rashid (DU)
 Prof. Dr. A. K. M. Azharul Islam (RU)
 Prof. Dr. M. Muniruzzaman (JU)
 Prof. Dr. Arun Kumar Deb (CU)
 Prof. Dr. Khairul A. Khan (RU)
 Prof. Dr. M. Aminul Islam (RU)
 Prof. Dr. Yasmeen Haque (SUST)
 Dr. Syed Mohammod Hossain (BAEC)

SUB-COMMITTEES

- Abstract Screening Committee** : Prof. Dr. Md. Golam Md. Bhuiyan (DU)
Prof. Dr. M. Khalilur Rahman Khan (RU)
Prof. Dr. Md. Rafiqul Islam (CU)
Prof. Dr. Suranjan Kumar Das (JnU)
Prof. Dr. Md. Nure Alam Abdullah (JnU)
Prof. Dr. Md. Mizanur Rahman (DU)
Prof. Dr. Md. Hamidur Rahman Khan (AUST)
Dr. Abu Zafur Ziauddin Ahmed (DU)
Dr. Mohammad Jellur Rahman (BUET)
Dr. Harinarayan Das (BAEC)
Dr. Mohammad Abdur Rashid (JUST)
- Programme Committee** : Dr. A. K. M. Abdul Hakim (BUET)
Prof. Dr. Syed Jamal Ahmed (DUET)
Prof. Dr. Ishtiaque M. Syed (DU)
Prof. Dr. Jahirul Islam Khandaker (JU)
Dr. Mohammad Amirul Islam (BAEC)
- Press & Publication Committee** : Prof. Dr. Md. Abu Hashan Bhuiyan (BUET)
Dr. Mohammad Khurshed Alam (BUET)
Dr. Ratan Chandra Gosh (DU)
Dr. Mohammad Jellur Rahman (BUET)
Dr. Harinarayan Das (BAEC)
Dr. Mohammad Kamrul Haque Bhuiyan (NCTB)
- Technical Committee** : Prof. Dr. Shibendra Shekher Sikder (KUET)
Prof. Dr. A.K.M. Moinul Haque Meaze (CU)
Prof. Dr. Abdullah Shams Bin Tariq (RU)
Prof. Dr. Mohammad Mohi Uddin (CUET)
Dr. Farhad Alam (IUB)
Dr. Ratan Chandra Gosh (DU)
Dr. Abu Zafur Ziauddin Ahmed (DU)
Dr. Mohammad Khurshed Alam (BUET)
Dr. Mohammad Jellur Rahman (BUET)
Dr. Harinarayan Das (BAEC)
Dr. Pretam Kumar Das (PUST)
Dr. Mohammad Abdur Rashid (JUST)

Bangladesh Physical Society

Executive Board (2020-2021)

1.	President	:	Prof. Dr. Mesbahuddin Ahmed	(BAC)
2.	Vice-President-1	:	Prof. Dr. Golam Mohammed Bhuiyan	(DU)
3.	Vice-President-2	:	Dr. A. K. M. Abdul Hakim	(BUET)
4.	Treasurer	:	Dr. Mohammad Khurshed Alam	(BUET)
5.	General Secretary	:	Dr. Mohammad Nazrul Islam Khan	(BAEC)
6.	Joint Secretary	:	Prof. Dr. Jahirul Islam Khandaker	(JU)
7.	Information & Publication Secretary	:	Dr. Harinarayan Das	(BAEC)
8.	Executive Member	:	Prof. Dr. Md. Abu Hashan Bhuiyan	(BUET)
9.	Executive Member	:	Prof. Dr. Shibendra Shekher Sikder	(KUET)
10.	Executive Member	:	Prof. Dr. M. Khalilur Rahman Khan	(RU)
11.	Executive Member	:	Prof. Dr. Md. Rafiqul Islam	(CU)
12.	Executive Member	:	Prof. Dr. Syed Jamal Ahmed	(DUET)
13.	Executive Member	:	Prof. Dr. A.K.M. Moinul Haque Meaze	(CU)
14.	Executive Member	:	Prof. Dr. Syed Jamal Ahmed	(DUET)
15.	Executive Member	:	Prof. Dr. Ishtiaque M. Syed	(DU)
16.	Executive Member	:	Prof. Dr. Abdullah Shams Bin Tariq	(RU)
17.	Executive Member	:	Prof. Dr. Md. Abdul Basith	(BUET)
18.	Executive Member	:	Prof. Dr. Mohammad Hamidur Rahman Khan	(AUST)
19.	Executive Member	:	Dr. Mohammad Amirul Islam	(BAEC)
20.	Executive Member	:	Dr. Mohammad Abdur Rashid	(JUST)
21.	Executive Member	:	Dr. Mohammad Kamrul Haque Bhuiyan	(NCTB)

BPS Webpage address: <http://www.bdphs.org>

Bangladesh Journal of Physics (BJP)

Email address: bjp_bps@yahoo.com

Year-wise Honorable President and Secretary of the Executive Board of Bangladesh Physical Society

Serial No.	President	Affiliation	Secretary	Affiliation	Duration
1.	Prof. M. Innas Ali	DU	Prof. A. M. Harun ar Rashid	DU	1973 - 1974
2.	Prof. A. K. M. Siddiq	DU	Dr. A. A. Ziauddin Ahmad	BAEC	1975 - 1976
3.	Prof. Ahmad Husain	DU			1977 - 1978
4.					1979 - 1980
5.	Prof. A. Matin Chaudhury	DU	Dr. M. Khaliquzzaman	BAEC	1981 - 1982
6.	Dr. Anwar Hossain	BAEC	Dr. M. Ibrahim	DU	1983 - 1984
7.	Prof. M. Shamsul Huq	DU	Dr. M. A. Wazed Miah	BAEC	1985 - 1986
8.	Prof. Muhtasham Hussain	DU	Dr. M. A. Wazed Miah	BAEC	1987 - 1988
9.	Dr. M. A. Mannan	BAEC	Prof. M. Ali Asgar	BUET	1989 - 1990
10.	Prof. A. M. Harun ar Rashid	DU	Prof. Sultana Shafee	DU	1991 - 1992
11.	Prof. A. M. Harun ar Rashid	DU			1993 - 1994
12.	Prof. Sadruddin A. Chawdhury	DU	Prof. Badrul Alam	DU	1995 - 1996
13.	Dr. M. A. Wazed Miah	BAEC	Prof. Mominul Huq	BUET	1997 - 1999
14.	Prof. R.I.M.A. Rashid	DU	Prof. Sultana Shafee	DU	2000 - 2001
15.	Prof. M. Ali Asgar	BUET	Dr. Farid Uddin Ahmed	BAEC	2002 - 2003
16.	Dr. C. S. Karim	BAEC	Prof. Md. Abu Hashan Bhuiyan	BUET	2004 - 2005
17.	Dr. C. S. Karim	BAEC	Prof. Md. Abu Hashan Bhuiyan	BUET	2006 - 2009
18.	Prof. M. Ali Asgar	EWU	Prof. Jiban Podder	BUET	2010 - 2011
19.	Dr. A. A. Ziauddin Ahmad	BRACU	Dr. Dilip Kumar Saha	BAEC	2012 - 2013
20.	Dr. A. A. Ziauddin Ahmad	BRACU	Dr. Dilip Kumar Saha	BAEC	2014 - 2015
21.	Prof. Ajoy Kumer Roy	DU	Prof. Dr. Ishtiaque M. Syed	DU	2016 - 2017
22.	Prof. Dr. Md. Abu Hashan Bhuiyan	BUET	Prof. Dr. Ishtiaque M. Syed	DU	2018 - 2019
23.	Prof. Dr. Mesbahuddin Ahmed	BAC	Dr. Mohammad Nazrul Islam Khan	BAEC	2020-2021

Sessions List

Sl. No.	Session Name	Session Number	Date	Time
1.	Theoretical & Computational Physics-I	I	06 August 2021	10.05 – 11.15
2.	Material Science-I	II	"	11.20 - 12.40
3.	Medical Physics	III	"	14.30 – 15.55
4.	Nuclear and Reactor Physics	IV	"	16.00 – 17.20
5.	Nanomaterials	V	"	17.25 –18.55
6.	Theoretical & Computational Physics-II	VI	07 August 2021	09.00 – 10.15
7.	Environmental Science and Meteorology	VII	"	10.20 – 11.35
8.	Materials Science-II	VIII	"	11.40 – 13.00
9.	Health Physics	IX	"	14.00 – 15.15
10.	Thin Film	X	"	15.20 – 16.35
11.	Poster Session		"	16.40 – 18.00
12.	Physics Education	XI	"	18.00 – 19.00

Invited Speakers List

Sl. No.	Session Name	Session Number	Invited Speaker
1.	Theoretical & Computational Physics-I	I	G. M. Bhuiyan
2.	Material Science-I	II	A. K. M. Akther Hossain
3.	Medical Physics	III	K Siddique-e Rabbani
4.	Nuclear and Reactor Physics	IV	Arun Kumar Basak S. I. Bhuiyan
5.	Nanomaterials	V	
6.	Theoretical & Computational Physics-II	VI	Muhammad N. Huda
7.	Environmental Science and Meteorology	VII	Nasir Ahmed
8.	Materials Science-II	VIII	M. M. Uddin
9.	Health Physics	IX	David Bradley
10.	Thin Film	X	Md. Akhtaruzzaman
11.	Poster Session		
12.	Physics Education	XI	

Sessions Chair List

Sl. No.	Session Name	Session Number	Date	Time	Session Chair and Co-chair
1.	Theoretical & Computational Physics-I	I	06 August 2021	10.05 – 11.15	Prof. Saleh Hasan Naqib Dr. Alamgir Kabir
2.	Material Science-I	II	"	11.20 - 12.40	Prof. S. S. Sikder Prof. Belal Ahmed
3.	Medical Physics	III	"	14.30 – 15.55	Prof. Dr. Kamila Afroj Quadir Dr. Prof. Abdul Hannan
4.	Nuclear and Reactor Physics	IV	"	16.00 – 17.20	Prof. Nure Alam Abdullah Dr. Md. Amirul Islam
5	Nanomaterials	VI	"	17.25 –18.55	Dr A K M Abdul Hakim Dr. Haniun Maria
6.	Theoretical & Computational Physics-II	VII	07 August 2021	09.00 – 10.15	Prof. Md. Rafiqul Islam Dr. Ratan C. Gosh
7.	Environmental Science and Meteorology	VIII	"	10.20 – 11.35	Prof. Md. Mahbubul Hoque Dr. A. K. Mallik
8.	Materials Science-II	IX	"	11.40 – 13.00	Prof. Faruque-Uz-Zaman Chowdhury Prof. A T M Kaosar Jamil
9.	Health Physics	X	"	14.00 – 15.15	Prof. Suranjan Das Dr. Abul Hasnat Rubel
10.	Thin Film	XI	"	15.20 – 16.35	Prof. Jiban Poddar Dr. Md. Tareq Chowdhury
11.	Poster Session		"	16.40 – 18.00	
12.	Physics Education	XII	"	18.00 – 19.00	Prof. Mesbahuddin Ahmed Dr. Md. Nazrul Islam Khan

National Conference on Physics – 2021 06-07 August 2021

PROGRAMME

6 August 2021 (Friday)

Inaugural Session : 09.00 – 10.00
Venue : Zoom online Platform
 : Welcome Address: Prof. G. M. Bhuiyan, Vice-President, BPS
 : Address by the Special Guest: Prof. Arun Kumar Basak, Professor Emeritus, RU
 : Address by the Chief Guest: Prof. M. Shamsheer Ali, Professor Emeritus, EU
 : Address by the Chairperson: Prof. Mesbahuddin Ahmed, President, BPS
 : Vote of Thanks: Dr. Md. Nazrul Islam Khan, General Secretary, BPS

Technical Sessions Programme

Session (I): Theoretical and Computational Physics-I

Venue: Zoom online Platform

Time: 10.05 - 11.15

Chair : Prof. Saleh Hasan Naqib
 Co-Chair : Dr. Alamgir Kabir

Invited Talk [20 minutes]

IT- I: Origin of segregation in liquid metallic binary alloys: G. M. Bhuiyan

Contributory Papers [10 minutes per paper]

- TCP-01:** Collective dynamic properties of liquid $\text{Na}_x\text{K}_{1-x}$ binary alloys: An orbital free molecular dynamic simulation study: **M. Alamgir Hossain, A. Z. Ziauddin Ahmed, Mohammad Riazuddin Molla, G. M. Bhuiyan**
- TCP-02:** DFT based prediction of pressure dependent structural, elastic, electronic, and optical properties of superconducting NaC_6 : **Nazmun Sadat Khan, B. Rahman Rano, Ishtiaque M. Syed, R.S. Islam, S. H. Naqib**
- TCP-03:** Electronic structure and optical properties of cubic BaTiO_3 (BTO): A DFT study: **Arpon Chakraborty, M. N. H. Liton, M. S. I. Sarker, M. M. Rahman, M. K. R. Khan**
- TCP-04:** Structural, magnetic, electronic and optical properties of $\text{Nd}_2\text{FeCrO}_6$ double perovskite: A first-principles study: **M. D. I. Bhuiyan, Rana Hossainnd, M. A. Basith**

Session (II): Materials Science-I

Venue: Zoom online Platform

Time: 11.20 – 12.40

Chair : Prof. S. S. Sikder
 Co-Chair : Prof. Md. Belal Hossen

Invited Talk [20 minutes]

IT-II: Perovskite type metal halides for photovoltaics and optoelectronic devices: **A. K. M. Akther Hossain**

Contributory Papers

[10 minutes per paper]

- MS-01:** Fabrication of spray pyrolysed Al/ZnO: Cd heterostructure: Effect of Cd on structure, current-voltage and capacitance-voltage characteristics: **M. A. Sattar, M. A. Rahman, M. A. Halim, M. Mozibur Rahman, M. K. R. Khan**
- MS-02:** Structural characterization of tensile strained $\text{Si}_{1-x}\text{Ge}_x$ grown on various Ge substrates: **Md. Mahfuz Alam Tanbhir Hasan, Youya Wagatsuma, Kazuya Okada, Michihiro Yamada, Kohei Hamaya, and Kentarou Sawano**
- MS-03:** Influence of manganese substitution on the structural and magnetic properties of nanocrystalline $\text{Li}_{0.2}\text{Zn}_{0.6-x}\text{Mn}_x\text{Fe}_{2.2}\text{O}_4$: **Benjir Ahmed, M. N. I. Khan, and A.K.M. Akther Hossain**
- MS-04:** Study on hydrogen isotopes behavior in rare-earth oxides: **M. Khalid Hossain, K. Hashizume, S. Jo, K. Kawaguchi, Y. Hatano**
- MS-05:** Multiferroic orders in Co-doped SrTiO_3 : **A. K. M. Sarwar Hossain Faysal, Shahrar Ahmed, M. N. I. Khan, M. A. Basith, Muhammad Shahriar Bashar, H. N. Das, S. I. Liba, Tarique Hasan and Imtiaz Ahmed**
- MS-06:** Complex permeability and dielectric property of Li-Cu-Mg-Zn ferrites: **M. Atikul Islam, M. Samir Ullah, Sm. Rubayatul Islam, M. A. Islam, F. A. Khan, Faruque Ahammed, F. Afrose Sonia and M. Mizanur Rahman**

Lunch and Prayer Break : 12.40 – 14.30

Session (III): Medical Physics

Venue: Zoom online Platform

Time: 14.30 – 15.55

Chair : Prof. Dr. Kamila Afroj Quadir

Co-Chair : Dr. Prof. Abdul Hannan

Invited Talk

[20 minutes]

IT-III: Filling a void in the century old cable theory of neural conduction, **K Siddique-e Rabbani**

Contributory Papers

[10 minutes per paper]

- MP-01:** Effects of electroporation on membrane electro-behavior in the cell like giant vesicles: **Md. Kabir Ahamed and Mohammad Abu Sayem Karal**
- MP-02:** Extraction of 3D ^{13}N distribution in inhomogeneous phantom by spectral analysis technique for proton therapy verification: **M. Rafiqul Islam, Masayasu Miyake, Mahabubur Rahman, Shigeki Ito, Shinichi Gotoh, Taiga Yamaya, Hiroshi Watabe**
- MP-03:** Investigation of molecular transport through a peptide induced nanopore and its size effects in the membrane of giant unilamellar vesicle using COMSOL: **T. Rahman, M. S. Ishtiaque, M. I. Hossain, M.A.S. Karal, Md. K. Alam**
- MP-04:** The molecular interactions of inhibitors with glucose transporter and glutaminase: In silico approach: **Suhrid Saha Pranta and Md Enamul Hoque**
- MP-05:** Effects of cholesterol on the anionic magnetite nanoparticles-induced deformation and poration of giant lipid vesicles: **Salma Akter, Sharif Hasan, and Mohammad Abu Sayem Karal**
- MP-06:** A new purification technique to obtain specific size distribution of giant lipid vesicles using dual filtration: **Tawfika Nasrin and Mohammad Abu Sayem Karal**

Session (IV): Reactor and Nuclear Physics**Venue: Zoom online Platform****Time: 16.00 – 17.20**

Chair : Prof. Nure Alam Abdullah

Co-Chair : Dr. Md. Amirul Islam

Invited Talk**[20+20 minutes]****IT-IV-A:, Arun Kumar Basak****IT-IV-B: VVER 1200 safety- protection against station blackout, S. I. Bhuiyan****Contributory Papers****[10 minutes per paper]**

- RNP-01:** Assessment of dose distribution of radionuclides due to a postulated accident of triga research reactor in Bangladesh: **M. Ajijul Hoq, Md. Abu Khaer, Mohammed Tareque Chowdhury, M. Mizanur Rahman**
- RNP-02:** Intracuclear cascade model for deuteron-induced reactions over a wide range of targets: **M. J. Kobra, Y. Uozumi**
- RNP-03:** Experimental cross section measurements for nuclear reactor technology: $^{55}\text{Mn}(n,\gamma)^{56}\text{Mn}$ reaction at two new thermal energies: **Md. Mustafa Zaved, Mohammad Amirul Islam**

Session (V): Nanomaterials**Venue: Zoom online Platform****Time: 17.25 – 18.55**

Chair : Dr A K M Abdul Hakim

Co-Chair : Dr. Kazi Haniun Maria

Contributory Papers**[10 minutes per paper]**

- NM-01:** Fast magnetization reversal of a magnetic nanoparticle driven by a chirp microwave field pulse at finite temperature: **M.T. Islam, M. A. J. Pikul, M. A. S. Akanda, and X. S. Wang**
- NM-02:** Tunable Exchange bias in $\text{Nd}_2\text{FeCrO}_6$ double perovskite: **Fahmida Sharmin, Ferdous Ara, M.D.I Bhuiyan, Subrata Das, Tetsu Sato, Tadahi Kameda, M. A. Basith**
- NM-03:** Structural and magnetic characteristic exploration of trivalent Al^{3+} ions substituted Ni-Zn-Co nano-spinel ferrites: **Nusrat Jahan, J. I. Khandaker, H. N. Das, and M. N. I. Khan**
- NM-04:** Comparison of structural and magnetic characteristics of $\text{CoNiFe}_2\text{O}_4$ @functionalized Cnts nanocomposite synthesized by different routes of hydrothermal process: **M. Al-Fahat Hossain, M. Al-Mamun, M. R. Rahman, Sheikh Manjura Hoque**
- NM-05:** Investigation of CuCo_2S_4 - moS_2 nanoparticles as electrode material for supercapacitor: **Sajjad Hasan, Subrata Das, Akter H. Reaz, Chanchal Kumar Roy, M A Basith**
- NM-06:** NM-06: Single crystal growth and anisotropic ionic conductivity of $\text{Li}_{3x}\text{La}_{(2/3-x)}\text{TiO}_3$: **Md. Shahajan Ali, Yuki Maruyama, Masanori Nagao, Satoshi Watauchi, Isao Tanaka**
- MN-07:** Investigation of the effect of Sm on magnetic and magnetodielectric properties of LaFeO_3 nanostructures: **Shovan Kumar Kundu, Dhiraj Kumar Rana, Soumen Basu**
- MN-08:** Synthesis and characterizations of ZnO nanoparticles and seed layers for subsequent growth of ZnO nanorods by hydrothermal process: **N. I. Tanvir, M. S. Hossain, N. Khatun, Md. Saidu Islam, S. Islam, and S.F.U. Farhad**
- MN-09:** Structural and improved dielectric, electrical and magnetic properties BFO-NiCuCd nano-composites: **M. Z. Islam, M. Belal Hossen**

7 August 2021 (Saturday)**Session (VII): Theoretical and Computational Physics-II****Venue: Zoom online Platform****Time: 09.00 - 10.15**

Chair : Prof. Md. Rafiqul Islam

Co-Chair : Dr. Ratan C. Gosh

Invited Talk [20 minutes]**IT-VII : Formation of polarons in metal-oxide based solar absorber materials, Muhammad N. Huda****Contributory Papers [10 minutes per paper]****TCP-05:** Density functional theory-based investigation of mechanical, electronic, optical and thermal properties of AC (A = Nb, Ta, Ti) binary metallic carbides: **Razu Ahmed, Md. Sohel Rana, Sajidul Islam, Md. Mahamudujjaman, S. H. Naqib****TCP-06:** Atomic transport properties of liquid simple metals: A perturbative approach: **Mahir Manna, R.C. Gosh****TCP-07:** Boron-rich chalcogenide semiconductor materials: Prospects for device applications via DFT study: **M. M. Hossain, M. A. Ali, M. M. Uddin, S. H. Naqib, A. K. M. A. Islam****TCP-08:** Magnetic flux dynamics of high quality YBCO single crystal: insights from field and frequency dependent AC susceptibility measurements: **M. Rakibu Hasan Sarkar and S. H. Naqib****Session (VII): Environmental Science and Meteorology****Venue: Zoom online Platform****Time: 10.20 – 11.35**

Chair : Prof. Md. Mahbub Alam

Co-Chair : Dr. M. A. K. Mallik

Invited Talk [20 minutes]**IT-VII:** Sustainable management of water resources using isotope techniques: Applications and active research areas in bangladesh: **Nasir Ahmed****Contributory Papers [10 minutes per paper]****ES-01:** Ensemble prediction of storm surge associated with cyclone Amphan using jma-mri storm surge model: **S.M. Quamrul Hassan and Syed Jamal Ahmed****ES-02:** Assessment of heavy metal distribution and contamination in water and sediments of the Kaptai Lake, Bangladesh: **Biplob Das, Mohammad Amirul Islam, Kamrun Naher, Rahat Khan, Umma Tamim, Farah Tasneem Ahmed, Mohammad Belal Hossen****ES-03:** Predictability of monsoon depression over the Bay of Bengal using weather research and forecasting model: **Md. Abul Hossen, M. A. K. Mallik, M. A. M. Chowdhury, Md. A. E. Akhter, Syed Jamal Ahmed and S. M. Quamrul Hassan****ES-04:** Sensitivity of microphysical parameterization scheme for the simulation of orographic rainfall event of 18 April 2015 over Bangladesh using WRF model: **Md. Omar Faruq, M. A. K. Mallik, M. A. M. Chowdhury, Md. A. E. Akhter, Md. Shadekul Alam, S. M. Quamrul Hassan and M. Arif Hossain**

- ES-05:** Hydrogeochemical evolution in deep aquifer systems of Kumilla, Bangladesh: **F. Islama, A. Zahid, A. H. A. N. Khan, M. Moniruzzaman, M. A. Q. Bhuiyan, M. A. Ahsan, S. Sultana, and R. K. Majumder**

Session (VIII): Materials Science-II

Venue: Zoom online Platform

Time: 11.40 – 13.00

Chair : Prof. Faruque-Uz-Zaman Chowdhury
Co-Chair : Prof. A T M Kaosar Jamil

Invited Talk [20 minutes]

- IT-VIII:** MXenes: 5th generation 2D materials go beyond graphene: **M. M. Uddin**

Contributory Papers [10 minutes per paper]

- MS-07:** Performance optimization of TCO-less back contact dye-sensitized solar cells utilizing indoline and porphyrin sensitizer based on cobalt electrolyte: **Md. Zaman Molla, Ajay Kumar Baranwal, Shuzi Hayase and Shyam S. Pandey**
- MS-08:** Growth and characterization of LiCoO₂ single crystals for the applications of all solid-state Li-ion batteries (LIBs): **Ruma Parvin, Yuki Maruyama, Masanori Nagao, Satoshi Watauchi, Isao Tanaka**
- MS-09:** Effect of vanadium substitution on structural, magnetic and transport properties of Ni-Zn-Co ferrites: **M. D. Hossain, M. N. I. Khan, R. Rashid, S. J. Ahmed, A. T. M. Kaosar Jamil**
- MS-10:** Analysis of the HTS Inductor design for optimum energy storage in SMES: **M. R. Islam, Jahangir Alam and M. A. A. Zaman**
- MS-11:** Impact of Lanthanum ions on structural, optical, and magnetic properties of Cobalt-Zinc ferrites: **Mohammad Osman Goni1, Nazia Khatun, Mohammad Sajjad Hossain, M. Al- Mamun, Mohammad Saiful Alam, Suravi Islam, Most. Hosney Ara Begum, Syed Farid Uddin Farhad and Mahmuda Hakim**
- MS-12:** Dielectric Properties and Impedance Spectroscopy of V₂O₅ added Li-Zn Ferrites: **Sm. Rubayatul Islam, M. Miftaur Rahman, S. Manjura Hoque and M. Samir Ullah**

Lunch and Prayer Break : 13.00 – 14.00

Session (IX): Health Physics

Venue: Zoom online Platform

Time: 14.00 –15.15

Chair : Prof. Suranjan Kumar Das
Co-Chair : Dr. Abul Hasnat Rubel

Invited Talk [20 minutes]

- IT-IX:** Towards development of radioluminescence sensors, **David Bradley**

Contributory Papers [10 minutes per paper]

- HP-01:** Study on Radiation Protection Infrastructure of different x-ray facilities in Habiganj district city with different thanas: **L. Begum, R. B. Rana, M. Akramuzzaman, M. M. Rahman, and M. Nahar**

- HP-02:** Real-time Environmental radiation monitoring in tejgaon thana following in-situ method: **M. A. Rahman Shuvo, M. S. Rahman, S. Yeasmin, Md. Kabir Uddin Sikder**
- HP-03:** Health effects of electromagnetic radiation from cell phone and towers: it's present scenario in Bangladesh: **Munima Haque, M. Quamruzzaman, Md. Shohag Hossain**
- HP-04:** Source apportionment and health risk assessment of heavy metals from indoor air dust of an industrial area, Savar, Bangladesh: **M. A. M. Mottali Sarkar, M.M. Hasan, M. S. Rahman, B.A. Begum**
- HP-05:** Analysis of circulating cell free DNA extracted from blood plasma of cancer patients and healthy persons and their Z-scan study: **H. Ara, S. A. Tarek, S. M. S. Al Din, M. K. Biswas, S. M. Sharafuddin, S B Faruque and Y. Haque**

Session (X): Thin Film**Venue: Zoom online Platform****Time: 15.20 – 16.35**

Chair : Prof. Jiban Poddar
 Co-Chair : Dr. Md. Tareq Chowdhury

Invited Talk**[20 minutes]**

- IT-X:** Materials for stable perovskite solar cells: advances, challenges and opportunities: **Md. Akhtaruzzaman**

Contributory Papers**[10 minutes per paper]**

- TF-01:** Thickness dependent thermal and optical characteristics of plasma polymerized N-benzylaniline thin films: **Rani Nasrin, Mohammad Jellur Rahman, A. T. M. K. Jamil, A. H. Bhuiyan**
- TF-02:** Comparative study of power and thickness dependent optical properties of AC plasma polymerized 3,4-Ethylenedioxythiophene thin films: **Md. Juel Sarder, Mohammad Jellur Rahman, Md. Mahmud Hasan, and A. H. Bhuiyan**
- TF-03:** Evolution in surface properties, band gap tuning and reversal in electrical conductivity of ZnO thin films achieved via B doping: **M. Sharmin, A. H. Bhuiyan, J. Podder and K. S. Hossain**
- TF-04:** Structural, optical and transport properties of Fe: Co₃O₄ thin films grown by spray pyrolysis technique: **M. Zahan and J. Podder**
- TF-05:** Characterization of the physical properties of Cu₂O thin films synthesized in the presence of NaCl by modified SILAR method: **A. Hossaina, N. I. Tanvir, S. F. U. Farhad, S. Majumder, B. C. Ghos, M. A. Rahman, T. Tanaka, Q. Guo, M. A. M. Patwary**

Poster Session : 16.40 – 18.00

Session (XI): Physics Education & Closing

Venue: Zoom online Platform

Time: 18.00 – 19.00

Chair : Prof. Mesbahuddin Ahmed

Co-Chair : Dr. Md. Nazrul Islam Khan

Contributory Papers

[10 minutes per paper]

- PE-01:** Gender issues in science classroom and female learner's participation in higher education science programs: **Anina Mahmud, Mohammad Nure Alam Siddique**
- PE-02:** status and reasons of current practice of science practical at the secondary level: **S. M. Hafizur Rahman, Md. Salimuzzaman, TahminaHoq**
- PE-03:** A study on the effectiveness of online classes in Bangladesh during the COVID-19 pandemic: **Shahid Uddin Fahim, Md. Tanjimul Islam, Md. Mahmudul Hasan, Humaira Khondokar Gim, Fatema Jahan, Humayra Ferdous, Tafazzal Hossain, Md. Ehasanul Haque**

List of Posters for Presentation

- PP-01:** Assessment of ambient air quality in Dhaka city and sources of pollutant identification: **M.M. Hasan, B.A. Begum, M.S. Rahman, M.A.M Mottalib Sarkar**
- PP-02:** Recent pre-monsoon thunderstorms scenario over Bangladesh: **Mohammed Mozammel Hoque, Syed Jamal Ahmed, M. A. K. Mallik, S. M. Quamrul Hasanand, Ishtiaque M. Syed**
- PP-03:** Synthesis and characterization of SWCNT modified biopolymer with super cyclic stability for transient energy storage application: **Rabeya Binta Alam, Md. Hasive Ahmad, Muhammad Rakibul Islam**
- PP-04:** Determination of essential elements in medicinal plants of the Sundarban mangrove forest by neutron activation analysis: **Md. Barkat Ullah Pappu, Mohammad Amirul Islam, Abdullah Al-mamun, Rinku Majumder**
- PP-05:** Simulation of a severe thunderstorm and its characteristics over Dhaka, Bangladesh using WRF Model: **Most. Marioum, M. A. K. Mallik, Suranjan Kumar Das, S.M. Quamrul Hassan and Md. Omar Faruq**
- PP-06:** Implementation of meteorological data and atmospheric dispersion model for radiological consequence analysis: **Md. Abu Khaer, S. Sultana Shiuli, Md. Ajijul Hoq, Mohammed Tareque Chowdhury, Mohammad Mizanur Rahman**
- PP-07:** Ternary scandium based antiperovskite $\text{Sc}_3\text{GaX}(\text{X}=\text{B},\text{N})$: DFT study: **Istiaq Ahmed, F. Parvin, A.K.M. A. Islam**
- PP-08:** Recent track climatology of cyclonic disturbances over the Bay of Bengal: **Shahanaj Sultana, M. A. K. Mallik, Md. Shadekul Alam, Md. Omar Faruq, Md. Abdul Mannan and S.M. Quamrul Hassan**
- PP-09:** Database from secondary data of concentration of NORM and making an absorbed dose map for overall Bangladesh: **Md. Ashik Azad Khan, A.K. M. Saiful Islam Bhuian, Shahadat Hossain and Quazi Muhammad Rashed Nizam**
- PP-10:** Radiation monitoring around cancer hospital campus and evaluation of radiological risk on public health: **Md. Arman Ali, M. S. Rahman, S. Yeasmin, Md. Kabir Uddin Sikder**
- PP-11:** Estimation of radiation risk on worker & public from radiological facility using thermoluminescent dosimeters: **Omar Faruk, M. S. Rahman, K. N. Sakib, M. M. Tasnim, S. Yeasmin**
- PP-12:** Real-time radiation monitoring around BIRDEM hospital campus and estimation of radiation risk on public health: **Sk. Sabbir Ahmed Shakil, M. S. Rahman, S. Yeasmin, Md. Kabir Uddin Sikder**
- PP-13:** Real-time radiation monitoring around LABAID hospital campus and evaluation of radiation risk on public: **A. A. Shuhan, M. S. Rahman, S. Yeasmin, Md. Kabir Uddin Sikder**
- PP-14:** Implementation of Meteorological data and atmospheric dispersion model for radiological consequence analysis: **Md. Abu Khaer, S. Sultana Shiuli, Md. Ajijul Hoq, Mohammed Tareque Chowdhury, Mohammad Mizanur Rahman**
- PP-15:** Real-time radiation monitoring at outdoor of mitford hospital campus and estimation of radiation risk on public: **L. A. Tonu, M. S. Rahman, Pretam K. Das, S. Yeasmin**
- PP-16:** Synthesis of gallium (Ga) Doped CdO/p-Si heterojunction and evaluation of junction parameters: **AbdurRouf, M. K. R. Khan, M. Saifur Rahman, M. S. I. Sarker and M. Mozibur Rahman**
- PP-17:** Surface morphology of Ca Doped $\text{Li}_{0.5}\text{Bi}_{0.5}\text{Fe}_{0.5}\text{Nb}_{0.5}\text{O}_3$ perovskite: **M. A. Rashid, K. A. Rahman and A. K. M. Akther Hossain**
- PP-18:** Reduced graphene oxide supported cobalt ferrite nanoparticles: a study of synthesis mechanism, structural, magnetic and thermal stability characterization: **Gobinda Chandra Mallick, M. Al-Mamun, M. R. Rahman, M. Al-Fahat Hossain, Sheikh Manjura Hoque**

- PP-19:** Structural, electrical and magnetic properties of Ce and Fe doped SrTiO₃: **Tarique Hasan, Arnab Saha, M. N. I. Khan, M. A. Basith, Muhammad Shahriar Bashar, H. N. Das, R. Rashid, Tarique Hasan, and Imtiaz Ahmed**
- PP-20:** Determination of thermo-optic coefficient, nonlinear absorption coefficient and nonlinear refraction coefficient in the thermal regime of L-tryptophan using closed aperture CW Z-scan: **S. A. Tarek, S. B. Faruque, S. M. Sharafuddin, K. M. E. Hasan, A. K. M. M. Hossain, H. Ara, M. K. Biswas, Y. Haque**
- PP-21:** Study on the iron-deficient non-stoichiometry driven electromagnetic and magnetoelectric properties of multiferroic composites: **Sharifa Nasrina, Tabassum Haque Joyee, A.K.M. Akther Hossain, and Md. D. Rahaman**
- PP-22:** Comparison of perovskite nanorod's bandgap obtained via diverse methods for optoelectronic applications: **Mohammad Tanvir Ahmed, Shariful Islam, Farid Ahmed**
- PP-23:** Performance optimization of TCO-less back contact dye-sensitized solar cells utilizing indoline and porphyrin sensitizer based on cobalt electrolyte: **Md. Zaman Molla, Ajay Kumar Baranwa, Shuzi Hayase and Shyam S. Pandey**
- PP-24:** Design and investigation of step-index core polymer directional coupler for board-level optical circuitry: **Fariha Tasnim, Md Omar Faruk Rasel, and Takaaki Ishigure**
- PP-25:** Effect of Gd substitution on the structural, dielectric and electric properties of Ni-Cu-Cd ferrite nanoparticles: **M. AnwarHossain, M. Belal Hossen**
- PP-26:** Synthesis and characterization of europium doped nickel zinc cobalt ferrite: **Imran Sardar, Md. Nazrul Islam Khan, Md. Rashedur Rahman, Md. Sohel Sikder**
- PP-27:** Facile method for synthesizing ZnO nanorods with controllable size: **M. Sultana, Mohammad Jellur Rahman, M. S. Bashar**
- PP-28:** Study of structural and initial permeability of strontium and nickel co-doped barium titanate sintered at 1250°C: **Mehedi Hasan, A. K. M. Akther Hossain**
- PP-29:** Structural and magnetic properties of Li-Cr-Zn ferrites: **Rowshon Satara, M. Firoz Uddin, M. Zaman Molla, Mahmudul Hasan, Faizus Salehin, S. Manjura Hoque, F. A. Khan and, M. Samir Ullah**
- PP-30:** Detailed electrical investigation on highly potential NCZA ceramics for MLCI and miniaturized device applications: **M Rahim Ullah, H M A R Maruf, N M Eman, N J Shirin and M Belal Hossen**
- PP-31:** Possible applications of multi-Josephson junction in superconductor as a quantum interferometer: **H.M.A.R. Maruf, Md. Abdullah Al Zaman, M.R. Islam and F.-U.-Z. Chowdhury**
- PP-32:** Analysis of beam contamination along the beam path by isotopes of ¹²C beam and their role in charge changing cross section measurement by PHITS: **Quazi Muhammad Rashed Nizam**
- PP-33:** Investigation of molecular transport through multipore into giant unilamellar vesicles using COMSOL simulation: **Md. Asaduzzaman, T. Rahman, M.S. Ishtiaque, M.I. Hossain, Md. A. S. Karal and Md. K. Alam**
- PP-34:** Synthesis of ZnO nanoparticles from waste materials: **Tanvir Ahmed Chowdhury, Jahirul Islam Khandaker, Md. Abdul Gafur**
- PP-35:** Rietveld analysis on the structural properties of Mn Substituted Ni-Cu-Cd bulk ferrites synthesized from nanocrystalline powders: **Mia Md Fakharuddin Ali Mazlobee, M. R. Shah and M. Belal Hossen**
- PP-36:** Graphene oxide and Reduced graphene oxide reinforced hydroxyapatite based nano composites for biomedical application: **Md. Ifat-Al-Karim, Md. Al Mamun, Md. Mahbubul Haque, Farzana Nahid**
- PP-37:** Reduced graphene oxide supported cobalt ferrite nanoparticles: a study of synthesis mechanism, structural, magnetic and thermal stability characterization: **Gobinda Chandra Mallick, M. Al-Mamun, M. R. Rahman, M. Al-Fahat Hossain, Sheikh Manjura Hoque**
- PP-38:** Analysis of grain growth, densification and reduction of porosity, coercivity and functional properties of Mn substituted Ni-Cu-Zn nanocrystalline ferrites: **Abdul Ahad, and A. K. M. Akther Hossain**

- PP-39:** Structural, electrical and magnetic properties inspection for rare-earth substituted magnetic dense ceramics synthesized from Nanoferrites: **M. Faishal Mahmood and M. Belal Hossen**
- PP-40:** Atomic-scale investigation of the formation of Al nanocluster in the pulsed laser ablation technique: **Samiul Hossain Sajal, Nithika Datta and Md Enamul Hoque**
- PP-41:** Hot injection synthesized lead-free CsSnCl_3 nanocrystals: an experimental investigation :**Yasir Fatha Abed, Md. Shahjahan Ali, Subrata Das, M. A. Basith**
- PP-42:** Study of the structural and magnetic properties of Gd doped CoFe_2O_4 nanoparticles synthesized via sol-gel route: **M. S. I. Sarker, Marufa Yeasmin, S. Manjura Haque, M. M. Rahman, M. K. R. Khan**
- PP-43:** Synthesis and Characterization of Co_3O_4 incorporated three-Dimensional MoS_2 nanostructure: **Muhammad Hasive Ahmad, Rabeya Binta Alam, S.F. U. Farhad, Muhammad R. Islam**
- PP-44:** Impact of particle size on the magnetic properties of highly crystalline Yb^{3+} substituted Ni-Zn nano ferrites: **N. Jahan, M.N.I. Khan, F.-U.-Z. Chowdhury, M. R. Hasan, H. N. Das, M.M. Hossain and M.M. Uddin**
- PP-45:** Dielectric, modulus, impedance spectroscopy and conductivity properties of Mg-substituted Cu-Zn-Al nano ferrites with structural rietveld refinement: **S. K. Ahmed and M. B. Hossen**
- PP-46:** Fabrication and characterization of the metallic nanoparticles using pulsed laser ablation technique: **Mustabi Mustafa Chowdhury and Md. Enamul Hoque**
- PP-47:** Effects of atomic number and pressure of different filling gases on soft X-ray yield from PF1000 plasma focus device: **M A Malek, L Akter, G S Rakib, M M Islam, M N Huda, and M K Islam**
- PP-48:** Design, development and simulation of a nuclear counting system using ATMEL microcontroller: **M. N. Islam, M. S. Alam and M. A. S. Haque**
- PP-49:** Data hiding using audio steganography considering less distortion of cover data for nuclear data: **Md. Shamimul Islam, Nayan Kumar Datta, Md. Mahbub Alam, Dr. Md. Dulal Hossain, Dr. Md. Shakil Ahmed**
- PP-50:** Theory of 3F4D universe (Beyond SM of Particle Physics): **Yogesh V. Chavan**
- PP-51:** Elastic, electronic, bonding, optoelectronic and thermophysical properties of SnTaS_2 : comprehensive insights from ab-initio calculations: **M. I. Naher, M. Mahamudujjaman, A. Tasnim, S. H. Naqib**
- PP-52:** MAX phase materials: prospect of MAX phase borides: **M. A. Ali, M. M. Hossain, M. M. Uddin**
- PP-53:** DFT based first principles calculation of lead-free CsSnCl_3 perovskite: A “GGA+U” Approach: **Md. Shahjahan Ali, Yasir Fatha Abed, Subrata Das, M. A. Basith**
- PP-54:** Elastic, electronic, bonding, optoelectronic and thermophysical properties of SnTaS_2 : comprehensive insights from ab-initio calculations: **M. I. Naher, M. Mahamudujjaman, A. Tasnim, S. H. Naqib**
- PP-55:** Structural, elastic and optoelectronic properties of CaZn_2X_2 (X = N, P, As) semiconductors: density functional theory-based investigations: **Md. Sajidul Islam, Md. Mahamudujjaman, S. H. Naqib**
- PP-56:** Insights into the physical properties of aCaCuO_3 and SrCuO_3 semi-metals: A DFT study **M. Monira, M.N.H. Liton, M.A. Helal and M. Kamruzzaman**
- PP-57:** Realization of the role of donor (F) impurity on the electronic structure and optical properties of ZnO: A first principles study: **M. N. H. Liton, M. K. R. Khan**
- PP-58:** Wigner rotation in different space time: **Md. Tarek Hossain**
- PP-59:** Analysis of the HTS inductor design for optimum energy storage in SMES: **M. R. Islam and Jahangir Alam and M A A Zaman**
- PP-60:** A computational molecular design of new potential molecules for D/A type OLED and investigating TADF properties for high luminescence: A DFT study: **Banasree Sarkar Mou, Ahsan Ullah, Dr Nazia Chawdhury**
- PP-61:** Thermophysical and optoelectronic properties of Nb_2P_5 : density functional theory-based insights: **M. I. Naher and S. H. Naqib**

- PP-62:** Simulation study of macrobending and microbending losses of a single mode step index optical fiber: **P. Roy and H. R. Khan**
- PP-63:** Density functional theory-based ab-initio insights into the physical properties of Mo_3P : **Md. Sohel Rana, Razu Ahmed, Sajidul Islam, Md. Mahamudujjaman, S. H. Naqib**
- PP-64:** Study on shielding effectiveness of a conceptual active radiation shield constructed with multi-wall carbon nanotube added YBCO-123 superconducting material: **Md. Abdullah Al Zaman, H. M. A. R. Maruf, Md. Rafiqul Islam**
- PP-65:** Ternary scandium based antiperovskite Sc_3GaX ($\text{X}=\text{B},\text{N}$): DFT study: **IstiaqAhmed1, F. Parvin, A.K.M. A. Islam**
- PP-66:** Dust-acoustic shock waves in nonthermal dusty plasmas with two population ions: **K. N. Mukta, I. Tasnim, M. M. Masud, and A. A. Mamun**
- PP-67:** Strategy of improving photovoltage and efficiency of FeS_2 based heterojunction solar cell through absorber, buffer and window layers optimization with SCAPS-1D software: **M. Kamruzzaman, R. Afrose, M. N. H. Liton, M. A. Helal and M. Aktary**
- PP-68:** Study of thermal and DC electrical properties of plasma polymerized 1,2-diaminocyclohexane thin films: **Md. Mahmud Hasan, Mohammad Jellur Rahman, Md. Saddam Sheikh, Md. Juel Sarder, Md. Masud Reza, and A. H. Bhuiyan**
- PP-69:** Optical and structural properties of spin coated $\text{Cu}_2\text{NiSnS}_4$ (CNTS) thin film: effect of thiourea concentration: **M.M. Rashid, S. Islam, F. Ahmed, M.S. Bashar, A.T.M.K. Jamil, S.J. Ahmed**
- PP-70:** Structural, morphological, and optical properties of CuO thin films synthesized by dip-coating technique for gas sensing applications: **A. M. M. Musa, M. A. Gafur, S. U. F. Farhad, and A. T. M. K. Jamila**
- PP-71:** Analysis of purification of charged giant vesicles in a buffer using their size distribution: **Marzuk Ahmed and Mohammad Abu Sayem Karal**
- PP-72:** An overview of global fusion energy R&D trends and current perspectives of bangladesh: **Md Mahbub Alam, Md Maidul Islam, Md Abdur Rob Sheikh**
- PP-73:** Challenges and approaches to develop and maintain a strong nuclear knowledge base for the country started construction of its first nuclear power reactor: **Md Mahbub Alam, Nayan Kumar Datta, Md. Shakil Ahmed**
- PP-74:** Precautions to reduce uncertainty during sample preparation for analysis: **M. A. Maksud, A.K.M. Atique Ullah, N. E. Alam, S. R. Khan, M. M. Hosen, L. N. Lutfa, T. R. Choudhury, S. B. Quraishi**

NATIONAL CONFERENCE ON PHYSICS-2021

06 – 07 August 2021

Theme: Physics for National Development

**INVITED & CONTRIBUTORY ABSTRACTS
FOR ORAL PRESENTATION**

Venue: Zoom Online Platform

Bangladesh Physical Society

6 August 2021 (Friday)

Session-I: Theoretical and Computational Physics-I

IT-I: Formation of polarons in metal-oxide based solar absorber materials

Muhammad N. Huda

Department of physics, The University of Texas at Arlington, TX 76019, USA

For solar energy-based renewable energy technologies, solar absorber materials with efficient optical absorption and charge transport properties are required. Hydrogen production from water splitting via the photo-electrochemical (PEC) process remains one of the most promising green technologies. The key materials for this technology are the photo-electrocatalysts that are required to absorb sunlight, form electron-hole pairs and transport the charge carriers efficiently towards the liquid-semiconductor interface to split water molecules. Metal-oxides are thought to be the most stable materials under intense interfacial reactive conditions. However, the overall solar to hydrogen production efficiencies are not as high as expected, even for those with near-suitable bandgap energies. One of the main reasons is attributed to the poor transport properties in metal-oxides, especially in the 3d transition metal-oxides, where electrons are strongly correlated. In strongly correlated systems, electrons can interact with phonons to form polarons. In this presentation, representative metal-oxides photo-catalysts will be considered to demonstrate the polaron formation mechanism. From detailed electronic structure calculations by density functional theory (DFT) based methods, the polaronic states in metal-oxides will be depicted. We will show how these polaronic states affect the transport properties and the photo-voltages of the PEC cell. We will also discuss how well these computational results compare with the recent experimental outcome. Computations were performed at the Texas Advanced Computing Center (TACC).

TCP-01: Collective dynamic properties of liquid $\text{Na}_x\text{K}_{1-x}$ binary alloys: An Orbital Free Molecular Dynamic Simulation Study

M. Alamgir Hossain^{a,1}, A. Z. Ziauddin Ahmed^{a,2}, Mohammad Riazuddin Molla^{a,b}, G. M. Bhuiyan^a

^aDepartment of Theoretical physics, University of Dhaka, Dhaka, 1000, Bangladesh

^bDepartment of Mathematics, University of Dhaka, Dhaka, 1000, Bangladesh

E-mail: ¹alamgirphysics5@gmail.com, ²abuzafur@yahoo.com

The collective properties of the liquid $\text{Na}_x\text{K}_{1-x}$ binary alloys such as intermediate scattering function, dynamic structure factor, velocity of sound and shear viscosity are studied by using orbital free *ab-initio* molecular dynamics (OF-AIMD) simulation technique. This study is carried out for three different concentration $x = 0.3, 0.5$ and 0.7 at thermodynamic states near their melting point (373 K). In OF-AIMD method, the Hohenberg-Kohn version of DFT is used for calculating the electronic energy functional. Here the local pseudopotential prescribed by Bhuiyan *et al.* is employed for approximating the electron-ion interaction energy functional. We have calculated adiabatic sound velocity from the dispersion relation which obtained from the peaks of dynamic structure factor $S(q, \omega)$ for different q values. The dynamic structure factor contain all the information regarding inter-particle correlations and their time evolution and is obtain from the Fourier transform of the intermediate scattering function $F(q, t)$. The results obtained are seems to be encouraging in comparison with experimental data and other theoretical works available in the scientific literature.

TCP-02: DFT based prediction of pressure dependent structural, elastic, electronic, and optical properties of superconducting NaC_6

Nazmun Sadat Khan^{1*}, B. Rahman Rano¹, Ishtiaque M. Syed¹, R.S. Islam², S. H. Naqib²

¹Department of Physics, University of Dhaka, Dhaka-1000, Bangladesh

²Department of Physics, University of Rajshahi, Rajshahi-6205, Bangladesh

*Email e-mail: nazmunsadat@gmail.com

NaC_6 belonging to the Im-3m (No-299) group is a material which exhibits superconductivity at high critical temperatures T_c . We have performed density functional theory (DFT) based calculations to investigate the elastic, electronic, thermodynamic and optical properties at various pressures in this study. The structural and elastic structures have been compared with available literature. The electronic band structure of the material has been studied. Pressure dependence of important parameters such as bulk modulus, Young's modulus and Poisson's ratio have been calculated. From these parameters, we've obtained Debye temperature of the material, which is unusually high and explains partially the high critical temperature. The optical parameters of the material have been studied in detail. NaC_6 displays high reflectance in the ultraviolet region. An analysis of the high critical temperature of the material has been performed in light of all these properties.

TCP-03: Electronic structure and optical properties of cubic BaTiO_3 (BTO): A DFT study

Arpon Chakraborty^a, M. N. H. Liton^b, M. S. I. Sarker^a, M. M. Rahman^a & M. K. R. Khan^a

^aDepartment of Physics, University of Rajshahi, Rajshahi-6205, Bangladesh

^bDepartment of Physics, Begum Rokeya University, Rangpur-5400, Bangladesh

*Email: iamarpon07@gmail.com

Now-a-days, the majority of the current research has concentrated on lead (Pb)-based ferroelectric materials for cutting edge technology and industrial applications. However, their high structural intricacy presents a problem to design utmost application. Many characteristics of solids linked to ferroelectricity have been discovered recently in barium titanate, BaTiO_3 (BTO), which has great scientific interest. Here in, first principle calculations were performed to investigate the ground state physical properties of cubic phase BTO based on density functional theory (DFT). To explore the electronic configuration of this prototype ferroelectric perovskite compound, calculations for the band structure, density of states (DOS), and phonon have been systematically conducted. The electronic band structure of BTO demonstrates the semiconducting nature with band gap of 1.75 eV revealed BTO phase is suitable for photocatalytic performance for water splitting and pollutant degradation. The absence of an imaginary phonon frequency in dispersion curve assured its dynamical stability. Furthermore, the energy dependent optical properties confirmed that the electron transition from the **O-2p to Ti-3d orbital is mainly responsible for the optical activity** of BTO which is consistent with the underlying density of states. The optical absorption and reflectivity spectra of BTO, as well as its static index of refraction, indicate that the compound has the potential to be exploited in the optoelectronic device industry.

Keywords: BaTiO_3 ; Electronic band structure; Optical properties; Phonon spectra; First principles calculations.

TCP-04: Structural, magnetic, electronic and optical properties of $\text{Nd}_2\text{FeCrO}_6$ double perovskite: A first-principles study

M. D. I. Bhuyan¹, Rana Hossain² and M. A. Basith¹

¹Nanotechnology Research Laboratory, Department of Physics,
Bangladesh University of Engineering and Technology (BUET), Dhaka-1205

²Department of Mechanical Science and Bioengineering, Osaka University, Osaka 560-8531, Japan.

Email: didar_bhuiyan@yahoo.com

In this investigation, the first-principles predictions on the crystallographic structure, magnetic, electronic and optical properties of B-site ordered $\text{Nd}_2\text{FeCrO}_6$ (NFCO) double perovskite have been reported. Spin-structure of the ground state has been selected by a series of GGA+U calculations by employing experimentally obtained structural parameters and optical band gap. Our calculation indicates in NFCO double perovskite, the ferrimagnetic (FiM) $\text{Fe}\uparrow\text{-O-Cr}\downarrow$ super-exchange interaction is more energetically favourable than ferromagnetic (FM) and antiferromagnetic (AFM) order and the magnetic phase transition temperature is calculated to be 265.7 K. Phonon structure and elastic constants analysis show that NFCO is both dynamically and mechanically stable and possess ductile nature. The spin polarized band structure and density of states suggest that NFCO double perovskite has a semiconductor nature with the possibility of a direct transition. The density of states show that hybridized O-2p+Cr-3d(t_{2g}) orbitals dominate at the top of the valence band whereas Fe-3d(t_{2g})+O-2p states dominate at the bottom conduction band. Moreover, the absorption coefficient spectrum shows double absorption edges in the visible range at 1.98 eV and 2.60 eV respectively, which are related to the transition from VBM to Fe-3d(t_{2g}) and Fe-3d(e_g) bands respectively. Due to the semiconducting nature and acceptable bandgap, we anticipate that NFCO double perovskite may be an ideal option for spintronic and optoelectronic devices.

Session-II: Materials Science

IT-II: Perovskite type metal halides for photovoltaics and optoelectronic devices

A.K.M. Akther Hossain

Department of Physics, Bangladesh University of Engineering and Technology,
Dhaka-1000, Bangladesh.

E-Mail: akmhossain@phy.buet.ac.bd

Perovskite type metal halides have fascinating optoelectronic properties such as tunable bandgap, high optical absorption, broad absorption spectrum, mechanically stable and highly ductile. These materials can be described by the general formula ABX_3 , where A is a cation, B is a metal ion and X is a halogen anion. These materials are nontoxic, abundant in nature, and inexpensive. Therefore, for fabrication of solar cell these materials would be cost-effective and more efficient compared to that of silicon-based photovoltaic technology. The Density Functional Theory (DFT) based first principles calculations on Mn- and Ni doped CsGeCl_3 halides show that the absorption edge of both Ni and Mn-doped CsGeCl_3 is shifted toward the low energy region (red shift) relative to the pristine one. Similar behaviour is also observed in Cr- and Mn-doped CsSnCl_3 . Mechanical properties demonstrate that the doped samples are mechanically stable and ductile as the pristine CsGeCl_3 and CsSnCl_3 . The electronic properties show that the excitation of photoelectrons is easier due to the formation of intermediate states in Mn-doped CsGeCl_3 , and the Cr- and Mn-doped CsSnCl_3 . As a result, Mn-doped CsGeCl_3 and CsSnCl_3 exhibits higher absorptivity in the visible region compared to that of corresponding pristine sample. Detailed investigation suggests that the Mn-doped CsGeCl_3 and CsSnCl_3 perovskites are suitable candidates for the application in high performance solar cells and other potential optoelectronic devices.

Keywords: CsGeCl_3 , CsSnCl_3 perovskite, DFT, metal-doping, electronic properties, optical properties, mechanical properties.

MS-01: Fabrication of spray pyrolysed Al/ZnO: Cd heterostructure: Effect of Cd on structure, current-voltage and capacitance-voltage characteristics

M. A. Sattar^a, M. A. Rahman^a, M. A. Halim^a, M. MoziburRahman^b, M. K. R. Khan^b

^aDepartment of Materials Science & Engineering, University of Rajshahi

^bDepartment of Physics, University of Rajshahi, Rajshahi 6205, Bangladesh.

E-mail: ykrkhan@yahoo.com

Al/ZnO: Cd heterojunctions were fabricated by depositing ZnO:Cd films on Al substrate using spray pyrolysis technique at 220 °C substrate temperature. X-ray diffraction (XRD) study showed that the prepared Cd-doped ZnO films are polycrystalline in nature, oriented in (101) plane. SEM images revealed that the grain structure changes from granular to tube or circular ring like with Cd doping. The rectifying behavior is observed for fabricated Al/ZnO: Cd junctions. The room temperature ideality factors are 4.5, 3.75 and 3.70 corresponding to 1, 3 and 5% doping concentration, respectively. The reverse saturation currents are 2.64×10^{-7} , 9.78×10^{-7} and 4.19×10^{-7} A for Al/ZnO: Cd junctions depending on Cd concentration. The reverse saturation current for Al/ZnO: Cd sample is increased slightly. The built-in-potential calculated from capacitance (C-V) data of Al/ZnO: Cd junctions are 2.36, 1.82 and 1.60 V for 1, 3 and 5% Cd doping concentration, respectively.

Keywords: Hetero-junction, Junction characteristics, Ideality factor, Built-in-potential, Spray pyrolysis

MS-02: Structural characterization of tensile strained Si_{1-x}Ge_x grown on various Ge substrates

Md. Mahfuz Alam^{1,2}, Tanbhir Hasan¹, Youya Wagatsuma², Kazuya Okada², Michihiro Yamada³, Kohei Hamaya³, and Kentarou Sawano²

¹Department of Physics, University of Barishal, Barishal-8254, Bangladesh

²Advanced Research Laboratories, Tokyo City University, 8-15-1 Todoroki, Setagaya-Ku, Tokyo 158-0082, Japan

³Center for Spintronics Research Network, Graduate School of Engineering Science, Osaka University, Toyonaka, Osaka 560-8531, Japan

Email: mahfuzalam08@yahoo.com

A high-quality Si_{1-x}Ge_x with high Ge contents plays an important role in the nano-electronics industry in recent years because of its several applications not only in strained SiGe-based electronics devices but also in Si/Ge heterostructures-based devices[1,2]. Recently, it has been reported that SiGe(111) can be used in spintronics devices as a channel layer while pure-spin-current transport with a long spin lifetime observed for the SiGe(111) channel layer [3]. Very common defects such as dislocations and stacking faults are generated as a strain relaxation mechanism whereas, stacking faults only formed under the tensile strain relieving process. Cracking is another relaxation mechanism to relieve tensile strain in SiGe layers which physically fractures the top epitaxial SiGe layers [4]. Still, now, there are very few reports on detailed crack formation mechanisms for the tensile strained SiGe epitaxial layer. In this work, the initial stage of line-shaped cracks correlated with ridge formation is studied in detail to investigate the experimental critical thickness (t_c) for cracks correlated with ridge formation in tensile strained Si_{1-x}Ge_x layers grown on Ge-on-Si(111), Ge(111), and Ge(100) substrates. We found that

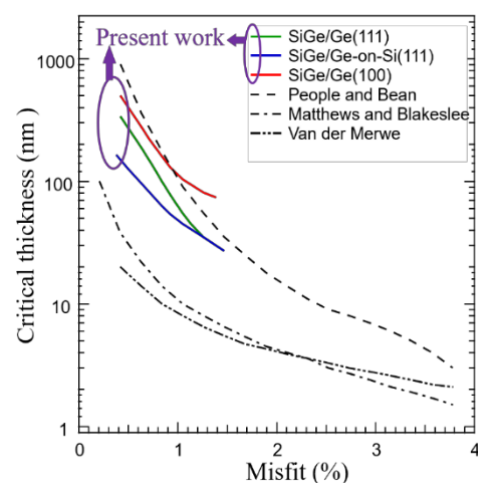


Figure 1: Comparison graph of our experimental results of

experimental critical thickness t_c for line-shaped cracks correlated with ridge formation on Si_{1-x}Ge_x/Ge(100) is very near to the reported theoretically predicted t_c while both are equal for 112nm and is higher than that on Si_{1-x}Ge_x/Ge(111) and Si_{1-x}Ge_x/Ge-on-Si(111) as shown in figure-1. The t_c of Si_{1-x}Ge_x/Ge-on-Si(111) is lower than that of Ge(111), since threading dislocation in substrate leads to the origin of misfit dislocation which contributes to form cracks in the SiGe layers. It can be said that these comparative studies of t_c for line-shaped cracks correlated with ridge formation are expected to open possibilities of the practical application of SiGe/Ge heterostructures to spintronics and high-performance Ge(111) based devices.

References:

- [1] L. Gomez, P. Hashemi, and J. L. Hoyt, IEEE Transactions on Electron Devices, 56(11), 2644 - 2651 (2009)
- [2] V. A. Shah, A. Dobbie, M. Myronov, D. J. F. Fulgoni, L. J. Nash, and D. R. Leadley Appl. Phys. Lett. 93,192103 (2008)
- [3] Takahiro Naito, Michihiro Yamada, Makoto Tsukahara, Shinya Yamada, Kentarou Sawano, and Kohei Hamaya, Appl. Phys. Express 11, 053006 (2018).
- [4] Md. Mafuz Alam, Y. Wagatsuma, K. Okada, Y. Hoshi, M. Yamada, K. Hamaya, and K. Sawano, Appl. Phys. Express 12, 081005 (2019).

MS-03: Influence of Manganese Substitution on The Structural and Magnetic Properties of Nanocrystalline Li_{0.2}Zn_{0.6-x}Mn_xFe_{2.2}O₄

Benjir Ahmed^{*,1}, M. N. I. Khan², and A.K.M. Akther Hossain¹

¹Department of Physics, Bangladesh University of Engineering and Technology, Dhaka-1000, Bangladesh.

²Materials Science Division, Atomic Energy Center, Dhaka, Bangladesh

*Email: 01989940598z@gmail.com

Manganese (*Mn*) substitution on the Lithium-Zinc-Manganese ferrite have been taken for a particular purpose in case the electromagnetic components and microwaves devices. In the present study, the structural, magnetic and dielectric properties of various Li_{0.2}Zn_{0.6-x}Mn_xFe_{2.2}O₄ are thoroughly investigated. No secondary phases are detected in the X-ray diffraction patterns, indicated that the sample possess fairly single-phase cubic spinel structure. The values of lattice constant of all samples follow Vegard's law. The SEM micrographs showed that *Mn* substitution has significant effect on the grain growth. Maximum value of real part of initial is obtained for the samples sintered at 1200 °C. Due to addition of *Mn* there is an increase of initial permeability and saturation magnetization. A combinational result suggests that the *Mn* doped Lithium-Zinc Ferrite can be extensively used in many electronic devices.

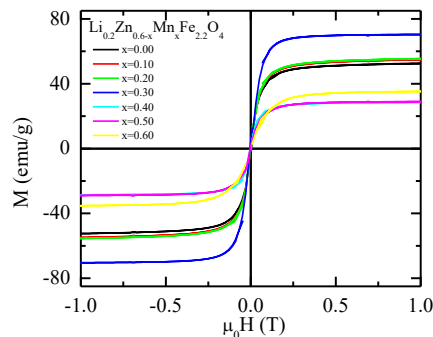


Fig. 1 M-H Hysteresis loops of various Li_{0.2}Zn_{0.6-x}Mn_xFe_{2.2}O₄.

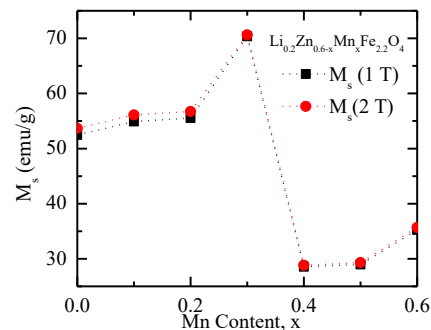


Fig. 2 Saturation magnetization as a function of *Mn* content

MS-04: Study on hydrogen isotopes behavior in rare-earth oxides**M. Khalid Hossain^{1, 2,*}, K. Hashizume¹, S. Jo², K. Kawaguchi², Y. Hatano³**¹Department of Advanced Energy Engineering Science, Interdisciplinary Graduate School of Engineering Science, Kyushu University, Fukuoka 816-8580, Japan.²Atomic Energy Research Establishment, Bangladesh Atomic Energy Commission, Dhaka 1349, Bangladesh.³Hydrogen Isotope Research Center, Organization for Promotion of Research, University of Toyama, Toyama 930-8555, Japan.*Email: khalid.baec@gmail.com, khalid@kyudai.jp

Oxide materials are one of candidates as tritium permeation barriers in fusion reactor applications. Therefore, tritium solubility and diffusivity in the oxide materials is a significant issue. Rare-earth oxides are also candidate materials of such a tritium permeation barrier. They have rare-earth C structure, in which lattice constants decrease with atomic number. The relationship between the lattice constants and hydrogen solubility is considered to be interesting, but have not been studied well. In the present study, hydrogen dissolution behavior in rare-earth oxides were examined by using high concentration tritium gas and imaging plate (IP). Specimens were prepared with conventional powder metallurgy: powders Y_2O_3 , Gd_2O_3 , Er_2O_3 and Yb_2O_3 of were pressed separately into discs and fired in air at 1650°C for 20 h. The densities of the prepared specimens exceeded 95% of the theoretical densities. After heating at 873K for 1h in vacuum, the specimens were exposed to 133Pa of a tritium-deuterium gas mixture at 873 K for 5h, and then quenched down to room temperature. The disc specimens were then cut into halves, and the cross sections were exposed to IP. Then the resultant tritium activity was converted to the dissolved hydrogen amount. The tritium distributions in cross sections of the specimens, except for Gd_2O_3 , was non-uniform representing a diffusion profile of tritium penetrating from surface. On the other hand, the distribution in Gd_2O_3 was uniform suggesting an equilibrating one, and its value was higher than the others, reaching to $10^{17}\text{H}/\text{cm}^3$. This result showed the clear relationship between lattice constants of the rare-earth oxides and tritium dissolution behavior. More detailed comparison on the tritium behavior will be discussed in the paper.

Keywords: Rare-earth oxides, Tritium gas exposure, Hydrogen Dissolution, Hydrogen Diffusion.**MS-05: Multiferroic orders in Co-doped SrTiO_3** **A. K. M. Sarwar Hossain Faysal¹, Shahran Ahmed¹, M. N. I. Khan², M. A. Basith³, Muhammad Shahriar Bashar⁴, H. N. Das², S. I. Liba², Tarique Hasan¹ and Imtiaz Ahmed¹**¹Department of Electrical and Electronic Engineering, University of Dhaka, Bangladesh²Materials Science Division, Atomic Energy Center, Dhaka – 1000, Bangladesh³Nanotechnology Research Laboratory, Department of Physics, Bangladesh University of Engineering and Technology, Dhaka – 1000, Bangladesh⁴Institute of Fuel Research and Development, Bangladesh Council of Scientific and Industrial Research, Dhaka – 1205, BangladeshE-mail: ni_khan77@yahoo.com, mtiaz@du.ac.bd

Strontium titanate SrTiO_3 (STO), Zr doped $\text{Sr}_{1-x}\text{Zr}_x\text{TiO}_3$ and (Zr, Ni) co-doped $\text{Sr}_{1-x}\text{Zr}_x\text{Ti}_{1-y}\text{Ni}_y\text{O}_3$ samples have been synthesized using solid state reaction techniques. We confirmed the cubic Pm-3m phase in our synthesized samples using Rietveld refinement of the powder X-ray diffraction pattern. The chemical species of the samples were identified using energy dispersive X-ray spectroscopy. The grain size of the synthesized materials was reduced significantly due to Zr doping as well as (Zr, Ni) co-doping in STO. We observed forbidden first order Raman scattering at 148, 547 and 797 cm^{-1} which may indicate nominal loss of inversion symmetry in cubic STO. The absence of absorption at 500 cm^{-1} and within $600 - 700\text{ cm}^{-1}$ band in the Fourier Transform Infrared spectra corroborates Zr and Ni as substitutional dopants

in our samples. Due to 4% Zr doping in $\text{Sr}_{0.96}\text{Zr}_{0.04}\text{TiO}_3$ sample dielectric constant, remnant electric polarization, remnant magnetization and coercivity were increased. Notably, in the 4% Zr and 10% Ni codoping, we have clearly observed the existence of both FE and FM hysteresis loops in the $\text{Sr}_{0.96}\text{Zr}_{0.04}\text{Ti}_{0.90}\text{Ni}_{0.10}\text{O}_3$ sample. In this co-doped sample, the remnant magnetization and coercivity were increased by ~ 1 and ~ 2 orders of magnitude respectively as compared to those of undoped STO. The coexistence of both FE and FM orders in (Zr, Ni) co-doped STO might have the potential for interesting multiferroic applications.

MS-06: Complex permeability and dielectric property of Li-Cu-Mg-Zn ferrites

**M. Atikul Islam¹, M. Samir Ullah^{2*}, Sm. Rubayatul Islam², M. A. Islam², F. A. Khan²,
Faruque Ahammed², F. Afrose Sonia¹ and M. Mizanur Rahman¹**

¹Department of Physics, University of Dhaka, Dhaka-1000

²Department of Physics, Bangladesh University of Engineering and Technology, Dhaka-1000

* Email: samirullah@phy.buet.ac.bd

The effects of Zn^{2+} substitution on the structural and magnetic properties of Li-Cu-Mg ferrites are studied. The samples were prepared by solid state reaction method and sintered at 1050°C . The crystal structure of all the samples was investigated by the X-ray diffraction (XRD) technique and it was found to be cubic spinel structure. The lattice parameter was calculated from XRD data and it increases with increasing of Zn content which could be attributed to the difference in ionic radii. The microstructural study reveals that the grain growths of Li-Cu-Mg ferrites are strongly depended on the Zn contents. The complex magnetic permeability of the prepared samples was investigated to obtain the initial magnetic permeability (μ'_i) and relative quality factor (RQF) using an impedance analyzer. It is observed that the enhancement of μ'_i is clearly evidenced on the Zn contents. The increase of μ'_i can be attributed to the densification of the samples and promote of grain growth. The resonant frequency shifts toward the lower frequency with Zn contents, which is expected according to Snoek's relation. Frequency dependent dielectric constant, ac conductivity and complex impedance spectroscopy of Li-Mg-Cu-Zn ferrites have been investigated at room temperature. The dielectric properties of the samples follow the Maxwell-Wagner type of polarization model. Ac conductivity measurement shows a sharp increase of conductivity at higher frequency region which could be attributed to the enhancement of the electron hopping between Fe^{2+} and Fe^{3+} ions at the octahedral site of the spinel lattice.

Session-III: Medical Physics

IT-III: Filling a void in the century old cable theory of neural conduction

K Siddique-e Rabbani

Retired Professor and founding Chairperson, Department of Biomedical Physics & Technology,
University of Dhaka

Email: rabbani@du.ac.bd

Nerve fibres in our body conduct sequential electrical pulses, called action potentials that represent messages to convey some physical condition, at speeds between a few metres/sec to almost a hundred metres/second. The slower nerve fibres are simply like tubes of diameter of the order of a few micrometres with electrically conducting fluids both inside and outside. The tube wall is a thin semipermeable insulating membrane, about 10nm thick, which normally remains electrically charged. A sudden localised change in this charge distribution creates an action potential, which through a complex

ionic process creates small localised current loops that physically transfer the action potential to a neighbouring region. The process keeps on repeating contributing to neural conduction along the fibre. The cable theory for neural conduction uses a model of the nerve fibre (also called axons), in terms of a few potential sources and a system of resistances (R) and capacitances (C). The time constant RC dictates the speed of conduction, the less the RC, greater is the conduction speed. Here the internal axonal resistance dominates this value of R and therefore, the only means of speeding up the signal conduction is through increasing the diameter of the fibre which reduces the axonal resistance. However, this is not practical for higher speeds as this would require a huge volume for the thousands and thousands of nerve fibres, required to carry the body signals. Instead, nature had an ingenious solution through covering small contiguous segments (of the order of a mm each) of the nerve fibre by thick fatty layers called 'myelin' with gaps in between, called 'nodes'. Here current loops can form between adjacent nodes only and the action potential 'jumps' from node to node, speeding up the conduction velocity by about ten times for a nerve fibre of the same diameter. The myelinated nerves have diameters of a few micrometres to about 20 micrometres, for the fastest.

The cable theory for neural conduction came around in the 1920s and evolved gradually to a matured state covering both unmyelinated and myelinated fibres. However, the present author found a void in the cable theory for myelinated fibres which no one thought of before. This void was revealed through some his original experimental findings. In these experiments his group studied the effect of sideways bending of the head on a new nerve conduction parameter called 'Distribution of F-Latency (DFL)', since such manoeuvre stretches and relaxes nerve trunks in the neck region. DFL was found to change instantaneously in a systematic way. DFL was introduced earlier by the present author and was used successfully by his group to detect cervical spondylotic neuropathy (radiculopathy/myelopathy, due to entrapment of nerve fibres at the vertebral region) at early stages. However, the observation of immediate change in conduction velocity due to head bending was criticised by expert reviewers arguing that there are no known mechanisms that explain such immediate changes in nerve conduction. This then led to a thorough search of literature by the author which came out with at least two investigations on direct measurements of Ulnar nerve conduction velocity (NCV) at the elbow due to systematic bending (flexion) of the hand to different angles. These studies were carried out on more than a hundred subjects and the results were consistent, which showed that with more bending the NCV increased instantaneously and reverted back to previous value on straightening the hand. In fact such bending resulted in different degrees of stretching of the Ulnar nerve reducing its diameter which was also supported by experimental findings by other investigators. Apparently, a decrease in the axonal diameter would increase the axonal resistance and consequently the existing cable theory would predict a decrease in NCV, contrary to the experimental findings. So this was a great anomaly. However, all these investigators were interested in the clinical aspects only and did not make any attempt to explain these findings. On the other hand, these findings somehow missed the attention of neuroscientists.

In order to address this anomaly, the author made a thorough search of published electron micrographs of myelinated nerves, particularly of the physical configuration of the structures at the nodes between two myelinated regions and came up with a plausible explanation of the experimental anomaly mentioned above. The myelin sheaths from two sides of a node did not leave a large gap which the existing cable theory assumed, rather these were interdigitated structures overlapping each other in 3 dimension around a nerve fibre. These caused an obstruction to ionic current flow between the immediate outside of the nerve axon and the extracellular fluid outside the myelin sheaths. The author argued that this resistance between the myelin sheaths at the node is the dominant one contributing to the time constant mentioned above which decreased significantly on stretching of the nerve, thus increasing the NCV, as observed. Thus he introduced this new resistance to the cable theory for the first time which would cover all the

previous experimental observations for myelinated nerve fibres, both for relaxed and stretched conditions. Since the axonal resistance loses its dominance, all the electrical elements of the cable theory has to be assessed anew and this would bring a big change to the fundamental aspects of this branch of neuroscience.

MP-01: effects of electroporation on membrane electro-behavior in the cell like giant vesicles

Md. Kabir Ahamed and Mohammad Abu Sayem Karal

Department of Physics, Bangladesh University of Engineering and Technology, Dhaka-1000, Bangladesh

Email: fbkabar@gmail.com

Electroporation attracts much attention to the researchers because this technique is used to investigate the rupture, deformation, and fusion of cells or vesicles by short, high-frequency electric pulses, and has been used in the past for destroying cell, tissue ablation, and treatment for certain diseases. It is also considered a promising tool as a model of biological cell and for delivering the drug to specific body organs. As a mimic of biomembranes of cells, lipid membranes of giant unilamellar vesicles (GUVs), with diameters equal or greater than 10 μm is synthesized by the natural swelling method. When external forces are applied to GUVs, lateral tension is induced in lipid membranes, causing stretching. Therefore, the tension reaches a critical magnitude, pore formation occurs, causing the rupture of cell membranes. Otherwise, deformation or electrofusion may be occurred. In this report, we developed the microcontroller-based electroporation technique for the study of membrane's response. Then membrane behaviors are investigated using an inverted phase constant fluorescence microscope. To obtain the rate constant of pore formation in GUVs induced by constant electric tension (due to electric field), the pulsed electric field of range 340-560 V/cm is applied on the targeted GUVs. All the membranes electro-behavior of GUVs can be explained based on the theoretical approach. These investigations provided valuable information that will help to elucidate the mechanism of electrically-induced pore formation, deformation and membranes fusion in the vesicles and cells in biological entities.

MP-02: Extraction of 3D ^{13}N distribution in inhomogeneous phantom by Spectral Analysis Technique for proton therapy verification

M. Rafiqul Islam^{1,2}, Masayasu Miyake¹, Mahabubur Rahman³, Shigeki Ito⁴, Shinichi Gotoh⁵, Taiga Yamaya⁶, Hiroshi Watabe¹

¹ Graduate School of Biomedical Engineering, Tohoku University, Sendai 980-8578, Japan.

² Institute of Nuclear Medical Physics, AERE, Bangladesh Atomic Energy Commission, Dhaka-1349, Bangladesh.

³ Nuclear Safety Security Safeguard Division, Bangladesh Atomic Energy Regulatory Authority, Dhaka-1207, Bangladesh.

⁴ Mrai Imaging Inc., Japan.

⁵ GO Proton Japan Inc., Japan

⁶ National Institute for Quantum and Radiological Science and Technology, Japan

Proton therapy is a recently developed state-of-the-art radiation therapy technique. It has the advantage of delivering a minimum dose to normal organs, while delivering a large dose to cancer cells, using a physical property known as the Bragg peak of the proton. This Bragg peak must be within the tumor to achieve higher accuracy and some method is necessary to verify it. However, there is a well-known inaccuracy regarding dose computation in heterogeneous media. The purpose of this study is to find the ^{13}N peaks near the Bragg peak position in the inhomogeneous medium that can be used for 3D PEM-based verification of proton therapy. PEM (Positron emission mammography) is a dedicated PET system for detecting breast cancer. In this simulation study, we applied the Spectral Analysis (SA) approach to extract the ^{13}N distribution at the voxel level in the inhomogeneous phantom. Actually, this is an

extension of our previous study where we applied the SA approach in the homogeneous medium for both simulations and experimental data (PEMGRAPH data) and found promising results. Simulations were performed with the PHITS version 3.22 Monte Carlo code. An 80 MeV mono-energetic (pristine) proton pencil beam and energy modulated SOBP (Spread-out Bragg peak) were used for irradiating the inhomogeneous target consisting of PMMA ($\rho = 1.18 \text{ g cm}^{-3}$), lung equivalent ($\rho = 0.26 \text{ g cm}^{-3}$), water ($\rho = 1.0 \text{ g cm}^{-3}$), and bone equivalent ($\rho = 1.85 \text{ g cm}^{-3}$) tissues labs that arranged to form interferences position perpendicular to the beam direction. The deposited energy and the positron-emitting nuclei were recorded as per proton. The simulation production data was converted into activity and made 1 minute dynamic frames for 30 minutes. Time-activity curves (TACs) were calculated of the 30-minute dynamic data. The SA approach was applied to the time-activity curves (TACs) and generated 3D SA images for both cases of pristine and SOBP of simulations are shown in Fig.1. The SA results showed the highest contribution of materials dependent ^{13}N radionuclide in the Bragg region, concurrent with our previous simulation and experimental results. From these qualitative results, we conclude that the SA approach could be a useful tool for PEM-based range verification of proton therapy.

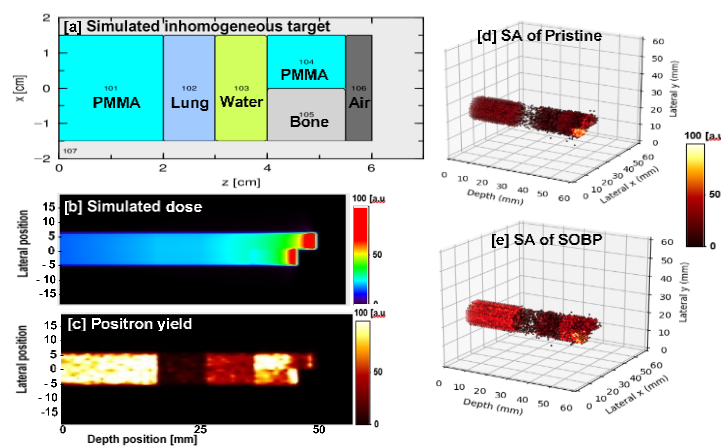


Fig. 1 (a) Simulated inhomogeneous phantom, (b)-(c) simulated dose and positron activity distribution for 80 MeV (pristine) proton beam in the inhomogeneous phantom, and (d)-(e) 3D illustration of Spectral Analysis results based on 30 min data sets for pristine and SOBP, respectively.

MP-03: Investigation of Molecular Transport Through a Peptide induced nanopore and its Size Effects in the Membrane of Giant Unilamellar Vesicle using COMSOL

¹**T. Rahman**, ¹M. S. Ishtiaque, ¹M. I. Hossain, ²M.A.S. Karal, and ^{*1}Md. K. Alam

¹Department of Physics, University of Barishal, Barishal-8200, Bangladesh.

²Department of Physics, Bangladesh University of Engineering and Technology, Bangladesh.

E-mail: khorshed_du@yahoo.com

Many biomedical applications such as gene transfection into cells, cancer chemotherapy, introduction of foreign proteins into cells, cell killing for sterilization and transdermal drug delivery can be possible if the molecules can transport through the nanopore in cell membrane with a controllable manner [1]. Antimicrobial peptides (AMPs) which are produced by various organisms such as amphibians, insects, plants and mammals, have activities that subdue bacteria and/or fungi. Among different AMPs, magainin 2, which was first isolated from the African clawed frog *Xenopus laevis*, has been extensively investigated [2]. Experimental studies reported that magainin interacts directly with the lipid bilayer rather than with a specific protein target within the cell membrane [3]. As a mimic of bio membranes of cells, lipid membranes of giant unilamellar vesicles (GUVs) with diameters 10 μm or more were used to investigate the pore formation induced by various membrane-active agents such as antimicrobial peptides that is magainin-2 [4]. To reveal the mechanism of pore formation clearly it is important to investigate the

kinetics of molecular transport through a single nanopore in the membranes of GUVs. Recently, simulation work has been performed to explore molecular transport into vesicles through a single nanopore in GUVs using COMSOL simulation [1,5] but still, many issues remained to be clarified like; for multipore and pore size in the membrane etc.

In this study, we investigated the molecular transport/leakage rate into the GUVs through nanopore and its size effect to unveil the kinetics molecular transport through nanopores in the membranes of GUVs. We have considered here for different fluorescent probes (Calcein, AFSBTI, FITC-BSA, TRD-3k, TRD-10k and TRD-40k) and artificially designed pore in membrane. Our simulation results $K_{\text{leak}}(\text{s}^{-1})$ has the good consistency with experimental results.

References:

1. V. Jayasooriya, D. Nawarathna, *13th COMSOL conference, Boston* (2017).
2. Y. Tamba, M. Yamazaki, *J PhysChem B*. 113:4846–4852 (2009).
3. Steve J. Ludtke, Ke He, William T. Heller, Thad A. Harroun, Lin Yang, and Huey W. Huang, *Biochemistry*, 35, 13723-13728(1996).
4. M.A.S. Karal, J.M. Alam, T. Takahashi et al. *Langmuir*.31:3391– 3401 ((2015)
5. M.A.S. Karal, M. K. Islam, Z.B. Mahbub, *EurBiophy J*. 49:59-69 (2020)

MP-04: The Molecular Interactions of Inhibitors with Glucose Transporter and Glutaminase: in Silico Approach

Suhrid Saha Pranta and Md Enamul Hoque*

Department of Physics, Shahjalal University of Science and Technology, Sylhet-3114, Bangladesh.

Email: mjonyh-phy@sust.edu

Excessive nutrient absorption is one of the fundamental characteristics of cancer cells. They can acquire energy and produce biosynthetic precursors by glucose and glutamine metabolism. By blocking these two metabolic pathways synergistically by introducing inhibitors, it is possible to starve the cancer cells to death. In this work, we have adopted the novel drug candidate Glutor for Glucose transporter and the CB-839 for Glutaminase as potential inhibitors for blocking those pathways. To observe their interactions, stability and their corresponding binding energy in the potential active sites, we have applied the docking, molecular dynamics, and free energy calculation for the Glutor with Glut-1, Glut-3 protein, and for CB-839 with Glutaminase enzyme. The studies of Glutor and CB-839 indicate that they can be potential drug candidates to treat cancer effectively.

Keywords: Molecular Dynamics, Free Energy Calculation, Docking, Cancer, Glutor, CB-839

MP-05: Effects of Cholesterol on the Anionic Magnetite Nanoparticles-Induced Deformation and Poration of Giant Lipid Vesicles

Salma Akter, Sharif Hasan, and Mohammad Abu Sayem Karal

Department of Physics, Bangladesh University of Engineering and Technology, Dhaka-1000, Bangladesh

Email: shammi1663973@gmail.com

The emission of nanoparticles (NPs) in the environment from various sources is one of the main causes for substantial mortality and morbidity in cardiorespiratory diseases. Medical implants, magnetic resonance imaging contrast agents, pesticides, food products processing are some sources of NPs entered the human body. Hence, the study of the interaction of NPs with cells is important for developing new medical and pharmacological technologies. In this study, we investigated the effects of cholesterol on the anionic magnetite NPs-induced deformation and poration of giant unilamellar vesicles (GUVs). The membrane of vesicles was prepared by a mixture of lipids and cholesterol using the natural swelling

method for obtaining more biological relevance. The fraction of deformed GUVs increased with time while the fraction of poration at first increased and then remained constant. Both the fractions decreased with cholesterol. The thin-walled closed shell model and bilayer coupling model explained the deformation of vesicles. The increased line tension of membranes due to cholesterol was one of the important causes for decreasing the poration.

MP-06: A New purification technique to obtain specific size distribution of giant lipid vesicles using dual filtration

Tawfika Nasrin and Mohammad Abu Sayem Karal

Department of Physics, Bangladesh University of Engineering and Technology, Dhaka-1000, Bangladesh

Email: tawfikatuli@gmail.com

A new purification technique is developed for obtaining distribution of giant unilamellar vesicles (GUVs) within a specific range of sizes using dual filtration. The GUVs were prepared using well known natural swelling method. For filtration, different combinations of polycarbonate membranes were implemented in filter holders. In our experiment, the combinations of membranes were selected with corresponding pore sizes – (i) 12 and 10 μm , (ii) 12 and 8 μm , and (iii) 10 and 8 μm . By these filtration arrangements, obtained GUVs size distribution were in the ranges of 6–26 μm , 5–38 μm and 5–30 μm , respectively. In comparison, the size distribution range was much higher for single filtration technique, for example, 6–59 μm GUVs found for a membrane with 12 μm pores. Using this technique, the water-soluble fluorescent probe, calcein, can be removed from the suspension of GUVs successfully. The size distributions were analyzed with lognormal distribution. The skewness became smaller (narrow size distribution) when a dual filtration was used instead of single filtration. The mode of the size distribution obtained in dual filtration was also smaller to that of single filtration. By continuing this process of purification for a second time, the GUVs size distribution became even narrower. After using an extra filtration with dual filtration, two different size distributions of GUVs were obtained at a time. This experimental observation suggests that different size specific distributions of GUVs can be obtained easily, even if GUVs are prepared by different other methods.

Session-IV: Reactor and Nuclear Physics

IT-IV: VVER 1200 safety- protection against station blackout

S. I. Bhuiyan

Former Professor, Department of Nuclear Engineering, King Abdulaziz University, Jeddah. KSA.

Former chairman, BAEC, Dhaka, Bangladesh

The term “station blackout” refers to the complete loss of alternating current (AC) electrical power to the essential and nonessential switchgear buses in a nuclear power plant. Failure of to restore alternate power within the station blackout cooping period results in loss of all instrumentation and control and consequential core damage. There is no Heat Rejection System from the Primary System Circuit, the Reactor gets Hotter and Hotter, the fuel began to melt down; You have a Big Accident. That’s the traditional system of Generation II NPPs. The Fukushima accident happened due to the failure of the auxiliary power supply. The key safety advantage of the latest generation VVER-1200 unit constructed by Rosatom is its capability to maintain safety without operator intervention in the case of station blackout and prevent fuel damage for at least 24 hours the on-site power generators concurrent with the loss of offsite power results in loss of all alternate current power sources. This event is known as station blackout. Failure in the event of blackout compounded by LOCA. In VVER a Passive System for heat Rejection (

Russian Acronym 'SPOT') can reject heat in this worst case of scenario. The Design aimed to minimize Human Factor. If Power of the Overall Unit is lost there will be a Natural Circulation in the primary Circuit that rejects heat in the secondary circuit. (Passive Heat Removal System Heat Exchangers). In the System Generators steam is generated and supplied to the SPOT. The System is activated by itself when the pressure is too high in the secondary circuit or 'STATION BLACKOUT' for more than 20 seconds. The steam is rising to the Air-heat exchangers and condensate the steam by air to water, the water falls back to the Steam Generator, and again can reject heat in a closed cycle. There is no loss of Feed Water. The System is capable to maintain safety without operator intervention virtually indefinitely in the case of Station Blackout and to prevent fuel damage for at least 24 hours in the event of blackout compounded by LOCA. The Long 'grace period' (72 hours) allows active intervention with mobile Power Units.

The reactor main cooling pump (RCP) is of GCNA-1391 type. The RCP is equipped with a flywheel providing smooth main coolant circulation rundown during accident scenarios with loss of power. This permits adequate cooling until the reactor is shut down and decay heat has dropped to level where it can be safely removed by natural circulation. The cooling of pump motor and lubrication of all bearing is provided by water. Oil free cooling and lubrication eliminates the risk of oil fire inside the reactor Containment Building. This eliminates the pump as a possible cause of a Reactor LOCA in the event long time loss of all electrical power. Emergency Core Cooling System (ECCS) and Passive Core Flooding System- maintains the coolant level required for the reactor cooling to prevent core damage. The System is made up of Hydraulic Accumulators that can independently ensure core cooling for 24 hours in the case of a leakage of any size. The Primary Accumulators start feeding Boric Acid solution to the core if the pressure drops below 5.9 Mpa. Secondary Accumulators provide long term maintenance (at least 24 hours), of the Primary Coolant Level required for reliable heat removal from the core. These Accumulators start feeding Boric Acid solution to the core if the primary pressure drops below 1.5 Mpa. Tusheva et al. (2014) have studied the effect of the operator's controlling actions on the heat removal from the core of the VVER-1000 reactor by depressurization of the primary and secondary circuits and injection of a coolant using passive systems.

Emergency heat removal through secondary circuit is not time-limited both in active and passive operation modes. Long (at least 72 hours) unmanned prevention of fuel damage beyond the limits set for design accident during station black out. This is How Post-Fukushima Nuclear Plant works, in such a worst event like the Fukushima –Daichi NPP has experienced.

The author assumes Spot Technology Pumps uses the Power of Fisonic Nozzle. Russia has used these pumps for over 50 years. It drives submarine safety cooling systems, side thrusters, and 200 Knt Torpedo's since 1970's; 400 Knt torpedo's since 1990's and the world's fastest (100 Knot) deepest diving (1Km) Nuclear powered military Sub. The Technology was invented in the late 1770's in France by lazy monks to get water without much manual labor. It used to be used in UK steam locomotives to supply boiler water in the late 1800's. This pump operating with NO Electricity- NO moving parts. That's some sort of ejector pump, it uses high pressure steam to derive liquid with its velocity, It was used since steam locomotive age, to push smoke out of the smoke stack by means of a steam jet to grab air throughout the Fire box. Now imagine if Every nuclear reactor feed and condensate, and cooling water pump were replaced with these- No loss of electricity would affect plant operation, except grid load tripping off the turbine-generator, but not the cooling. All power reactors designed with passive core cooling the SG are physically located higher than the reactor. Reactors trips, RCPS shut off - Control Rods are inserted stopping the fission reactions, and any decay heat is sent up (heat rises) to the SGs and there is a steam powered auxiliary feed pump assuming there is a loss of electrical power and the motor driven auxiliary feed pumps can't start. Think of a water wheel on one side that will take about the lowest quantity stream you can imagine turning a pump that injects water into the SGs Steam generator (SG) secondary-side depressurization through the SG valve(s) is one of major AM measures to cool and depressurize the primary system via natural circulation (NC) because of steam condensation in the SG U-tubes especially when high-pressure injection system of emergency core cooling system (ECCS) is totally failed during accidents and transients in a pressurized water reactor. The variability of estimated station blackout likelihood is potentially large, ranging from approximately 10^{-3} to 10^{-5} per reactor-year. A "typical" estimated frequency is on the order of 10^{-5} per reactor-year. The implications of station blackout on several other safety issues were reviewed for significance. These include: loss-of-coolant-accident initiators; anticipated transients without scra. A program should be set up to further evaluate the risks.

All modern reactor designs have some form of passive cooling built-in in the design. Most reactors are 40+ years old, so don't have passive cooling. There are many existing reactors yet that could be back fit to give existing reactors passive long term, non-electrical cooling capacity by using the technology as mentioned. Grid stability and security, and the ability to restore power to a nuclear plant site with a grid blackout is of serious concern.

RNP-01: Assessment of dose distribution of radioxenon due to a postulated accident of TRIGA research reactor in Bangladesh

M. AjijulHoq, Md. Abu Khaer, Mohammed Tareque Chowdhury, M. Mizanur Rahman

Institute of Energy Science, Bangladesh Atomic Energy Commission, Dhaka, Bangladesh.

Assessment of dose distribution due to radioactive release or atmospheric dispersion during accidental conditions is essential for ensuring the safe operations of nuclear reactors. During normal operation mode, nuclear research reactors do not release any significant amount of radioactive material to the environment. But a considerable portion of the radionuclide inventory in the core may be released to the environment under accidental conditions with severe core damage. However, direct radiation exposure of the public may happen due to the release of radionuclides through the stack. In this work, assessment of radiological dose due to the deposition of ^{131m}Xe , ^{133m}Xe , ^{133}Xe , ^{135m}Xe , ^{135}Xe , and ^{138}Xe on ground and immersion considering a hypothetical accident of TRIGA Mark-II research reactor at AERE, Bangladesh has been made. Radiological doses have been investigated in different directions using the Gaussian Diffusion Model (GDM). Meteorological parameters like average wind speed, frequency, etc. in different directions around the TRIGA reactor site have also been evaluated. The maximum dose due to ^{131m}Xe , ^{133m}Xe , ^{133}Xe , ^{135m}Xe , ^{135}Xe , ^{138}Xe and the total ($^{131m}\text{Xe} + ^{133m}\text{Xe} + ^{133}\text{Xe} + ^{135m}\text{Xe} + ^{135}\text{Xe} + ^{138}\text{Xe}$) were found within the range $3.03\text{E-}7$ – $1.23\text{E-}4$ $\mu\text{Sv/hr}$, $1.01\text{E-}5$ – $4.09\text{E-}3$ $\mu\text{Sv/hr}$, 0.0003 – 0.14 $\mu\text{Sv/hr}$, $2.29\text{E-}5$ – $9.26\text{E-}3$ $\mu\text{Sv/hr}$, 0.002 – 1.111 $\mu\text{Sv/hr}$, $1.11\text{E-}5$ – $4.55\text{E-}3$ $\mu\text{Sv/hr}$, and 0.003 – 1.269 $\mu\text{Sv/hr}$, respectively for all the dominant directions. The contribution of dose from immersion due to ^{135}Xe is dominant (87.55%). The extracted result can be used to establish the radiological protective measures in and around the reactor site.

RNP-02: Intranuclear cascade model for deuteron-induced reactions over a wide range of targets

M. J. Kobra^{1*}, Y. Uozumi²

¹Department of Physics, Rajshahi University, Rajshah - 6205, Bangladesh

²Department of Applied Quantum Physics and Nuclear Engineering, Kysushu University, Fukuoka, Japan

*Email: mjkobra@gmail.com

In our previous work, an intranuclear cascade model was expanded successfully for cluster-induced nuclear reactions incorporating breakup reactions and trajectory deflections (M.J. Kobra *et al.*, JNST **55** 209-216 (2018)). However, the validity was confirmed only for ^{27}Al . In the present work, we widen the applicable range of masses of the target nucleus at incident energies 20-100 MeV. First the ground state of projectile and target and determined. Then we search for the optimal parameters: deuteron nuclear potential and maximum impact parameter. The breakup of loosely bound projectiles and trajectory deflection of projectiles or their fragments at initial or final interaction with the target is considered. The calculations are executed to verify the extended code followed by an evaporation model for double-differential cross-sections of $(d, d'x)$, (d, px) and (d, nx) reactions over a wide range of targets. The calculation results show good agreement with the experimental spectra for various targets at different incident energies.

Keywords: Deuteron-induced reactions, projectile breakup, trajectory deflection, intra-nuclear cascade model, double-differential cross-sections.

RNP-03: Experimental Cross Section Measurements for Nuclear Reactor Technology: $^{55}\text{Mn}(n,\gamma)^{56}\text{Mn}$ reaction at two new thermal energies

Md. Mustafa Zaved^{1,2}, Mohammad Amirul Islam^{1,2*}

¹Institute of Nuclear Science and Technology, Atomic Energy Research Establishment, Ganakbari, Ashulia, Dhaka-1349, Bangladesh

²Department of Nuclear Science & Engineering, Military Institute of Science and Technology, Dhaka 1216, Bangladesh

*Email: liton80m@yahoo.com

The investigations of neutron-induced reaction cross sections are very important in the fundamental research in Nuclear & Reactor Physics and Engineering as well as practical applications in dosimetry, radiation safety and developing evaluated nuclear data libraries. In nuclear science, the reaction $^{55}\text{Mn}(n,\gamma)^{56}\text{Mn}$ is used as a neutron flux monitor. Moreover, Mn as a target for (n, γ) reaction is of great interest in neutron transport calculations of nuclear structural material such as nuclear grade stainless steel 304L and 316L which contain 2% of manganese. In this study, thermal neutron capture cross sections of $^{55}\text{Mn}(n,\gamma)^{56}\text{Mn}$ reaction were measured for the first time at 0.0334 eV and 0.0536 eV energies by using a monochromatic neutron beam from TRIGA MARK-II research reactor. Neutron fluxes during the experiments were measured by using $^{197}\text{Au}(n,\gamma)^{198}\text{Au}$ monitor reaction. After considering all the correction factors such as neutron self-shielding and gamma-ray attenuation effects, the cross sections obtained at 0.0334 eV and 0.0536 eV are 11.07 ± 0.64 b and 9.03 ± 0.52 b, respectively. Our experimental data at 0.0334 eV and 0.0536 eV are 4.3% and 1.0% lower than the theoretical evaluated data of ENDF/B-VIII.0 and JENDL-4.0 data libraries, respectively. By following $1/v$ dependence in the thermal energy region, the resultant cross section values extrapolated to the average thermal neutron energy 0.0253 eV were calculated and compared with reported literature values. Our experimental data for this reaction would be helpful to ensure the reliability of the cross-sectional data evaluated by $1/v$ relation in the nuclear data libraries.

Keywords: Neutrons of 0.0334 eV and 0.0536 eV; TRIGA MARK II reactor; Neutron capture cross section; Gamma-ray attenuation; Manganese target; Neutron activation analysis.

Session-V: Nanomaterials

NM-01: Fast magnetization reversal of a magnetic nanoparticle driven by a chirp microwave field pulse at finite temperature

M.T. Islam^{1*}, M. A. J. Pikul¹, M. A. S. Akanda¹, and X. S. Wang²

¹Physics Discipline, Khulna University, Khulna 9208, Bangladesh.

²School of Physics and Electronics, Hunan University, Changsha 410082, China

*Email: torikul@phy.ku.ac.bd

We investigate, at room temperature, the magnetization reversal of a single-domain magnetic nanoparticle driven by a linear down-chirp microwave magnetic field pulse (DCMWP). The findings based on the Schostacastic Landau-Lifshitz-Gilbert equation reveal that a down-chirp microwave pulse is solely capable of inducing fast magnetization reversal. With a certain range of initial frequency and chirp rate, the required field amplitude is much smaller than that of a constant-frequency microwave field. The fast reversal is because the down-chirp microwave field pulse triggers stimulated microwave absorptions (emissions) by (from) the spin before (after) it crosses over the energy barrier. It is also found that any one of the three controlling parameters of a DCMWP, i.e. the amplitude, chirp rate, or initial frequency, decreases with increasing temperature while the other two are fixed. The maximal temperature

at which the reversal can happen increases with enlarging the system size. These phenomena are related to the facts that the energy barrier induced by anisotropy increases with the system volume, and the effective magnetization decreases with temperature. Our findings provide a way to realize low-cost and fast magnetization reversal.

NM-02: Tunable Exchange bias in $\text{Nd}_2\text{FeCrO}_6$ double perovskite

Fahmida Sharmin¹, Ferdous Ara², M.D.I Bhuyan¹, Subrata Das¹, TetsuSato³, Tadahiro Komeda² and M.A. Basith¹

¹Nanotechnology Research Laboratory, Department of Physics, Bangladesh University of Engineering and Technology, Dhaka-1205

²Institute of Multidisciplinary Research of Advanced Materials, Tohoku University, 2-1-1, Katahira, Aoba-ku, Sendai 980-0877, Japan

³Department of Chemistry, Graduate School of Science, Tohoku University, 6-3 Aramaki Aza Aoba, Aoba-ku, Sendai, Miyagi 980-8578, Japan

E-mail: soni_bd@yahoo.com

The exploration of exchange bias (EB) on the nanoscale provides a novel approach towards improving the magnetic properties of nanoparticles for prospective applications in magnetic read heads, random-access memories, and other spintronics devices. In this regard, we have synthesized polycrystalline double perovskite oxide $\text{Nd}_2\text{FeCrO}_6$ (NFCO) for the first time using a facile citrate based sol-gel method and systematically investigated its structural and magnetic properties. Rietveld refinement analysis of the powder X-ray diffraction pattern of the synthesized NFCO nanoparticles confirmed their single phase monoclinic structure with $P2_1/n$ space group. Average particle size was estimated to be ~ 72 nm from the field emission scanning electron microscopy images. X-ray photoelectron spectroscopy confirmed the presence of mixed valence states of Fe and Cr. Temperature (M-T) and field (M-H) dependent magnetic data have been recorded in a wide temperature range of 4 to 400 K under 100 Oe, and field range of ± 7 T at different temperatures. The M-T curves exhibited magnetic reversal behavior in this double perovskite at a low temperature of 6 K in the field cooled mode. The M-H hysteresis loops demonstrated the coexistence of weak ferromagnetic and antiferromagnetic domains in NFCO nanoparticles. Interestingly, exchange bias effect was observed in this double perovskite material while the sample was cooled down from 300 K to 10 K i.e., through *Néel* temperature and cooling magnetic fields (H_{cool}) were applied. The exchange bias field values showed an increasing trend as H_{cool} rises at 10 K. We anticipate that the newly synthesized NFCO double perovskite with magnetically tunable exchange bias due to the interaction between the Nd and Fe/Cr sublattices maybe a promising option to be used in innovative multifunctional devices.

NM-03: Structural and magnetic characteristic exploration of trivalent Al^{3+} ions substituted Ni-Zn-Co nano-spinel ferrites

NusratJahan^{a,b,*}, J. I. Khandaker^a, H. N. Das^c and M. N. I. Khan^c

^aDepartment of Physics, Jahangirnagar University, Savar, Dhaka 1342, Bangladesh

^bDepartment of Physics, American International University Bangladesh (AIUB), Dhaka 1229, Bangladesh

^cMaterials Science Division, Atomic Energy Centre, Dhaka 1000, Bangladesh

*Email: nusrat1974@yahoo.co.uk

This study explored the structural, morphological, optical, and magnetic characteristics of $\text{Ni}_{0.4}\text{Zn}_{0.35}\text{Co}_{0.25}\text{Fe}_{2-x}\text{Al}_x\text{O}_4$ ($0 \leq x \leq 0.12$) nano-spinel ferrites. Nanocrystalline cubic structure formation and weight loss percentage determined by thermogravimetric analysis and differential scanning calorimetry (TGA-DSC). Single-phase cubic spinel structures with $Fd3m$ space group of synthesized

samples confirmed by Rietveld refinement X-ray diffraction (XRD) data. The particle sizes were found to be in the range of 6.7 nm - 5.25 nm, and agglomeration occurs inside the ferrite samples. The atomic planes and strong crystallinity identified through SAED images. The characteristic peaks of the Raman spectra identified the bonding between the cations and anions in the sub-lattices. An inverse relationship followed between the particle sizes and bandgap energies with compositions. S-shape hysteresis (*M-H*) loops with low coercivity identified the superparamagnetic natures of the nano samples. Finally, these studies explored the potential applications of these nano samples for biomedical engineering.

NM-04: Comparison of structural and magnetic characteristics of CoNiFe₂O₄@functionalized Cnts nanocomposite synthesized by different routes of hydrothermal process

M. Al-Fahat Hossain^{*a}, M. Al-Mamun^{*b}, M. R. Rahman^a, Sheikh ManjuraHoque^b

^a Physics Discipline, Khulna University, Khulna-9208, Bangladesh.

^b Materials Science Division, Atomic Energy Centre Dhaka, Dhaka, Bangladesh

^{*}Corresponding author- md.afhr@gmail.com and mamunfh@yahoo.com

In this study, multi-walled carbon nanotubes (MWCNT) were prepared by the chemical vapor deposition method and functionalized successfully through a two-step procedure, namely sonication and acid reflux. Functionalized multi-wall carbon nanotubes (FMWCNT) were decorated with crystalline nickel substituted cobalt ferrite nanoparticles (CNF) by the two different routes of hydrothermal method to form CNF@FMWCNT nanocomposite. The nanocomposites with different weight ratios of CNF and FMWCNT were characterized by X-ray diffraction analysis (XRD), thermogravimetric analyzer (TGA), Fourier-transform infrared spectra analyzer (FTIR), Raman spectroscopy, and physical property measurement system (PPMS). The XRD patterns revealed the formation of the cubic phase spinel structure of CNF with the optimized 1:1 weight ratio composite with a crystallite size of 11.55 nm, accordingly the W-H method. XRD also showed the adhesion between ferrite and FMWCNTs in composites. FTIR study confirmed the functionalization of MWCNT and the presence of other functional groups in CNF@FMWCNT nanocomposites. The study of the Raman spectra provided useful information about the quality of MWCNT and its degree of functionalization, and the quality of nanocomposites. TGA study revealed that different nanocomposites were found to have dissimilar thermal stability depending on the different synthesis routes. The magnetic study showed CNF@FMWCNT nanocomposite of 1:1 weight percent composition, produced by in-situ growth method, obtained significant magnetization features among all the samples. Nanocomposites prepared by the in-situ growth method show improved characteristics than the separate addition technique.

NM-05: Investigation of CuCo₂S₄-MoS₂ Nanoparticles as Electrode Material for Supercapacitor

Sajjad Hasan¹, Subrata Das¹, Akter H. Reaz², Chanchal Kumar Roy² & MA Basith¹

¹Nanotechnology Research Laboratory, Department of Physics, Bangladesh University of Engineering and Technology, Dhaka-1000, Bangladesh

² Department of Chemistry, Bangladesh University of Engineering and Technology, Dhaka-1000, Bangladesh

Recently, supercapacitors have attracted considerable attention due to their high-power density, efficient charging-discharging rate, and extended durability compared to conventional batteries and capacitors. Bimetal sulfide such as CuCo₂S₄ has emerged as a potential electrode material for supercapacitors because of its higher theoretical specific capacitance, low cost, and high electrochemical activity, but it suffers from low conductivity and volume expansion during charging-discharging. However, MoS₂ is a prominent candidate that can alleviate these issues because of its excellent active sites and interlayer structure. In this work, we have prepared CuCo₂S₄ and CuCo₂S₄-MoS₂ nanoparticles using a facile hydrothermal method. To compare the physical properties (structural, morphological) and

electrochemical characteristics, these two nanoparticles were systematically investigated. The structural investigation using XRD revealed an improvement in crystallinity, increment in d-spacing and the absence of impurity phase in the $\text{CuCo}_2\text{S}_4\text{-MoS}_2$ in comparison with CuCo_2S_4 . The improvement in surface morphology and incorporation of multilayer MoS_2 with reduced agglomeration was also observed via FESEM. These advances of $\text{CuCo}_2\text{S}_4\text{-MoS}_2$ resulted in a high specific capacitance of 820 Fg^{-1} compared to CuCo_2S_4 (249 Fg^{-1}) in a 0.5 M aqueous Na_2SO_4 electrolyte at a current density of 0.5 Ag^{-1} in a three-electrode system. Furthermore, the $\text{CuCo}_2\text{S}_4\text{-MoS}_2$ exhibited an excellent energy density of 114 Whkg^{-1} at a power density of 250 Wkg^{-1} . Thus, the improved capacitive performance of $\text{CuCo}_2\text{S}_4\text{-MoS}_2$, achieved by enhanced accessible surfaces, reduced stacking of MoS_2 , low aggregation of CuCo_2S_4 , and improved ions transport routes, makes it more desirable as an electrode material for designing high-performance power storage devices.

NM-06: Single crystal growth and anisotropic ionic conductivity of $\text{Li}_{3x}\text{La}_{(2/3-x)}\text{TiO}_3$

Md. Shahajan Ali*, Yuki Maruyama, Masanori Nagao, Satoshi Watauchi, Isao Tanaka

Center for Crystal Science and Technology, University of Yamanashi, 7-32 Miyamae, Kofu, Yamanashi, Japan.

*E-mail: msali@pust.ac.bd

In the case of conventional lithium-ion batteries, fire accidents and explosion occur due to use of flammable organic electrolyte. Solid electrolytes between the electrodes can be used to overcome these problems. $\text{Li}_{3x}\text{La}_{2/3-x}\text{TiO}_3$ is a candidate of solid electrolyte with ionic conductivity more than $10^{-3} \text{ S}\cdot\text{cm}^{-1}$ at room temperature. The single crystal of $\text{Li}_{3x}\text{La}_{2/3-x}\text{TiO}_3$ (LLT) with different Li composition ($x = 0.083 \sim 0.15$) were grown successfully by the traveling solvent floating zone (TSFZ) method. Fig. 1. shows the single crystal of LLT with $x = 0.10$ nominal composition. As this material shows incongruent melting behavior, Li rich and $\text{La}_2\text{Ta}_2\text{O}_7$ -poor solvent were used. Crack- and inclusion-free single crystals were obtained in all compositions. The directions of the grown crystal were $[100]$ to be confirmed by two dimensional XRD analysis. The quantity of lithium in the grown crystals were found to be lower ($x = 0.045 \sim 0.12$) than the nominal composition due to the vaporization in the melt during growth and shows linear behavior. The ionic conductivity of LLT is anisotropic and depends on the Li-composition. The anisotropic ionic conductivity of the annealed crystal was found to be maximum with the composition of $x = 0.059$. The ionic conductivity along $[100]$ direction, $\sigma_{[100]} = 1.75 \times 10^{-3} \text{ S}\cdot\text{cm}^{-1}$ is higher than the $[001]$ directions $\sigma_{[001]} = 7.0 \times 10^{-4} \text{ S}\cdot\text{cm}^{-1}$.

NM-07: Investigation of the Effect of Sm on Magnetic and Magnetodielectric Properties of LaFeO_3 Nanostructures

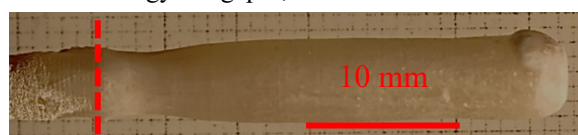
Shovan Kumar Kundu^{ab*}, Dhiraj Kumar Rana^b, Soumen Basu^b

^aDepartment of Physics, Faculty of Science and Technology, American International University-Bangladesh, Dhaka, Bangladesh-1229

^bDepartment of Physics, National Institute of Technology Durgapur, India-713209

*E-mail of Email: shovan1608@gmail.com

Nanotechnology is a topic that spans the area of science and engineering disciplines. It takes place at on a tiny scale range which is larger than the level of atoms and molecules but within the range of 1-100 nanometers. Multiferroic devices possess electric field controlled magnetic orderings which consumes significantly less power than magnetic field controlled, which requires electric currents to generate the



Seeding point → Growth direction

Fig. 1: Single crystal of $\text{Li}_{0.059}\text{La}_{0.57}\text{TiO}_3$ annealed in oxygen at 1000 C for 24 h .

magnetic field. Because of strong magneto-electric coupling, multiferroic materials have a vast area of application in spintronics devices, information storage devices, quantum electromagnets, microelectronics devices, and different types of sensors. Interestingly, it was found that Lanthanum Ferrite (LaFeO_3), a member of the centrosymmetric rare earth ortho-ferrite (RFeO_3) family (having a distorted orthorhombic perovskite structure), possesses magnetically tunable ferroelectricity due to the exchange striction mechanism. XRD patterns, along with Rietveld refinement analysis, were discussed to ensure the phase formation and crystallographic nature. Reduction of particle size and nanocrystallinity nature was studied in TEM analysis. Physics behind electronic states of different atoms was illustrated by XPS analysis. Magnetic (M - H loops and FC-ZFC curves), ferroelectric (P - E loops) and magneto-dielectric properties ensure the multiferroic property in Sm-doped LaFeO_3 system. The enhancement of multiferroic property by virtue of Sm doping is discussed. Positive magneto-dielectric coupling is observed in the samples where coupling increases with doping which states that the Sm doped LaFeO_3 can be good candidate in in magneto-electric industries.

NM-08: Synthesis and characterizations of ZnO nanoparticles and seed layers for subsequent growth of ZnO nanorods by hydrothermal process

N.I. Tanvir^{1,2}, M.S.Hossain¹, N. Khatun¹, Md. Saidul Islam³, S.Islam¹, and S.F.U. Farhad^{1,2*}

¹Energy Conversion and Storage Research Section, Industrial Physics Division, BCSIR Labs, Dhaka 1205, Bangladesh Council of Scientific and Industrial Research (BCSIR), Bangladesh

²Central Analytical and Research Facilities (CARF), Dhaka 1205, Bangladesh Council of Scientific and Industrial Research (BCSIR), Bangladesh

³Institute of Fuel Research Division (IFRD), Bangladesh Council of Scientific and Industrial Research (BCSIR), Bangladesh

*Email e-mail: sf1878@my.bristol.ac.uk; s.f.u.farhad@bcsir.gov.bd

Preferential (0002) oriented ZnO nanorods (NRs) are highly desirable to fabricate optoelectronic devices such as photovoltaic cells, LEDs, (photo)electrochemical sensors etc. ZnO nanoparticles (NPs) assisted seed layer (SL) could improve the alignment of ZnO NRs along the substrate normal. In this study, high energy ball mill (HEBM) facilitated top-down approach was adopted to produce ZnO NPs from ZnO microcrystalline powder with milling durations of 5, 10, 15, 20, and 25 hours. Ball-mill derived (BMD) ZnO NPs were ultra-sonicated with isopropanol alcohol for spin-coating on quartz substrates to produce ZnO seed layers followed by air-annealed at 250°C for 1h. ZnO NRs were then grown by hydrothermal process on pre-deposited ZnO SLs and then heated at temperature of 250°C for 1h in air. The structural and morphological properties of ZnO NPs, SLs, and NRs were carried out by X-ray diffractometers (XRD) and scanning electron microscopy (SEM). SEM micrographs exhibit that ZnO NPs with 25 milling hours produced the most compact and coherent ZnO SLs and induced well-aligned ZnO NRs. XRD analyses revealed a decreasing trend in crystallites size (~30-13 nm) with milling hours which is consistent with the peak broadening from Raman spectroscopy. The optical bandgap of the nanostructured ZnO samples was calculated from UV-VIS-NIR diffuse reflection spectra within the range of 3.23-3.28 eV. The room temperature photoluminescence analyses revealed that ZnO NRs exhibit a sharp near-band-edge luminescence peak at ~380 nm and the ZnO nanorod arrays are notably free from defect-related green-yellow emission peaks.

NM-09: Structural and improved dielectric, electrical and magnetic properties BFO-NiCuCd nano-composites

M. Z. Islam^{*1}, M. Belal Hossen²

¹Department of Physics, Chittagong college, Chattogram, 4203, Bangladesh

² Department of Physics, Chittagong University of Engineering & Technology, Chattogram, 4349, Bangladesh

Email: zahir.phycu@gmail.com

Multiferroics are prominent multifunctional material which bear two or more ferroic orders such as ferromagnetism, ferroelectricity and ferroelasticity simultaneously. The cohesion between ferromagnetism and ferroelectric possesses magnetoelectric (ME) effect. ME effect create enormous interest due to their plenty of application in magnetic field sensors, MeRAM, logic memory devices, read head, resonator and logic memory devices. One of the effective ways to achieve the required ME properties is to introduce the suitable materials with BFO to form the nano-composites. In this investigation, the $\text{Ni}_{0.5}\text{Cu}_{0.02}\text{Cd}_{0.3}\text{La}_{0.03}\text{Fe}_{1.97}\text{O}_4$ (NCCLFO) has been selected as the ferromagnetic phase and BiFeO_3 (BFO) as the ferroelectric phase which were prepared by sol-gel auto combustion technique. This powder were mixed thoroughly by grinding in acetone media for 2–3 h in weight proportions to obtain nano composites $(1-x)\text{BFO}-x\text{NCCLFO}$ ($x = 0.00-0.40$). The XRD analysis confirms the coexistence of orthorhombic perovskite BFO and spinel NMCLFO phases and also reveals that there is no chemical reaction between them. The dielectric constant shows usual dielectric dispersion at lower frequencies due to Maxwell–Wagner type interfacial polarization and reduces with the ferrite content and does not obey the sum rule. The highest value of the loss tangent is decreasing and moves to a lower frequency range to increase the NCCLFO content. The electric modulus increases from zero towards a high frequency and the dispersion shift to the high frequency region as increasing NMCLFO concentration. The imaginary dielectric modulus shows a considerable shift of maximum value towards lower frequency with broadening of peaks with increasing NMCLFO.

Session-VI: Theoretical and Computational Physics-II

IT-VI: Origin of segregation in liquid metallic binary alloys

G. M. BHUIYAN

Department of Theoretical Physics
University of Dhaka, Bangladesh

A complete understanding of the basic mechanisms, from the point of inter ionic interaction, about how and why segregation in some metallic alloys occurs at and under certain thermodynamic state specified by temperature and pressure is far from over although several attempts have been made from the point of experiments and empirical theoretical models. In this talk we intend to address this issue from the point of microscopic theory that includes theory of metals, perturbation approach and the statistical mechanics. The theory of metals we have engaged here deals with the electron-ion and ion-ion interaction through a local pseudo potential model. The perturbative approach handles the procedure how thermodynamic quantities can be calculated effectively. The essential ingredient for this study is the knowledge of liquid structure which is derived by using the statistical mechanics involving the interionic interactions. Thermodynamics of mixing namely the energy of mixing, enthalpy of mixing and entropy of mixing are calculated at different temperatures for $\text{Al}_{1-x}\text{Bi}_x$ binary alloys to dig out the cause of segregation. Finally a finishing touch is paid to the critical behaviours of segregation.

Keywords: Segregation, Thermodynamics of mixing, Electronic theory of metals, Critical temperature and critical concentration, Perturbative approach.

TCP-05: Density functional theory-based investigation of mechanical, electronic, optical and thermal properties of AC ($A = \text{Nb, Ta, Ti}$) binary metallic carbides

Razu Ahmed*, Md. Sohel Rana, Sajidul Islam, Md. Mahamudujjaman, S. H. Naqib

Department of Physics, University of Rajshahi, Rajshahi-6205, Bangladesh

*Email: razuphy135@gmail.com

Binary metallic carbides belong to technologically prominent class of materials. We have explored the mechanical, electronic, optical and some thermal properties of AC ($A = \text{Nb, Ta, Ti}$) binary metallic carbides in details employing density functional theory based first-principles method. Study of elastic constants and moduli shows that AC ($A = \text{Nb, Ta, Ti}$) possess low level of elastic anisotropy, reasonably good machinability, mixed bonding characteristics with ionic and covalent contributions, brittle nature and high Vickers hardness with high Debye temperature. The mechanical stability conditions are fulfilled. The bulk modulus and Young's modulus of TiC are lower than those of NbC and TaC . AC ($A = \text{Nb, Ta, Ti}$) compounds are mostly hard compounds. The electronic band structures with high electronic density of states at the Fermi level reveal metallic character of AC ($A = \text{Nb, Ta, Ti}$) compounds. Unlike notable anisotropy in elastic and mechanical properties, the optical parameters are found to be almost isotropic. The optical absorption, reflectivity spectra, and the static index of refractive of AC ($A = \text{Nb, Ta, Ti}$) show that the compounds hold promise to be used in optoelectronic device sector. Debye temperature, melting temperature and minimum phonon thermal conductivity of the compounds under study are high and show excellent correspondence with the elastic and bonding characteristics. Calculated values of different thermal properties indicate that AC binary metallic carbides have the potential to be used as thermal barrier coating material.

Keywords: Binary carbides; Density functional theory; Elastic properties; Optoelectronic properties; Thermophysical properties

TCP-06: Atomic Transport Properties of Liquid Simple Metals: A Perturbative Approach

Mahir Manna, R.C. Gosh*

Department of Physics, University of Dhaka, Dhaka 1000, Bangladesh

*Email: ratan@du.ac.bd

Self-diffusion coefficient, D , of some liquid simple metals namely Bi, Tl, Sn, Cd, Pb, In, Sb and Zn has been investigated using linear trajectory (LT) and small step (SS) diffusion theories. Friction coefficients originated from the hard, soft and crossed hard-soft parts of the potential are the main ingredients of the applied theories. For interionic interaction in metals, we have chosen Brettonet–Silbert (BS) pseudopotential model. The perturbation approach, Linearized Weeks-Chandler-Andersen (LWCA), has been applied for the liquid structure. We observe that, both theories provide slightly larger values than the available experimental and simulated data. If we compare both of the applied theories to calculate diffusion coefficients, LT comes out better. The probable reason behind may be the contribution coming from the crossed hard-soft forces which is neglected in the SS diffusion theory. If Carnahan-Stirling (CS) approximation is applied to the friction coefficient of the hard part of the potential, both theories provide excellent results for the diffusion coefficients of the concerned systems.

TCP-07: Boron-rich chalcogenide semiconductor materials: Prospects for device applications via DFT study

M. M. Hossain^{1,*}, M. A. Ali¹, M. M. Uddin¹, S. H. Naqib², A. K. M. A. Islam^{2,3}

¹Department of Physics, Chittagong University of Engineering and Technology (CUET), Chattogram-4349, Bangladesh

²Department of Physics, University of Rajshahi, Rajshahi 6205, Bangladesh

³Department of Electrical and Electronic Engineering, International Islamic University Chittagong, Kumira, Chittagong, 4318, Bangladesh

Email: mukter_phy@cuet.ac.bd

Boron rich chalcogenide semiconductor materials are of keen interest due to its extraordinary physical and chemical properties in the development of modern industry to meet emergent technological demands. To disclose the potential optoelectronic and mechanical applications, we have studied structural,

electronic, optical and mechanical properties using density functional theory for the first time. The estimated structural lattice parameters were consistent with the reported experimental constants. The materials are mechanically stable with brittle in nature and elastically anisotropic. Furthermore, the values of fracture toughness and mechanical hardness predict as prominent members of the class of hard compounds. The electronic band profiles confirm the indirect band gap semiconductor. Bulk optical anisotropy, visible light absorption coefficient and very low value of reflectivity spectra ($\sim 10\%$) are noted. Such favorable features give promise to the compounds under investigation to be used in optoelectronic and mechanical equipment applications.

Keywords: Chalcogenides; Mechanical properties; Electronic properties; Optical anisotropy; DFT

TCP-08: Magnetic flux dynamics of high quality YBCO single crystal: insights from field and frequency dependent AC susceptibility measurements

M. Rakibul Hasan Sarkar^{1*} and S. H. Naqib²

¹Department of Physics, Bangladesh Naval Academy, Patenga, Chattogram, Bangladesh

²Department of Physics, University of Rajshahi, Rajshahi-6205, Bangladesh

*Email: mrhs1987@gmail.com

The magnetic field and frequency dependent AC susceptibility (ACS) of a very high-quality YBCO single crystal was studied at different temperatures around the superconducting T_c . Magnetic field (H) was applied both parallel and perpendicular to the CuO_2 planes. It was found that the magnitude of the loss peak was slightly higher in the perpendicular field configuration. The height of the loss peak saturates when full penetration of magnetic field was achieved. Significant shifts in both real (χ') and imaginary (χ'') parts of the ACS to lower temperatures were observed as the applied magnetic field was increased for both perpendicular (HIIc) and parallel (HIIab) field configurations. The magnitudes of peak temperature (T_p) varied differently with different orientations of magnetic fields which illustrated the anisotropy in the magnetic flux dynamics. But T_p was found to be insensitive to frequency. The diamagnetic onset temperature was obtained from ACS signal. The superconducting transition width increased weakly with magnetic field and the rate of increment is relatively more prominent for HIIc case. The Cole-Cole plot [$\chi''(\chi')$] shows qualitatively and quantitatively identical features for both HIIc and HIIab configurations. The general features of $\chi''(\chi')$ implies that, there was no flux creep for the applied range of AC field and frequency. The results obtained here were compared with existing experimental and theoretical results and discussed in this presentation.

Keywords: AC susceptibility; YBCO single crystal; Vortex dynamics; Cole-Cole plot

Session-VII: Environmental Science

IT-VII: Sustainable Management of Water Resources Using Isotope Techniques: Applications and Active Research Areas in Bangladesh

Nasir Ahmed*

Bangladesh Atomic Energy Commission, Dhaka, Bangladesh

*E-mail: nasirbaec@gmail.com

Sustainable human development is dependent on the availability of water. So, a key to sustainable management of water resources is having the knowledge needed to make the right decisions. Isotope hydrology is a nuclear technique that uses both stable and radioactive environmental isotopes to trace the movements of water in the hydrological cycle. The application of isotopic techniques in Bangladesh over the last few years in determining groundwater residence times, recharge mechanisms, recharge areas,

inter-aquifers hydraulic interactions and connectivity between different water bodies have proved valuable to improve our understanding on the behaviour of groundwater systems. Bangladesh Atomic Energy Commission has been participating actively in IAEA's technical cooperation programs on isotope hydrology for the last couple of years. Maximum benefits are derived from the application of isotope techniques when they are complemented with conventional techniques in an integrated manner. Based on the determination of the stable and radioactive isotope composition, these isotope hydrology projects give important results and form the basis for the decision of the future protection and exploitation of the aquifers. The isotopic information is critical in guiding Bangladesh policy of deep aquifer exploitation and was used in the World Bank funded projects for arsenic-free rural water supply. Integration of isotope techniques in the hydro-geologic characterization work in Bangladesh has provided information rapidly and at much lower cost than is possible with non-isotopic techniques alone. Stable isotope signatures in precipitation are useful indicators of climate variability and provide critical information regarding regional and global water processes. Daily and event-based precipitation stable isotopes have improved the understanding of the influence of moisture transport processes in the region under survey. As observed from the daily stable isotope plot, in tropical area like Bangladesh, temperature and amount of precipitation have a rather weak influence on stable isotopes in precipitation, with the primary controls thought to be the relative humidity and the degree of airmass rainout during moisture transport. The stable isotopes of precipitation are enriched at the beginning of pre-monsoon and gradually depleted at the end of post-monsoon.

ES-01: Ensemble Prediction of Storm Surge associated with Cyclone Amphan using JMA-MRI Storm Surge Model

S.M. Quamrul Hassan^{1,2*} and Syed Jamal Ahmed¹

¹Dhaka University of Engineering & Technology, Gazipur, Bangladesh

²Bangladesh Meteorological Department, Agargaon, Dhaka, Bangladesh

*corresponding author: smquamrul77@yahoo.com

Bangladesh is prone to disaster due to its geographical location and low lying coastal topography. Cyclone induced storm surges constitutes a significant threat to life and property over coastal area of Bangladesh. Uncertainty is inherent in all forecasts, storm surge predictions also have an associated uncertainty. The main source of this uncertainty is thought to be arises from the uncertainty of meteorological forcing used in storm surge prediction. Ensemble prediction system is a technique used to assess uncertainty in weather forecasting, where small errors in input can modify model outputs significantly and can obtain the best forecast from the individual forecasts. The ensemble system works by running not only one but several forecasts, using slightly different initial conditions, boundary conditions, and/or model physics. In this study, an ensemble prediction system for operational forecasting of storm surge in the Bay of Bengal is presented and applied to simulate storm surge generated by severe cyclone Amphan along West Bengal-Bangladesh coast on 20 May 2020 based on an ensemble of 20 simulations using JMA-MRI (Japan Meteorological Agency-Meteorological Research Institute) storm surge model. It is shown that simulated storm surge peaks are very close to the observation, but storm surge peaks correspond to the maxima of uncertainty and the uncertainty in storm surge level to be linked to the uncertainty of the meteorological forcing.

Key words: Storm Surge, Amphan, Ensemble, MRI.

ES-02: Assessment of heavy metal distribution and contamination in water and sediments of the Kaptai Lake, Bangladesh

Biplob Das¹, Mohammad Amirul Islam^{2*}, Kamrun Naher², Rahat Khan², Umma Tamim², Farah Tasneem Ahmed², Mohammad Belal Hossen¹

¹Department of Physics, Chittagong University of Engineering & Technology,
Chittagong-4349, Bangladesh

²Institute of Nuclear Science & Technology, Atomic Energy Research Establishment, Ganakbari, Ashulia, Dhaka-1349, Bangladesh

E-mail: liton80m@yahoo.com

In this study, thirty-two surface sediment samples and 10 water samples were collected from different locations of the Kaptailake, Bangladesh to examine heavy metal distribution patterns, assess the level of contamination and identify the pollutant sources. Total concentration of 9 heavy metals (Cr, Fe, Co, Ni, Cu, Zn, As, Cd and Pb) in water and sediments of the lake were determined using atomic absorption spectroscopy (AAS) and neutron activation analysis (NAA) techniques. Quality of the analyses was evaluated by analyzing certified reference materials IAEA-SL-1 (lake sediment), IAEA-Soil-7 and NIST-SRM-1643e (water). The total metal concentrations in the water followed the descending order: Fe>Pb>Zn>Ni>Co>Cr>Cu>Cd>As, and whereas for sediments the descending order was: Fe>Zn>Cr>Cu>Co>Ni>Pb>As, where Cd was below the detection limit. Among the metals the average concentrations of Fe, Co and Pb in water were exceeded some standard limits. Different pollution indices, indicates that Kaptai lake sediments are minorly enriched by only Zn and As. The calculated pollution load index (PLI) values suggest deterioration of sediment quality in 4 sampling stations. Pearson correlation analysis of the metal concentrations in sediments were applied to find out origin of the metal sources. This study recommended that continuous monitoring of Fe, Co and Pb in water; sediment and other aquatic biota of Kaptailake should be directed to assess risk of the toxic metals to safe ecology of the lake.

Keywords: Heavy metal, Neutron activation analysis, Atomic Absorption Spectroscopy, Kaptai lake.

ES-03: Predictability of monsoon depression over the Bay of Bengal using weather research and forecasting model

Md. Abul Hossen¹, M. A. K. Mallik^{2*}, M. A. M. Chowdhury³, Md. A. E. Akhter⁴, Syed Jamal Ahmed⁵ and S. M. Quamrul Hassan²

¹Direcrorate of Secondary and Higher Education, Ministry of Education, Dhaka, Bangladesh

²Bangladesh Meteorological Department, Dhaka, Bangladesh

³Department of Physics, Jahangirnagar University, Savar, Dhaka, Bangladesh

⁴Department of Physics, Khulna University of Engineering and Technology, Bangladesh

⁵Department of Physics, Dhaka University of Engineering and Technology (DUET)

*Corresponding author E-mail :mallikak76@yahoo.com

An attempt has been made to check the predictability of monsoon depression over the Bay of Bengal and its associated rainfall using Weather Research and Forecasting (WRF) model. The model was run on a single domain of 10 km horizontal resolution using Morrison 2-moment microphysics with the combination of Kain-Fritsch cumulus parameterization scheme, Yonsei University (YSU) planetary boundary layer scheme, MM5 surface layer physics scheme, Unified Noah LSM land surface physics, Rapid Radiative Transfer Model (RRTM) for long-wave and Dudhia scheme for short-wave scheme respectively. The NCEP high resolution Final (FNL) 6-hourly data is used for initial and lateral boundary conditions. GrADS is used to visualize the different graphics. The model predicting capability is evaluated by analyzing Mean Sea Level Pressure (MSLP), wind pattern, vorticity, vertical wind shear, reflectivity and temperature and rainfall distribution. The model has captured the system, its initial condition, propagation, landfall time and location reasonably well. The model has simulated rainfall, wind and relative humidity sensibly well and compared with the observed data by BMD and Tropical Rainfall Measuring Mission (TRMM). It is found that the WRF model with perfect arrangement of domain, horizontal resolution and parameterization schemes is capable to predict the monsoon depressions over the Bay of Bengal and its associated rainfall over Bangladesh.

Keywords: Reflectivity, Vorticity, TRMM, NCEP and wind shear.

ES-04: Sensitivity of microphysical parameterization scheme for the simulation of orographic rainfall event of 18 April 2015 over Bangladesh using WRF model

Md.Omar Faruq^{1,2*}, M. A. K. Mallik¹, M. A. M. Chowdhury², Md. A. E. Akhter³, Md. Shadikul Alam¹, S. M. Quamrul Hassan¹ and M. Arif Hossain¹

¹Bangladesh Meteorological Department, Agargaon, Dhaka, Bangladesh

²Jahangirnagar University, Savar, Dhaka, Bangladesh

³Khulna University of Engineering & Technology, Khulna, Bangladesh

Email: omarfaruq_78@yahoo.com

An effort has been made to simulate the orographic rainfall event of 18 April 2015 over Bangladesh. The model was run on a single domain of 10 km horizontal resolution of 18 microphysics scheme with the combination of Kain–Fritsch cumulus scheme and Yonsei University PBL scheme. The NSSL 2-moment microphysics scheme was finally selected for simulating the orographic heavy rainfall event among 18 microphysics of the model which represents the lowest error in terms of RMSE. The model performance was evaluated by analyzing mean sea-level pressure, wind, moisture, wind shear, vorticity, convective available potential energy, convective inhibition, lifted index, K-index, total index and rainfall. The analysis shows that the CAPE of magnitude 80-1000 J/Kg, positive vorticity of $(8-10) \times 10^{-5} \text{ s}^{-1}$ and relative humidity of 80-100% up to 300 hPa level are highly supportive for the formation of thunderstorm and heavy rainfall which are well-matched to the observation.

Keywords: WRF-ARW Model, CAPE and CIN.

ES-05: Hydrogeochemical evolution in deep aquifer systems of Kumilla, Bangladesh

F. Islam^a, A. Zahid^b, A. H. A. N. Khan^a, M. Moniruzzaman^a, M. A. Q. Bhuiyan^a, M. A. Ahsan^a, S. Sultana^a, and R. K. Majumder^a

^aIsotope Hydrology Division, Institute of Nuclear Science and Technology, AERE, Savar, Dhaka

^bGroundwater Hydrology Circle, Bangladesh Water Development Board, Green Road, Dhaka

Email: farhanaislam.geoscience@gmail.com

This paper accounts the results of a study that has investigated the hydrogeochemical evolution of the 25 deep groundwater samples of central-eastern aquifer systems of Bangladesh. These analyses help to interpret the major hydrogeochemical evolution processes occurring in the aquifer and for deducing the material sources of the ions in the groundwater. Among the cations Na^+ is the most dominant and K^+ is the lowest constituents, whereas Cl^- is most abundant and NO_3^- is the minor constituents in anions. The mean abundance of major cations in the studied groundwater samples follow the order of $\text{Na}^+ > \text{Ca}^{2+} > \text{Mg}^{2+} > \text{K}^+$, while the general dominance of anions was in the order of $\text{Cl}^- > \text{HCO}_3^- > \text{SO}_4^{2-} > \text{NO}_3^-$. Except HCO_3^- and NO_3^- , TDS shows strong and positive correlation with Na^+ ($R = 0.89$), Ca^{2+} ($R = 0.56$), Mg^{2+} ($R = 0.70$), K^+ ($R = 0.78$), Cl^- ($R = 0.99$) and SO_4^{2-} ($R = 0.73$). The elevated Cl^- and higher proportions of Na^+ relative to Ca^{2+} , Mg^{2+} , and K^+ in groundwater suggest the influence by a source of Na^+ and Cl^- . Moreover, the strong relationship between Na^+ and Cl^- (0.83) also conforms the dissolution of halite. However, the positive and significant correlations between Mg^{2+} and Cl^- (0.78), Ca^{2+} and Cl^- (0.65) suggest that cation exchange can also play a significant role to affect groundwater composition. However groundwater in this study area has a higher ratio (averaged 0.75) of $(\text{Na}^+ + \text{K}^+)$ versus total cation, depicting the contribution of cations via silicate weathering and soils, to some extent. In conclusion, silicate weathering is the dominant process in the studied aquifer system of Kumilla that influencing the material source of ions followed by the halite dissolution and ion exchange.

Keywords: Hydrogeochemical evolution, aquifer, silicate weathering and halite dissolution.

Session-VIII: Materials Science

IT-VIII: MXenes: 5th generation 2D materials go beyond graphene

M. M. Uddin

Department of Physics, Chittagong University of Engineering and Technology (CUET), Chattogram 4349, Bangladesh

* mohi@cuet.ac.bd

MXenes are a new family of two-dimensional (2D) early transition metal carbides, carbonitrides and nitrides that were discovered in 2010 and emerged in the world of 2D materials beyond graphene. The key advantage explored so far is their high metallic electronic conductivity and ability to produce transparent conductive films beyond already been commercialized graphene. MXenes can be used in many applications such as lithium-ion and sodium-ion energy storage systems, electromagnetic interference (EMI) shielding (due to their good flexibility, easy processing, and high conductivity with minimal thickness having highest EMI shielding effectiveness of all synthetic materials of similar thickness), water purification, printable 5G and many more. They are also promising antibacterial agents, with higher efficiency than graphene oxide (GO) in diminishing bacterial cell viability. The archetypical MXenes with high metallic conductivity, hydrophilicity and high negative surface charge that allows dispersion in water, forming stable colloidal solutions of single-layer flakes that combine the best properties of GO and reduced graphene oxide (rGO) and take those to extreme (5-10 times higher conductivity compared to rGO films). MXenes are making ink-jet printed patterns with conductivity ten times that of printed graphene and not requiring heat treatment opens many opportunities. Therefore, researchers are interested to explore useful properties that enable applications of MXenes and hype (yesterday- nanotubes, today - graphene, or tomorrow – MXene). In this talk, the prospects and outlook of the MXenes research have been discussed.

MS-07: Performance optimization of TCO-less back contact dye-sensitized solar cells utilizing indoline and porphyrin sensitizer based on cobalt electrolyte

Md. Zaman Molla^{*1}, Ajay Kumar Baranwal², Shuzi Hayase² and Shyam S. Pandey³

¹Ahsanullah University of Science and Technology, Dhaka-1208, Bangladesh

²Info-Powered Energy System Research Center, University of Electro-Communications, Tokyo, 182-8585, Japan

³Graduate School of Life Science and Systems Engineering, Kyushu Institute of Technology, 2-4 Hibikino, Wakamatsu, Kitakyushu, 808-0196, Japan

E-mail: zaman.molla.as@aust.edu, whyzaman@gmail.com

Transparent conductive oxide-less (TCO-less) back contact (BC) dye-sensitized solar cell (DSC) employing stainless steel (SS) metal mesh coated with nanoporous TiO₂ film as a flexible photoanode utilizing cobalt complex redox shuttle is being reported. A thin layer of titanium (Ti) metal on the SS metal mesh was proved to be effective to retard the back-electron transfer, which was ensured by the dark current measurements. It was assured by electrochemical impedance spectroscopy (EIS) that NP TiO₂ with 30 nm particle size demonstrated less charge transport resistance at TiO₂-dye-electrolyte interface as compared to TiO₂ with the particle size of 15-20 nm. TCO-less BC-DSC using dye cocktail of indoline dyes D-205 and D-131 (1:1) with comparatively larger NP of TiO₂ of 30 nm as compared to smaller NP of TiO₂ of 15-20 nm demonstrated improved photoconversion efficiency (PCE) of 4.02 %. In order to enhance the PCE further, TCO-less BC-DSC with cobalt redox shuttle sensitized with porphyrin sensitizer (YD2-o-C8) with a larger optical area was explored. An optimum thickness of 10 μm of TiO₂ film was proved to be the best leading to an improved PCE of 5.26%

MS-08: Growth and characterization of LiCoO₂ Single crystals for the applications of all solid-state li-ion batteries (LIBs)

Ruma Parvin*, Yuki Maruyama, Masanori Nagao, Satoshi Watauchi, Isao Tanaka

Center for Crystal Science and Technology, University of Yamanashi, 7-32 Miyamae, Kofu, Yamanashi, Japan.

*E-mail: rparvin4391@gmail.com

The effects of the mirror tilt angle on the molten zone shape during the growth of LiCoO₂ crystals were investigated for the first time for the traveling solvent floating zone (TSFZ) technique using a tilting-mirror-type image furnace. In our experiments, it was found that the interface shape of the molten zone formed under both tilted and non-tilted conditions was convex. The convexities (h/r) of the feed-liquid and crystal-liquid interface were minimum at the tilt angle of $\theta = 10^\circ$. We successfully grew large (single crystals of LiCoO₂ approximately 7 mm in diameter and 50 mm in length (Figure 1)). For the TSFZ growth of larger diameter single crystals of LiCoO₂, the growth conditions, such as the excess Li content in the feed, amount of Li-excess solvent and the filament shape of the heating lamps, were optimized for various crystal diameters using a tilting-mirror-type image furnace. We successfully grew LiCoO₂ single crystals with a diameter of 10 mm and 13 (more than $\frac{1}{2}$ inch) and a length of 50 mm under the optimum growth conditions. The charge-discharge characteristics of the grown LiCoO₂ single crystals were studied using LiCoO₂ single crystals as cathode and liquid, gel and solid electrolytes. The discharge capacities of Li-ion batteries (LIBs) using LiCoO₂ single crystals cathode was 145 mAhg⁻¹ with liquid electrolyte. Almost all solid-state LIBs were designed using LiCoO₂ single crystals cathode with gel electrolyte. The discharge capacities of almost all solid-state LIBs were 90 mAhg⁻¹.

MS-09: Effect of vanadium substitution on structural, magnetic and transport properties of Ni-Zn-Co ferrites

M. D. Hossain¹, M. N. I. Khan², R. Rashid², S. J. Ahmed¹, A. T. M. Kaosar Jamil¹

¹Dept. of Physics, Dhaka University of Engineering & Technology (DUET), Gazipur-1707

²Materials Science Division, Atomic Energy Centre, Dhaka

Email: dulal_901@yahoo.com



The composition Ni_{0.7}Zn_{0.2}Co_{0.1}Fe_{2-x}V_xO₄ ($0 \leq x \leq 0.12$) ferrites was synthesized by a standard solid-state reaction method and all samples were crystallized with a single-phase cubic spinel structure that belongs to the $Fd\bar{3}m$ space group. The lattice constants are found to decrease gradually from 8.3673 Å to 8.3602 Å for substituting V⁵⁺ ions. Moreover, the average grain size (D_{SEM}) decreases from 6.92 to 1.99 μm and porosities (P_i and P_s) are also increased due to the substitution of V⁵⁺ at Fe³⁺ of B-site. The bond lengths and force constants of ions have been estimated from Raman and infrared spectra. Moreover, the absorption peaks of FTIR spectra have been utilized to evaluate the elastic properties and the thermodynamic properties of the studied samples. From the room temperature magnetization, a $Y-K$ type magnetic ordering is observed for samples with $x = 0.07$ and 0.12. In addition, a ferromagnetic

to paramagnetic phase transition is observed in all samples, and the Curie temperatures (T_C) are shifted to the lower temperature side with V^{5+} substitution. The transport properties for all samples were studied by the DC resistivity with a variation of temperature from 300 to 600 K and the higher activation energy (E_a) is observed for V^{5+} substitution. The conduction mechanism of the prepared samples has been evaluated from the electric modulus and AC conductivity (σ_{ac}) within 20 Hz to 100 MHz. Localization of relaxation mechanism in the studied samples has been derived from the imaginary part of the impedance (Z'') and electric modulus (M''). The RLC behavior and phase angles between 10 Hz to 100 MHz indicate that pure Ni-Zn-Co ferrite is fully resistive below 100 Hz while the V doped samples range from inductive to capacitive. The contributions of the capacitance, as well as resistance from the grains and grain boundaries were calculated from the relaxation peak of Z'' and M'' .

MS-10: Analysis of the HTS Inductor Design for Optimum Energy Storage in SMES

M. R. Islam, *Jahangir Alam and M. A. A. Zaman

Department of Physics, University of Chittagong, Chittagong-4331, Bangladesh

*Corresponding author email: Jahangir.phy@cu.ac.bd

Superconducting magnet coils are the major component parts of energy storage in SMES (Superconducting Magnetic Energy Storage). To maximize the storage energy, the coil must be designed to have the maximum inductance for a given length of conductor as its operating current. This report will discuss the design optimization for a superconducting solenoid made of silver sheathed first generation high- T_C superconductor (1G HTS) BSCCO-2223 tape conductor and consider various practical issues regarding the choice for a prototype. We have performed the inductance calculation for specific design and shown the effects of variation of parameters related to it. Numerical results suggest that the optimum inductance value (L) depends on the geometrical parameters *i.e.*, size ratios (α , β) and height of pancake layers (H) and so on. Finally, storage energy calculation with specific design and necessary explanations has been included.

Keywords: SMES (Superconducting Magnetic Energy Storage), HTS (High Temperature Superconductor), Size ratio, BSCCO-2223 (Bismuth Strontium Calcium Copper Oxide)

MS-11: Impact of lanthanum ions on structural, optical, and magnetic properties of Cobalt-Zinc ferrites

Mohammad Osman Goni¹, Nazia Khatun², Mohammad Sajjad Hossain², M. Al- Mamun³, Mohammad Saiful Alam¹, Suravi Islam², Most. Hosney Ara Begum², Syed Farid Uddin Farhad² and Mahmuda Hakim⁴

¹Applied Chemistry and Chemical Engineering, Noakhali Science and Technology University, Noakhali-3814, Bangladesh.

²Industrial Physics Division, Bangladesh Council of Scientific and Industrial Research, BCSIR, Dhaka-1205, Bangladesh

³Materials Science Division, Bangladesh Atomic Energy Center, BAEC, Shah bag Dhaka-1000, Bangladesh.

⁴Biomedical and Toxicology Research Institute (BTRI), BCSIR, Dhaka-1205, Bangladesh

Email: shariyerosman123@gmail.com

Lanthanum-doped Cobalt-Zinc ferrite with $\text{CoLa}_x\text{ZnFe}_{2-x}\text{O}_4$ ($x=0.00, 0.05, 0.10, 0.15, \text{ and } 0.20$) compositions were synthesized by the sol-gel auto combustion method sintered at 700°C for 4 hr. The XRD analysis confirmed the formation of the single-phase cubic spinel structure with minor impurity well over from $x=0.05$. The mean crystallite size decreases with increasing La^{3+} concentration in the range of 26-41 nm. Two major functional groups were found from FTIR spectra confirmed the presence of

metal oxide bond within the range 600 to 350 cm. Microstructural analysis from FE-SEM revealed the irregular-shape grain morphology with size in the range of ~60-78 nm. The EDX spectra of the samples confirmed the presence of Co, Zn, La, and Fe elements. The optical band gap (E_g) estimated from the UV-VIS-NIR diffuse reflection data of the powder samples was found to vary (~1.62 -1.76 eV) and consistently increased with the increase of La^{3+} content. The magnetic properties of the sample's such as saturation magnetization (M_s), magnetic moment (μ_B), and coercivity (H_C) were obtained from the respective hysteresis loops and revealed that La-doped Cobalt-zinc ferrites are soft ferrite nature and may be integrated for suitable device applications.

MS-12: Dielectric properties and impedance spectroscopy of V_2O_5 added Li-Zn ferrites

Sm. Rubayatul Islam¹, M. Miftaur Rahman², S. Manjura Hoque³ and M. Samir Ullah^{1*}

¹Department of Physics, Bangladesh University of Engineering and Technology, Dhaka-1000

²Department of Materials and Metallurgical Engineering, BUET, Bangladesh

³Materials Science Division, Atomic Energy Center, Dhaka-1000

Email: samirullah@phy.buet.ac.bd

Dielectric properties and impedance spectroscopy of V_2O_5 added Li-Zn ferrites have been investigated as a function of frequency at room temperature. The samples were prepared by the double sintering method. The crystal structure of the prepared samples has shown the single phase cubic structure. From the microstructural study, it was observed that V_2O_5 accelerated the densification and promoted the grain growth of Li-Zn ferrites as a sintering aid during the sintering process. It shows that the enhancement of the grain growth is clearly depended on V_2O_5 addition. The dielectric property of the samples showed the dispersive behavior following the Maxwell-Wagner type of polarization. Frequency dependent ac conductivity measurement at room temperature shows a sharp rise of conductivity which could be attributed to increase of exchange of electrons between Fe^{2+} and Fe^{3+} ions. The complex impedance gives the information about the resistive (Z') and reactive (Z'') components of the samples. The frequency independent nature of Z' and Z'' are observed at higher frequencies which may be related to the reduction of space charge polarization at the grain boundaries. The complex impedance spectroscopy through Cole-Cole plot revealed that the conduction process is dominated by only grain boundary of the samples. It is also ensured that all the impedance spectroscopy results are in good agreement with V_2O_5 content and suggesting the relaxation process is non-debye type.

Session-IX: Health Physics

IT-IX: Towards development of radioluminescence sensors

David Bradley

Centre for Applied Physics and Radiation Technologies, Sunway University, UK

Up until recent times our studies of such devices have largely focused on developing radioluminescence (RL) systems that allow for dosimetry of medical irradiating apparatus, with investigations concerning doped silica optical fibers and time-resolved radiation dosimetry. Away from pulsed sources of radiation and focusing within the low dose regime of naturally occurring radioactive materials (NORM), presently available devices have a number of operational limitations, including an inability to conduct investigations of hard to access locations, also an inability to operate in aqueous environments. Characterization has been made of an optical fiber system based on a $\text{LYSO}:\text{Ce}$ scintillator, compared against Geiger Muller (GM) device, tested thus far using monazite and xenotime at in-contact dose rates down to 20 $\mu\text{Gy/h}$. With measurements comparable to that of the GM counter, and with intrinsically safe RL remote capabilities, the study points to RL potential in a variety of industrial scenarios.

HP-01: Study on Radiation Protection Infrastructure of Different X-Ray Facilities in Habiganj District City with Different Thanas

L. Begum*, R. B. Rana, M. Akramuzzaman, M. M. Rahman, and M. Nahar

Radiation, Transport and Waste Safety Division, Bangladesh Atomic Energy Regulatory Authority,
Agargaon, Dhaka-1207, Bangladesh

*Email: aeclutfun@yahoo.com

A regulatory survey was carried out of different diagnostic X-ray facility in Habiganj district city with different thanas to study radiation protection infrastructure of those X-ray facility. Regulatory data of X-ray installations was collected and a detailed comparison was made on the present regulatory data with the previous inspection data. There were 43 X-ray facilities having 50 X-ray machines in Habiganj district city with 4 thanas. In 90% installations, the radiation dose level was within regulatory limit. From the study of year 2000, it was seen that 27% control panel were in open condition where's it reduced to 7% in 2019. From the survey study of 2000, it was seen that among the total of 17 X-ray machines 06 of them were 50 mA machines, while in the year 2019 among the total of 50 X-ray machines none of them were found to be 50 mA machine. Among all the X-ray machines, largest numbers of X-ray machines were seen 250 mA. In 2019 it was seen that, 97% of X-ray room wall had 10 inch brick wall where's in 2000 only 41% of them had 10-inch wall. Earlier in the year 2000, none of the radiation worker had TLD badge, but in 2019 percentage of workers using TLD badge was 53. In year 2019, 57% of them had satisfactory performance in compliance with the regulatory requirements, where in year 2000, none of the X-ray installation were in satisfactory condition. From the analysis of data of year 2000 to 2019, it was seen that radiation safety and protection of X-ray installation has been improved significantly.

HP-02: Real-time environmental radiation monitoring in Tejgaon thana following in-situ method

M. A. Rahman Shuvo¹, M. S. Rahman^{2*}, S. Yeasmin², Md. Kabir Uddin Sikder¹

¹Department of Physics, Jahangirnagar University, Savar, Dhaka, Bangladesh

²Health Physics Division, Atomic Energy Centre, 4 Kazi Nazrul Islam Avenue, Shahbag, Dhaka-1000, Bangladesh

*Email: msrahman1974@yahoo.com

Real-time environmental radiation monitoring is very important for generation of the baseline database. The baseline database is required to know the changes after operation of the nuclear facility in the country. In this study, real-time environmental radiation monitoring was performed at area of Tejgaon Thana under Dhaka city. The real-time radiation monitoring was carried out using digital portable radiation monitoring devices. The digital portable devices were placed at 1 meter above the ground on tripod and data collection time for each monitoring point (MP) was 1 hour. Total 32 MPs were selected for collection of the data in the outdoor environment of Tejgaon Thana from December 2020-January 2021. The MPs were marked-out using Global Positioning System (GPS) navigation. The measured dose rates were ranged from $0.110 \pm 0.003 \mu\text{Sv/hr}$ to $0.219 \pm 0.008 \mu\text{Sv/hr}$ with an average of $0.138 \pm 0.018 \mu\text{Sv/hr}$ for outdoor measurement. The annual effective dose to the public due to the outdoor environmental radiation was varied from $0.201 \pm 0.038 \text{ mSv}$ to $0.308 \pm 0.017 \text{ mSv}$ with an average of $0.242 \pm 0.032 \text{ mSv}$. Excess Life time Cancer Risk (ELCR) on public is calculated based on the real-time radiation monitoring data. These values are lower than India & higher than Sweden, China, Czech Republic, Italy, Canada, Turkey, Indonesia, Belgium, Albania, New Zealand and some other counties. This kind of study is required to detect the presence of natural radionuclides and artificial radionuclides (if any) releasing from nuclear & radiological installations in the country or from neighboring countries in normal operations or in case of

accident/incident. From the study, it can be concluded that there is no radiation burden to environment due to man-made sources.

Key Words: Outdoor; Tejgaon Thana; Radiation; In-Situ; Public.

HP-03: Health effects of electromagnetic radiation from cell phone and towers: It's present scenario in Bangladesh

Munima Haque¹, M. Quamruzzaman^{2*}, Md. Shohag Hossain²

¹Dept. of MNS, Brac University

²Dept. of ETE, Daffodil International University

Email: ext.munima.haque@bracu.ac.bd, *mqzaman60@gmail.com

Mobile/cell phone has converted the world into a global village. It is proved to be so useful that it has become the most popular and a part of daily life in modern society. The number of cell phone uses around the world has reached more than 8 billion according to ITU and in Bangladesh, the number is increasing very fast and has exceeded 160 million in 2021. Electromagnetic radiation (EMR) emitted by cell phone/towers (in Mega Hertz range) has been named as Non-Ionizing Radiation (NIR) as it does not ionize the media while propagating. There is public concern that the EMR/NIR from cell phone and tower is harmful for not only the human but also on living system and environment disturbing the ecological balance. It is reported from various studies around the world, that NIR causes various health problems like chronic cold, flu, headache, mind fogs, ataract, insomnia, indigestion, depression, dizziness, memory loss, child behavior problem and many other diseases like Cancer are also suspected to be related with NIR after prolonged use. The objective of this study was to explore and verify, whether the EMR/NIR from cell phones and towers are within maximum permissible dose (MPD) which is 1.6W/Kg or 10mW/cm² for cell phone and 9.25W/m² for 1850 MHz from towers, as suggested by ICNIRP 1998 guideline. It is necessary to be acquainted with the harmful effects of EMR/NIR to develop awareness and to take corrective measures for minimizing or controlling the health hazards as far as practicable.

Keywords: EMR, NIR, MPD, ICNIRP.

HP-04: Source apportionment and health risk assessment of heavy metals from indoor air dust of an industrial area, Savar, Bangladesh

M.A.M. Mottalib Sarkar, M.M. Hasan, *M.S. Rahman, B.A. Begum

Air Particulate Research Laboratory, Chemistry Division, Atomic Energy Centre, Dhaka, Bangladesh

Urban dust especially in industrial area is influenced by both the natural and anthropogenic factors. Their impacts, therefore, amend the concentration of heavy metals in the dust. This research work was carried out in the industrial area in order to determine the composition of trace elements in dusts deposited at homes, identifying different sources of elements and also for their possible health impacts because of these industries. A total of 15 deposited dust samples were collected from households near industrial area of Savar, Ziranibazar. Samples were analyzed using energy dispersive X-ray Fluorescence (EDXRF) spectroscopy and Ca, Fe, K, Ti, Zn, Mn, Zr, Sr, Rb, Cu, Pb and Co were found in these samples. Pearson correlation analysis, Principal component analysis and Hierarchical cluster analysis (HCA) were used to identify the possible sources of these heavy metals. From this multivariate statistical analysis, it was found that anthropogenic sources especially industrial activity, combustion, smelting, vehicular emission and household cooking are the main sources of trace elements in the study areas. The non-carcinogenic and carcinogenic health risks indicated that children are more vulnerable for non-carcinogenic effects whereas the values of cancer risk for both the child and adult are below the acceptable limit of European Union and USEPA.

HP-05: Analysis of circulating cell free DNA extracted from blood plasma of cancer patients and healthy persons and their Z-scan study

H. Ara¹, S. A. Tarek¹, S. M. S. Al Din², M. K. Biswas¹, S. M. Sharafuddin^{1*}, S. B. Faruque¹ and Y. Haque¹

¹Department of Physics, Shahjalal University of Science and Technology, Sylhet, Bangladesh

²Invent Technologies Ltd, Banani, Dhaka, Bangladesh

*Email: sharif-phy@sust.edu

Circulating cell free DNA (ccfDNA) detection can be applied qualitatively and quantitatively for the early detection of cancer. Detection of ccfDNA in cancer patients and healthy persons and its qualitative and quantitative analysis to compare the DNA profiles can be useful in early stage diagnosis of malignancies. Our objective is to determine the concentration of ccfDNA in plasma for early detection of cancer. In our study we have collected plasma samples from 40 different cancer patients and 40 healthy individuals. Circulating cell free DNA extractions from cancer and non-cancer plasma samples were done by Maxwell system. The total concentration of ccfDNA was determined using a fluorometry method and Nano Drop, and Z-Scan technique was used for investigating the corresponding nonlinear optical response of a sample. Our results showed that ccfDNA concentrations were significantly higher in cancer patients as compared to healthy individuals. The median levels of the ccfDNA concentration in patients with cancer were significantly higher than those in controls (both $P < 0.001$). The aim of this study was to determine the levels of ccfDNA in cancer patients and to assess their concentration for early detection of cancer using Z-scan technique based on nonlinear optical response of the samples.

Key Words: Circulating Cell Free DNA (ccfDNA), Biomarker, Nucleic acid, Maxwell System, Fluorometer, Nano Drop Spectrophotometer, Z-Scan, Nonlinear Optical Response (NLO).

Session-X: Thin Film

IT-X: Materials for stable perovskite solar Cells: Advances, challenges and opportunities

Md. Akhtaruzzaman

Solar Energy Research Institute (SERI), The National University of Malaysia (@Universiti Kebangsaan Malaysia) (UKM), 43600 UKM-Bangi, Selangor, Malaysia

Email: akhtar@ukm.edu.my

Organic-inorganic hybrid perovskite solar cells (PSCs) have recently gained a lot of attention as promising photovoltaic technology to the academic and industrial community due to their lightweight, flexible and low-cost manufacturing processes. The most advantages of using perovskite materials possess some interesting optoelectronic properties such as tunable bandgap, high absorption coefficient, long diffusion lengths ($>1 \mu\text{m}$), easy and low-cost solution processability together with cheap and available raw materials. Typically, a PSC is a sandwich structure having a perovskite absorber layer (e.g. MAPbX_3 ; $\text{MA} = \text{CH}_3\text{NH}_3^+$ and $\text{FA} = \text{CH}_3(\text{NH}_2)_2^+$, $\text{X} = \text{Cl}^-$, Br^- , I^- , BF_4^- , PF_6^- , SCN^-) sandwiched between the electron transport layer (ETL) (e.g. TiO_2 , ZnO , C_{60} -derivatives) and the hole transport layer (HTL) (e.g. spiro-OMeTAD, PEDOT: PSS, NiOx) with front and back contact electrodes. Light passing through the transparent electrode of a PSC onto the photosensitive perovskite layer generates electron-hole (e^-/h^+) pairs. The charged particles separate and migrate through the ETLs and HTLs to their

respective metal electrodes, thereby generating an electric current. Despite the current progress of PSCs, many issues remain to be resolved for further progress in this area of research, such as reproducibility, water and ambient moisture instability, carrier recombination process, interface defects, oxygen/moisture sensitivities of the electron/hole transport layer, low charge carrier mobility, poor crystallinity and solubility, efficient front contact, expensive counter-electrode (e.g. Au), cost-effectiveness etc., which restrict the commercial production opportunity. Therefore, new materials and strategies have been designed and screened to make the best heterojunction using suitable ETLs or stable inorganic HTL, with minimized interface recombination and bulk defects for enhancing PSCs stability and efficiency in large areas.[1-3]

References

1. M. Shahiduzzaman*, M. I. Hossain, S. Visal, T. Kaneko, W. Qarony, S. Umezu, K. Tomita, S. Iwamori, D. Knipp, Y. H. Tsang, Md. Akhtaruzzaman*, J.M. Nunzi, T. Taima, and M. Isomura*, *Optimized Multi-layer Front Contact Design for Realizing Efficient Perovskite Solar Cells* - **Nano-Micro Letters**, **2021**, **13**, 1014
2. Md Shahiduzzaman*, Ersan Y Muslih, AK Mahmud Hasan, LiangLe Wang, Shoko Fukaya, Masahiro Nakano, Makoto Karakawa, Kohshin Takahashi, Md Akhtaruzzaman*, Jean-Michel Nunzi, Tetsuya Taima - *The Benefits of Ionic Liquids for the Fabrication of Efficient and Stable Perovskite Photovoltaics* - **Chemical Engineering Journal**, **2021**, **411**, 128461
3. Mohammad Ismail Hossain, A. K. Mahmud Hasan, Wayesh Qarony, Md. Shahiduzzaman, M. A. Islam, Yasuaki Ishikawa, Yuki Haru Uraoka, Nowshad Amin, Dietmar Knipp, Md. Akhtaruzzaman*, Yuen Hong Tsang - *Electrical and optical properties of nickel-oxide films for efficient perovskite solar cells* - **Small Method**, **2020**, **4**, 2000454

TF-01: Thickness dependent thermal and optical characteristics of plasma Polymerized N-benzylaniline thin films

Rani Nasrin^{a*}, Mohammad Jellur Rahman^a, A. T. M. K. Jamil^b, A. H. Bhuiyan^{a,c}

^aDepartment of Physics, Bangladesh University of Engineering and Technology, Dhaka-1000, Bangladesh

^bDepartment of Physics, Dhaka University of Engineering & Technology, Gazipur-1707, Bangladesh

^cUniversity of Information Technology and Science, Baridhara, Dhaka-1212, Bangladesh

*Email: rnasrin_drnc@yahoo.com

Plasma polymerized N-benzylaniline (PPNBA) thin films of different thicknesses are prepared onto cleaned glass substrates at room temperature from N-benzylaniline (NBA) precursor by a parallel plate capacitively coupled glow discharge plasma system. The thermo-gravimetric analysis and differential thermal analysis indicate that thermal stability of the as-deposited PPNBA thin films increases with film thickness, d . Optical properties of these films are investigated at room temperature from ultraviolet-visible (UV-Vis) spectroscopic measurements. The absorbance spectra reveal that as-deposited PPNBA thin films have high absorbance and double peaks in between ultraviolet-visible regions due to π - π^* transition. The indirect and direct optical band gaps, E_{gi} and E_{gd} , of the studied PPNBA thin films vary from 2.04 to 2.11 eV and 3.1 to 3.2 eV, respectively and the values of Urbach energy, E_u , decrease from 0.63 to 0.56 eV as d increases. The increase in E_g and the decrease in E_u with increasing d may be due to some reduction of localized electronic states in the E_g and are related to the extent of conjugation between adjacent rings of quinoid and benzenoid structure in the PPNBA thin films. At 325 nm, the values of extinction coefficient are observed to be as small as 0.124–0.152 and those of refractive index values are as high as 6.77–17.39 depending on d as well as cluster size. The dissipation factor is low over the entire wavelength region, which indicates that the thin films have good homogeneity and the higher thickness films are more efficient than those of lower thickness for device applications. Optical conductivity of the

thin films increases with the increase of d indicating the formation of localized states in the gap owing to new defects. Thus, it can be inferred that the PPNBA thin films may find applications in electronic and optoelectronic devices.

TF-02: Comparative study of power and thickness dependent optical properties of AC plasma polymerized 3,4-Ethylenedioxythiophene thin films

Md. JuelSarder^a, Mohammad Jellur Rahman^{a*}, Md. Mahmud Hasan^a, and A. H. Bhuiyan^{a,b}

^aDepartment of Physics, Bangladesh University of Engineering and Technology, Dhaka-1000, Bangladesh

^bUniversity of Information Technology and Sciences, Baridhara, Dhaka-1212, Bangladesh

*Email: mjrahman@phy.buet.ac.bd

Organic polymer thin films have attained significant research attention in the last few decades. Plasma polymerization is a distinctive technique for direct polymeric thin films deposition from different organic monomers. The organic compound 3,4-ethylenedioxythiophene (EDOT) has been chosen as monomer to deposit plasma polymerized EDOT (PPEDOT) thin films. The polymerization is carried out by using a capacitively coupled glow discharge reactor by optimizing the plasma parameters, where the plasma is created at line frequency (50 Hz). Thicknesses of the thin films are varied by synthesizing PPEDOT thin films for different deposition times and input powers. Optical parameters of the deposited PPEDOT thin films such as the absorbance, absorption coefficient, optical band gap energies, Urbach energy, extinction coefficient, refractive index, etc. are obtained from UV-visible spectra and are correlated to understand their applicability. From the UV-Vis analysis, it is observed that the values of direct band gap energy, $E_{g(d)}$, varies from 3.94 to 3.86 eV and that of the indirect band gap energy, $E_{g(i)}$, varies from 3.62 to 3.20 eV for the PPEDOT thin films of different thicknesses. The decrease of $E_{g(d)}$ and $E_{g(i)}$ values with the increasing thicknesses is due to the increase in fragmentation/cross-linking in the bulk of the material due to the impact of plasma on the surface of the thin films during polymerization. The values of the Urbach energy varies from 0.00364 to 0.00258 eV with the variation of thickness owing to the increase of disorder in the PPEDOT thin films.

Keywords: 3,4-ethylenedioxythiophene, plasma polymerization, thin films, optical bandgap, UV-Visible spectroscopy

TF-03: Evolution in surface properties, band gap tuning and reversal in electrical conductivity of ZnO thin films achieved via B doping

M. Sharmin^{1*}, A. H. Bhuiyan^{1,2}, J. Podder¹ and K. S. Hossain³

¹Department of Physics, Bangladesh University of Engineering and Technology, Dhaka-1000, Bangladesh

²University of Information Technology and Sciences, Baridhara, Dhaka-1212, Bangladesh

³Department of Physics, University of Dhaka, Dhaka-1000, Bangladesh

E-mail: proggaph@gmail.com

Zinc oxide (ZnO) and boron (B) doped ZnO thin films were deposited onto microscope glass slides by spray pyrolysis technique. The amount of B doping was varied between 1 and 5 at% in ZnO thin films. An evolution in surface morphology from nanofibrous to nanoflakes pattern has been observed in B doped ZnO thin films by field emission scanning electron and atomic force microscopies images. The chemical structure and composition of the films are confirmed by Energy dispersive X-ray and X-ray photoelectron spectroscopy analyses. The films show a polycrystalline wurtzite structure with the preferential (002) orientation in X-ray diffraction analysis. Crystallite size is found in the range of 18 to 32 nm. The films are transparent in the Vis-NIR region and the optical band gap is found between 3.20 and 3.29 eV. Direct current electrical resistivity and carrier concentration of B doped ZnO thin films are

found in the order $10^{-2} \Omega\text{-cm}$ and 10^{20} cm^{-3} , respectively. The films show a change of majority charge carriers from n-type to p-type for 5 at% B doping. The highest carrier mobility is found to be $1.44 \text{ cm}^2 \text{V}^{-1} \text{s}^{-1}$ for 1 at% B doped ZnO thin film. The results of various investigations presented in the paper suggest the suitability of B doped ZnO thin films in optoelectronic applications.

TF-04: Structural, optical and transport properties of Fe: Co₃O₄ thin films grown by spray pyrolysis technique

M. Zahan and J. Podder

Department of Physics, Bangladesh University of Engineering and Technology, Dhaka, Bangladesh

Email: muslimazahan30@gmail.com

Iron (Fe) doped cobalt oxide (Co₃O₄) nanostructured thin films (Fe:Co₃O₄) were prepared by a spray pyrolysis deposition technique to explore their structural, morphological, optical and transport properties suitable for glucose sensing abilities. Many useful characteristics were observed in the growth process, phase transformation and remanent magnetization due to the addition of Fe concentration in the range of 0 to 10 at %. Powder X-ray diffraction (PXRD) pattern of the deposited thin films showed the spinel cubic structure of lattice parameters $a = b = c = 8.0764 \text{ \AA}$ and well agrees with the JCPDS card file no. 42-1467. Fe concentration strongly influenced the crystallite size of Co₃O₄ analyzed by scanning electron microscope. The crystallite sizes were also calculated using the Scherer's formula and were found 29, 31, 35, 32, 30 and 27 nm variation with 0-10 at% Fe doping concentration respectively. The optical band gap energies in the UV region were found about 2.02, 1.96, 1.73, 1.89, 2.15 and 2.21 eV respectively. Williamson-Hall plot results indicated the appearance of strain for Fe doping. Electrical resistivity's were obtained in the order of $10^4 \Omega\text{-cm}$ and minimum resistivity was observed at 4 at% Fe concentrations. Maximum carrier concentration was obtained at 4 at% Fe concentration using Hall Effect measurement. The glucose sensitivity measurements revealed that Fe doping concentration greatly affected on the sensing abilities of Co₃O₄ thin film. Highest glucose sensing response was recorded about 45% at 5 minutes for 4 at% Fe concentrations.

Keywords: Thin films, spray pyrolysis, PXRD, transport properties, glucose sensing.

TF-05: Characterization of the physical properties of Cu₂O thin films synthesized in the presence of NaCl by modified SILAR method

A. Hossain^a, N. I. Tanvir^b, S. F. U. Farhad^b, S. Majumder^a, B. C. Ghos^b, M. A. Rahman^{a, c}, T. Tanaka^d, Q. Guo^d, M. A. M. Patwary^{a, d*}

^aPhysical Chemistry Research Laboratory, Department of Chemistry, Comilla University, Cumilla-3506, Bangladesh

^bSolar Energy Conversion and Storage Research Section, Industrial Physics Division, BCSIR Laboratories, Dhaka-1205, Bangladesh

^cDepartment of Chemistry, Kumamoto University, Kumamoto, 860-8555, Japan

^dDepartment of Electrical and Electronic Engineering, Saga University, Saga, 840-8502, Japan

*Email: mamajedp@gmail.com

Cu₂O is an attractive material in thin film technology due to its notable optoelectronic properties such as non-toxicity, high absorption coefficient, direct band gap nature, high hole mobility and 20% theoretical efficiency under 1.5 AM solar illumination. In this work, we have synthesized Cu₂O thin films by the modified SILAR method on soda lime glass by varying the concentration of NaCl used as an electrolyte and the physical properties of the deposited Cu₂O thin films have been investigated. The XRD pattern revealed that Cu₂O thin films were polycrystalline with (111) preferential growth. In addition to XRD, Raman also exhibited characteristic peaks for phase pure Cu₂O. Surface resistivity of the Cu₂O thin films

decreased from 15,142 to 685 Ωcm with the increase of concentration until 4mmol of NaCl, then showed opposite tendency with the further increase of the concentration. Optical band gap of the deposited Cu₂O thin films were in between 1.88 and 2.36 eV, while the temperature dependence activation energies of the films were found as about 0.14~0.21 eV. Surface SEM images exhibited Cu₂O nanorod as well as densely packed spherical grains with the variation of NaCl concentration. Cu₂O phase was stable up to 230 °C which was consistent with respective to the band gap results. The film deposited at 4 mmol of NaCl exhibited the lowest resistivity and activation energy as well as excellent nanorod formation. Therefore, structural, electrical, and optical properties of the Cu₂O thin films have a great influence in presence of NaCl electrolyte, which could have significant impact in photovoltaic research.

Session-XI: Physics Education

PE-01: Gender issues in science classroom and female learner's participation in higher education science programs

Anina Mahmud¹, Mohammad Nure Alam Siddique²

¹Content Developer, JAAGO Foundation

²Institute of Education & Research (IER), University of Dhaka.

Email: anina.mahmud@jaago.com.bd, siddique.mna@du.ac.bd

According to the Board of Intermediate and Secondary Education, 2017 and University Grant Commission (2017), the rate of women transitioning from higher secondary science to higher education science discipline is considerably low in Bangladesh. A number of gender issues in science classrooms affect female learners' participation in higher level science courses and science careers. In this study we explore the gender issues in higher secondary science classroom in Bangladesh that influence female learner's participation in higher education science courses. And for this we explore answers to research questions focusing on- the gender issues existing in science classroom, teachers' views about these issues and the reasons underlying these issues. We utilized qualitative multiple case study research design and accordingly, classroom observations, teacher interviews and student FGDs were used to collect qualitative data. The findings generated in this study indicates- many gender issues exist in the science classrooms, including rigid instruction portraying science as objective and value free, male domination in classroom instruction and management process, low engagement of female learners in science classroom. It is also found that teachers are not aware of gender issues in their classroom and they have gendered assumptions about female learners' and male learners' abilities and interests in different science subjects. Students' family background and expectation is found as one of the reasons behind lack of female participation in higher education science. We recommend increased research and training initiatives to be in place, to make teachers, educators and science classroom gender sensitive for increased female participation in higher education science programs.

Key words: Gender Issues, Science Education, Female Learners, Gendered assumption, Gender sensitive.

PE-02: Status and reasons of current practice of science practical at the secondary level

S. M. Hafizur Rahman¹, Md. Salimuzzaman², Tahmina Hoq¹

¹Institute of Education and research (IER), University of Dhaka-100, Bangladesh

²National Academy for Educational Management (NAEM), Dhaka-1205, Bangladesh

Email: hafiz.rahman@du.ac.bd

National Educational Policy 2010 of Bangladesh has noted science practical work as a valuable part in science education. However, most of the stakeholders are not satisfied with the current practice of practical work at the secondary level. The major objective of this study was therefore to explore the status and reasons of current practices of science practical work at the secondary level. This research used Convergent Parallel Mixed design and collected data from secondary science students and teachers, SSC practical examiners, examination board representative, and science education experts using appropriate sampling strategies. The data also collected from observation of practical class and reviewed relevant policy documents. The findings revealed that the irregularity in taking science practical class is a reality for both rural and urban contexts. Most of the science teachers are not enough competent to conduct practical class and they assign practical marks to students based on the marks of theory part of science classes. A very few students are assessed as per examination guidelines at the SSC examination. SSC candidates mostly do not need to perform experiment during SSC examination. The major reasons behind this invalid and unreliable assessment process in SSC examination include: exam center management; lack of apparatus at SSC center, and lack of monitoring like theory part. The findings of the study set recommendations for all stakeholders includes exam authority, local education officials to practice better ethical standard as well as to curriculum authority to design proper guidelines of practical work.

Keywords: Practical work; Investigation in science, Practical Examination guidelines, Assessing practical work

PE-03: A study on the effectiveness of online classes in Bangladesh during the COVID-19 pandemic

Shahid Uddin Fahim¹, Md. Tanjimul Islam¹, Md. Mahmudul Hasan¹, Humaira Khondokar Gim¹, Fatema Jahan², Humayra Ferdous³, Tafazzal Hossain³, Md. Ehasanul Haque^{4*}

¹Department of Computer Science & Engineering, American International University-Bangladesh, Dhaka-1229, Bangladesh

²Department of Aquaculture, Khulna Agricultural University, Sonadanga, Khulna, Bangladesh

³Department of Physics, American International University-Bangladesh, Dhaka-1229, Bangladesh

⁴Department of Industrial & Production Engineering, American International University-Bangladesh, Dhaka-1229, Bangladesh

*Email: ehasanul@aiub.edu

Education system has been affected badly in all over the world due to COVID-19 pandemic. The outbreak of COVID-19 caused the prompt closure of almost all level of educational institutions and forced them to initiate online teaching-learning system. However, it was difficult to switch on online education system overnight specially for developing countries like Bangladesh. We investigated the impact of COVID-19 pandemic on online education in Bangladesh through a questionnaire-based survey. Around 310 students were surveyed to find their perspectives about online education in Bangladesh. The Linear Regression method was used for data analysis. We found around 60% people are satisfied on online education system in our country due to getting close interaction and enough effort from the teacher. On the contrary, the remaining students are unhappy by considering their health and mental issues as they are attending long time online classes. It is recommended to improve the internet speed, and provide sufficient educational materials, technical training on online education to students in Bangladesh to enhance the effectiveness of online education system during this pandemic period.

Keywords: COVID-19, Questionnaire-Based Survey, Linear Regression, Educational materials.

NATIONAL CONFERENCE ON PHYSICS-2021

06 – 07 August 2021

Theme: Physics for National Development

**INVITED & CONTRIBUTORY ABSTRACTS
FOR POSTER PRESENTATION**

Venue: Zoom Online Platform

Bangladesh Physical Society

PP-01: Assessment of ambient air quality in Dhaka city and sources of pollutant identification

M.M. Hasan, B.A. Begum, M.S. Rahman, M.A.M Mottalib Sarkar

Air Particulate Research Laboratory, Chemistry Division, Atomic Energy Centre, Dhaka, Bangladesh. Particulate air pollution is the major concern in Bangladesh and thus it is necessary to understand the characteristics of the pollutant as well as sources for further improvement of the air quality. In this research work, particulate matter (PM) sampling was done between September 2019 to August 2020 at a residential site (Atomic energy centre, AECD) in Dhaka. PM sampling was performed using a GENT sampler, which collects samples in two size fractions: $PM_{2.5}$ and $PM_{2.5-10}$. A total no of 128 fine samples were analyzed for mass, black carbon (BC) and elemental compositions. Mean $PM_{2.5}$ and BC concentration was found to be $77.06 \mu g m^{-3}$ and $15.52 \mu g m^{-3}$ respectively. The impact of meteorological variables on particulate matter was also studied which shows $PM_{2.5}$ and BC both makes negative correlation with the variables. Data on the concentrations of 17 elements (Na, Mg, Al, Si, S, Cl, K, Ca, Ti, V, Mn, Fe, Ni, Cu, Zn, Br, and Pb), black carbon, and mass were available for data analysis. Source apportionment of the trace elements in $PM_{2.5}$ was done by using Positive Matrix Factorization (PMF) technique. The identified sources include brick kilns, soil dust, road dust, motor vehicle, fugitive Pb, Zn source, Biomass burning and sea salt sources. Among them, Brick kiln contributes the highest followed by road dust and motor vehicle. It was found that more than 49.5% of the fine particle mass comes from anthropogenic source such as brick kilns, biomass burning, and motor vehicles.

PP-02: Recent Pre-monsoon Thunderstorms Scenario over Bangladesh

Mohammed Mozammel Hoque^{1*}, Syed Jamal Ahmed¹, M. A. K. Mallik², S. M. Quamrul Hasan² and Ishtiaque M. Syed³

¹Department of Physics, Dhaka University of Engineering and Technology (DUET), Bangladesh

²Bangladesh Meteorological Department, Agargaon, Dhaka, Bangladesh

³Department of Physics, Dhaka University, Dhaka, Bangladesh

Corresponding Author Email: mozammelpysics@gmail.com

Study is done to understand the frequency of Thunderstorms (TSs) which are locally known as Nor'westers or Kal-baishakhis, took place over Bangladesh during the pre-monsoon season (March-May) in the last 10 years (2012-2021). The data are collected from Bangladesh Meteorological Department (BMD), Agargaon, Dhaka, Bangladesh. It is found that, most of the severe TSs with wind speed 121-149 km/h which are embedded within squall lines and accompanied by lightning, thunder, hailstorms and heavy rains took place in the month of May whereas most of the moderate and light TSs took place in the month of April. According to the data analysis the no. of severe TSs took place in the last 10 years in the month of March, April and May are 0, 4 and 17 whereas No. of Moderate TSs are 4, 18, 17 and the No. of Light TSs are 29, 112 and 84 respectively. During the study period (2012-2021) there were about 06 severe TS events took place in Chattogram out of 11 events of the whole country. But the highest speedy TS (148 km/h) took place at Badalgachi, Naogaon on 24.4.2015. At same period highest 12 No. of Moderate TSs with wind speed (91-120) km/h took place in Chattogram region where as 06, 05 and 05 events took place in Dhaka, Sylhet, Barishal and Patuakhali regions. Out of 304 light TSs with wind speed (61-90) km/h, the highest 95 events took place in Chittagong region, 47 events in Dhaka region, 37 events in Sylhet region, 27 events in Rangpur region and 09 events in Mymensingh region. In the current study it is found that highest incidence of TSs occurs in Chattogram region whereas the second highest occurs in Rangpur region.

PP-03: Synthesis and Characterization of SWCNT modified Biopolymer with Super Cyclic Stability for Transient Energy Storage Application

RabeyaBintaAlam, Md. Hasive Ahmad, Muhammad Rakibul Islam*

Department of Physics, Bangladesh University of Engineering and Technology (BUET)

*Corresponding Author: rakibul@phy.buet.ac.bd

The wide-scale production of non-biodegradable e-waste from electrical appliances is causing great harm to the environment. The use of bio-polymer-based nanomaterials may offer a promising approach for the fabrication of eco-friendly sustainable devices. In this work, gelatin / single walled carbon nanotube (Gel/SWCNT) nanocomposites were prepared by a simple and economical aqueous casting method. The effect of SWCNT on the structural, surface-morphological, electrical, and electrochemical properties of the nanocomposite was studied. Fourier transform infrared spectroscopy (FTIR) and field emission scanning electron microscope (FESEM) showed an improved degree of interaction between the SWCNTs and Gel matrix. The surface wettability of the nanocomposites was found to be changed from hydrophilic to hydrophobic due to the incorporation of SWCNTs into the Gel matrix. The incorporation of SWCNTs was also found to reduce the DC resistivity of the nanocomposite by 4 orders of magnitude. SWCNTs also increase the specific capacitance of the nanocomposite from 124 mF/g to 467 mF/g at a current density of 0.3 mA/g. The electrochemical impedance spectroscopy analysis revealed an increase of the pseudocapacitance increased from 9.4 μ F to 31 μ F due to the incorporation of SWCNT. The Gel/SWCNT nanocomposite showed cyclic stability with capacitive retention of about 98% of its initial capacitance after 2000 charging/discharging cycles at a current density of 100 mA/g. The nanocomposite completely dissolves in water within 12 h, demonstrates it as a promising candidate for transient energy storage applications. The Gel/SWCNT nanocomposite may offer a new route for the synthesis of eco-friendly, biodegradable, and transient devices.

PP-04: Determination of essential elements in medicinal plants of the Sundarban mangrove forest by neutron activation analysis**Md. Barkat Ullah Pappu^{1,2}, Mohammad Amirul Islam^{1*}, Abdullah Al-mamun², Rinku Majumder²**¹Institute of Nuclear Science & Technology, Atomic Energy Research Establishment, Ganakbari, Ashulia, Dhaka-1349, Bangladesh²Physics Discipline, Khulna University, Khulna-9208, Bangladesh

E-mail of the corresponding author: liton80m@yahoo.com

In this research work, Neutron Activation Analysis (NAA) method was employed to assess the essential elements present in two medicinal plants (*Cynodon dactylon*, *Acanthus ilicifolius*) collected from three different locations of the Sundarbans, Bangladesh. The rhizosphere soil of the respective plants and surface soil from those locations were also examined for elemental analysis. Two standard samples (IAEA-CRM-SL-1 and NIST-SRM-1547) were allowed to evaluate the accuracy of the analysis. For quantification of the elements by NAA, all these samples were irradiated in rabbit irradiation facility of 3 MW TRIGA MARK-II research reactor of Bangladesh Atomic Energy Commission (BAEC) and gamma-ray spectrometry of the irradiated samples was performed using a high-resolution HPGe detector system at neutron activation analysis (NAA) laboratory of BAEC. A total of 9 elements (Al, Ca, Cl, Dy, K, Mn, Na, Ti and V) in the plant samples and 8 elements (Al, Ca, Dy, K, Mn, Na, Ti and V) in the soil samples were found. The concentration values of those elements in the plant samples were found to be safe for consumption. No such toxic elements were determined rather most of those are very essential for humans and animals. In the future, the elemental concentration in different parts of such plants can be monitored to assess the average daily intake of these parts by the local people and health hazard quotient with the assistance of the results of this study.

PP-05: Simulation of a severe thunderstorm and its characteristics over Dhaka, Bangladesh using WRF model

Most. Marioum^{1*}, M. A. K. Mallik², Suranjan Kumar Das¹, S.M. Quamrul Hassan² and Md. Omar Faruq²

¹Department of Physics, Jagannath University, Dhaka, Bangladesh

²Bangladesh Meteorological Department, Agargaon, Dhaka, Bangladesh

Email: marioum43411@gmail.com

An attempt has been made to simulate a thunderstorm event which was occurred over Dhaka on 23 April 2020 using Weather Research and Forecasting (WRF-ARW version 4.2.1) model. The WRF model was run for 48 hours on a single domain of 09 km horizontal resolution utilizing six hourly Global Final (FNL) datasets from 0000 UTC of 22 April 2020 to 0000 UTC of 24 April 2020 as initial and lateral boundary conditions. The model has been run using Yonsei University (YSU) scheme as Planetary Boundary Layer (PBL), Kessler scheme for microphysics, Kain-Fritsch (KF) scheme for cumulus physics, Revised MM5 scheme for surface layer physics, Rapid Radiative Transfer Model (RRTM) for longwave radiation, Dudhia scheme for shortwave radiation respectively. One hourly model output is visualized by Grid Analysis and Display System (GrADS). The model performance is evaluated by analyzing Mean Sea Level Pressure (MSLP), temperature, Relative Humidity (RH), wind pattern at various pressure levels, vertical wind shear, latent heat, Convective Available Potential Energy (CAPE), and Rainfall and compared with the observed data of BMD. From the comparison it is found that the performance of WRF model is reasonably well to predict the thunderstorm event over Dhaka, Bangladesh.

Keywords: Thunderstorm, WRF-ARW Model, FNL and CAPE.

PP-06: Implementation of meteorological data and atmospheric dispersion model for radiological consequence analysis

Md. Abu Khaer, S. Sultana Shiuli¹, Md. Ajijul Hoq, Mohammed Tareque Chowdhury, Mohammad Mizanur Rahman

Institute of Energy Science, Bangladesh Atomic Energy Commission, Dhaka, Bangladesh.

¹Department of Physics, Hajee Mohammad Danesh Science and Technology University, Dinajpur-5200, Bangladesh

For evaluation of radiological safety and emergency response, appropriate selection of dispersion model and their efficient implementation is crucial. In the case of radiological consequence and emergency management, there are three kinds of atmospheric dispersion models, such as Gaussian Plume Model (GPM) (1960s – 1970s), Lagrangian Gaussian Puff Model (LPGM), and Particle Random Walk Model (PRWM) (1980s – 1990s), and Computational Fluid Dynamics Model (CFDM) is under development (2000s). In radiological safety evaluation and emergency response, it is important to select how and which dispersion model can be used efficiently. Until now the GPM and LPGM have been used for radiological consequence assessment and emergency management. We studied the radiological safety and emergency response of the VVER-1200 type nuclear power plant using the RASCAL 4.3 and HOTSPOT 3.1.2 codes for INES levels 5, 6, and 7 reactor accidents due to Station Black Out (SBO) concomitant with Loss of Coolant Accident (LOCA) for both dry and rainy seasons. The simulation was performed using GPM and LPGM for short and long-range, respectively. In this work, meteorological data was used for the model calculation at atmospheric dispersion of radionuclides in both time and space up to 48 hours and 40.2 km, respectively from the RNPP site. In this study, two times of the year, corresponds to dry and rainy seasons, around the RNPP site was considered for the measurement of the radioactive dispersion and the accidental consequence. The weather data of the Ishwardi area, Pabna district was collected from the www.worldweatheronline.com website.

PP-07: Ternary scandium based antiperovskite Sc_3GaX ($X=\text{B},\text{N}$): DFT study**Istiaq Ahmed¹, F. Parvin¹, A.K.M. A. Islam^{1,2}**¹Department of Physics, Rajshahi University, Rajshahi-6205, Bangladesh²International Islamic University Chittagong, Kumira-4318, Chittagong, Bangladesh

We present an investigation on structural, mechanical, electrical, thermal and optical properties of the cubic inverse perovskite Sc_3GaX ($X=\text{B},\text{N}$) by first-principles density functional theory (DFT). The optimized lattice parameters, three independent elastic constants, bulk moduli, shear moduli, Young's moduli, Pugh's ratio, Poisson's ratio are estimated and discussed. Changes in the mechanical properties are noticed when B is replaced by N. The electronic properties such as band structure and partial density of states of Sc_3GaX ($X=\text{B},\text{N}$) at zero pressure are studied. The band structure shows considerable hybridization of Sc-*d* states with the *p*-states of B/N. Thermal properties such as Debye temperature, specific heats, thermal expansion coefficient have also been studied in the pressure range 0 to 50 GPa and the temperature range 0 to 1000 K. Optical functions are calculated and the prominent features discussed. The high reflectivity of 95-80% in the IR region and 50-55% above this region up to 8 eV would predict these to be good coating materials.

PP-08: Recent track climatology of cyclonic disturbances over the Bay of Bengal**Shahanaj Sultana*, M. A. K. Mallik, Md. Shadikul Alam, Md. Omar Faruq, Md. Abdul Mannan and S.M. Quamrul Hassan**

Bangladesh Meteorological Department, Agargaon, Dhaka, Bangladesh

Corresponding Author Email: Shahanaj76@yahoo.com

Compared to global perspective the Bay of Bengal (BoB) is an important frequently tropical cyclone forming basin. Track climatology of Cyclonic Disturbances (CDs) is imperative to minimize casualties and damages. An attempt has been made to construct the seasonal distribution of cyclones over the BoB during 1891-2020 using Bangladesh Meteorological Department (BMD) and India Meteorological Department (IMD) e-Atlas data. The most devastating cyclones' tracks of 1991, 1994, 2007, 2008, 2009 and 2020 are also drawn over the BoB. The number and frequency of cyclone over the BoB varies year to year. The analysis represents that the category of cyclonic stage are 35, 123, 97 and 28 in pre-monsoon, monsoon, post-monsoon, winter seasons respectively whereas correspondingly severe cyclonic storms are 58, 33, 103 and 26 over the BoB during 1891-2020. Initially, the cyclone of all intensity over the BoB follows Westward/Northwestwards tracks, some of them re-curved and follows North/Northeastwards tracks. Sometimes looping track is also found over the BoB. It is also found that some cyclones have completed their course of journey in the BoB without making any landfall. This variation of cyclone makes the BoB basin more vulnerable and more challenging for track forecasting.

PP-09: Database from secondary data of concentration of NORM and making an absorbed dose map for overall Bangladesh**Md. Ashik Azad Khan¹, A.K. M. Saiful Islam Bhuian², Shahadat Hossain² and Quazi Muhammad Rashed Nizam¹**¹Department of Physics, University of Chittagong, Chittagong-4331, Bangladesh²Atomic Energy Center Chittagong, Bangladesh Atomic Energy Commission, Bangladesh

Natural radioactivity emanates from extraterrestrial sources as well as from naturally occurring radioactive materials (NORM) existing in the earth crust and varying with different geological formation of various rocks. It is important to have a background and baseline data for the concentration of NORM

for the future use and safety from the radiation protection point of view. Keep that in mind, many researchers are measuring the environmental samples from the overall Bangladesh since few decades. But because of lacking organized data or sampling points, accumulation of measured data points, researchers were measuring the samples from the locations of insignificant distance. To avoid that redundancy of sampling points for future measurement of environmental NORM concentrations we accumulate all the measured data points overall Bangladesh since 1990- 2020 from the published paper and unpublished thesis in this study. We divide the whole country into 2094 grids of 5'x5' area which is about 25 square miles by using geographical information system (GIS). Then we overlap the measured data locations into this grid. From this, we found that some of the locations (grid) have been chosen by the researchers for environmental NORM measurement many times (max 13). Also, we found the maximum of the country regions has not been measured yet for a single time. So, there are a lot of blank region which is needed to consider for future measurement.

In this study we focus on the appraisal of absorbed dose due to NORM from ^{238}U and ^{232}Th series, ^{40}K , ^{137}Cs and the corresponding geographical information system (GIS) predictive mapping for the secondary data collected from previously done a total of 95 research works of Bangladesh within a time period 1990-2020. With GIS, all the collected secondary data was accumulated as a whole, but there were many locations where no research work or previous study had done. So, inverse distance weighting (IDW) technique was used to interpolate the scattered data for absorbed doses and NORM concentrations by converting measured points into continuous surfaces.

The resulting GIS prediction maps and distribution study of radionuclides could be used to understand the variation and cause of variation and to explain the trend of variation of absorbed dose and activity concentration of NORM.

PP-10: Radiation monitoring around cancer hospital campus and evaluation of radiological risk on public health

Md. Arman Ali¹, M. S. Rahman^{2*}, S. Yeasmin², Md. Kabir Uddin Sikder¹

¹Department of Physics, Jahangirnagar University, Savar, Dhaka, Bangladesh

²Health Physics Division, Atomic Energy Centre, Shahbag, Dhaka-1000, Bangladesh

*Corresponding author, e-mail: msrahman1974@yahoo.com

The medical usage of ionizing radiation offers great benefit to patient through diagnosis & treatment. The National Institute of Cancer Research & Hospital (NICRH) is the only tertiary level centre of the country connecting in multidisciplinary cancer patient management. Even though modern radiation generating equipment has significantly increased patient care, improper or unsafe handling of the radiation generating equipment may also cause potential health risks for patients, workers and also public. Therefore, real-time radiation monitoring around the NICRH campus is needed in order to detect the presence of the radiation hazard arising from medical use of ionizing radiation. The aim of the study is to monitor the real-time radiation around the NICRH campus and evaluation of radiological risk on public health. The real-time radiation monitoring around the NICRH campus was carried out using digital portable radiation monitoring devices and those devices were placed at 1 meter above the ground on tripod. 32 locations around the NICRH campus were selected for monitoring the real-time radiation and data collection time for each monitoring point (MP) was 1.0 hour. The MPs were marked-out using the Global Positioning System (GPS) device. The real-time radiation dose rates were ranged from 1.15 - 4.05 $\mu\text{Sv.h}^{-1}$ with an average of $1.781 \pm 0.310 \mu\text{Sv.h}^{-1}$. The annual effective doses to the public from the natural as well as hospital radiation were ranged from 2.255- 4.712 mSv and the mean was found to be $3.111 \pm 0.556 \text{mSv}$. The excess life-time cancer risk (ELCR) on public health were ranged from 8.972×10^{-3} - 18.747×10^{-3} with an average of 12.378×10^{-3} . It is observed from the study that the annual effective doses and ELCR on public around the NICRH campus is higher than those of the prescribed limit of the International Commission on Radiological Protection (ICRP).

Key Words: NICRH; In-Situ; Radiation; ELCR; Public.

PP-11: Estimation of radiation risk on worker & public from radiological facility using thermoluminescent dosimeters**Omar Faruk¹, M. S. Rahman^{2*}, K. N. Sakib¹, M. M. Tasnim¹, S. Yeasmin²**¹Department of Physics, MawlanaBhashani Science and Technology University, Santosh, Bangladesh²Health Physics Division, Atomic Energy Centre, Shahbag, Dhaka-1000, Bangladesh*Corresponding author, e-mail: msrahman1974@yahoo.com

Atomic Energy Centre Dhaka (AECD) is a radiological facility which uses radioactive substances & radiation generating equipments for service, training, research & development activities. Radiation generating equipments and radioactive substances in the radiological facility has to be handled very carefully for the protection of the people and the environment from undue radiation hazard. The aim of the study is to continuous indoor radiation monitoring at AECD campus using Thermoluminescent Dosimeter (TLD) and estimation of radiation risk on workers & public. Continuous radiation monitoring was performed at the AECD campus from February-June 2020 using the TLDs. Twenty locations were selected at the AECD campus for continuous radiation monitoring and each location one TLD was placed at one meter above the ground. The annual effective dose to workers and public were calculated based on the continuous radiation monitoring data and ranged from 0.301 ± 0.021 mSv to 0.459 ± 0.023 mSv with an average of 0.399 ± 0.038 mSv. The excess life-time cancer risk (ELCR) on workers & public were estimated based on the annual effective dose and ranged from 1.197×10^{-3} to 1.826×10^{-3} with an average of 1.590×10^{-3} . The average annual effective dose and ELCR on workers & public were lower than those of the worldwide permissible values as per recommendation of the International Commission on Radiological Protection (ICRP). Continuous radiation monitoring is very important for identification of malfunction of the radiation generating equipments and improper handling of the radioactive substances at the radiological facility. The study would help for minimization of the radiation risk on workers & public and for detection of the abnormal situation at radiological facility.

PP-12: Real-time radiation monitoring around BIRDEM Hospital campus and estimation of radiation risk on public health**Sk. Sabbir Ahmed Shakil¹, M. S. Rahman^{2*}, S. Yeasmin², Md. Kabir Uddin Sikder¹**¹Department of Physics, Jahangirnagar University, Savar, Dhaka-1342, Bangladesh²Health Physics Division, Atomic Energy Centre, Shahbag, Dhaka-1000, Bangladesh*Corresponding author, e-mail: msrahman1974@yahoo.com

Ionizing radiation plays an important role for diagnosis & treatment of patient in the hospital. More than 90% public radiation exposure comes from the medical procedures from the man-made radiation sources. Public who are living beside the large hospital campus is usually getting higher radiation comparing to others. The aim of the study is to monitor the real-time radiation around the BIRDEM Hospital campus, Shahbag and estimation of excess life-time cancer risk (ELCR) on public based on annual effective dose. The real-time radiation monitoring was performed from February-March 2021 using digital portable radiation monitoring devices and GARMIN eTrex HC Series Personal Navigator for location identification. The digital portable radiation monitoring device was placed at 1 meter above the ground on tripod and data collection time for each monitoring point (MP) was 1 hour. 32 MPs were selected for taking real-time radiation data around the BIRDEM Hospital campus. The measured dose rates due to natural and man-made radionuclides were ranged from 1.451 ± 0.247 to 3.512 ± 1.579 μ Sv/hr with an average of 2.343 ± 0.452 μ Sv/hr. The annual effective dose to the public due to hospital's radiation was varied from 2.542 ± 0.432 to 6.153 ± 2.767 mSv with an average of 4.105 ± 0.792 mSv. ELCR on public around the BIRDEM hospital campus based on annual effective dose was calculated and varied from 10.114×10^{-3} to 24.480×10^{-3} with an average value of 16.333×10^{-3} . Real-time radiation monitoring around hospital is important for detection of the equipment's fault and improper operation of the radiation

generating equipments. It is observed from the study that in every thousand people, sixteen persons are at the risk of developing cancer caused by the scattered radiation exposure from the BIRDEM hospital during his/her lifetime.

PP-13: Real-time Radiation Monitoring around LABAID Hospital Campus and Evaluation of Radiation Risk on Public

A. A. Shuhan¹, M. S. Rahman^{2*}, S. Yeasmin², Md. Kabir Uddin Sikder¹

¹Department of Physics, Jahangirnagar University, Savar, Dhaka-1342, Bangladesh

²Health Physics Division, Atomic Energy Centre, Shahbag, Dhaka-1000, Bangladesh

*Corresponding author, e-mail: msrahman1974@yahoo.com

Public are usually exposed to radiation from natural and man-made sources. The usage of radiation in medical applications continues to increase worldwide. There is a probability of getting cancer, if public received small amount of ionizing radiation during long time. Hospital workers, public who are living nearby are getting higher radiation dose because of increasing usage of diagnostic and therapeutic procedures to patients. The purpose of this study is to monitor the real-time radiation around the LABAID Specialized Hospital campus, Dhanmondi and evaluation of excess life-time cancer risk (ELCR) on public health based on annual effective dose. The real-time radiation monitoring was performed using digital portable radiation monitoring device and GARMIN eTrex GPS device for location identification. The portable radiation monitoring device was placed at 1 meter above the ground on tripod and data acquisition time for each monitoring point (MP) was 1 hour. 32 MPs were selected for collection of radiation dose rates at different locations around LABAID Hospital campus. The radiation monitoring was performed in October 2020. The measured dose rates due to natural and man-made radionuclides were ranged from 0.02-1.48 $\mu\text{Sv/hr}$ with an average of $0.178 \pm 0.096 \mu\text{Sv/hr}$. The annual effective dose to the public due to radiation was varied from 0.222-0.528 mSv with an average of $0.311 \pm 0.054 \text{ mSv}$. ELCR on public based on annual effective dose was calculated and varied from 0.881×10^{-3} - 2.102×10^{-3} with an average value of 1.22×10^{-3} . Real-time radiation monitoring around hospital is required for minimizing unnecessary exposure to the public from man-made sources and thereby ensure the safety of the public. It can be estimated from the result that in every thousand people, one person is at the risk of developing cancer caused by the scattered radiation exposure from the LABAID hospital.

PP-14: Implementation of Meteorological Data and Atmospheric Dispersion Model for Radiological Consequence Analysis

Md. Abu Khaer, S. Sultana Shiuli¹, Md. Ajjil Hoq, Mohammed Tareque Chowdhury, Mohammad Mizanur Rahman

Institute of Energy Science, Bangladesh Atomic Energy Commission, Dhaka, Bangladesh.

¹Department of Physics, Hajee Mohammad Danesh Science and Technology University, Dinajpur-5200, Bangladesh

*khaetaperapece08@gmail.com

For evaluation of radiological safety and emergency response, appropriate selection of dispersion model and their efficient implementation is crucial. In the case of radiological consequence and emergency management, there are three kinds of atmospheric dispersion models, such as Gaussian Plume Model (GPM) (1960s – 1970s), Lagrangian Gaussian Puff Model (LPGM), and Particle Random Walk Model (PRWM) (1980s – 1990s), and Computational Fluid Dynamics Model (CFDM) is under development (2000s). In radiological safety evaluation and emergency response, it is important to select how and which dispersion model can be used efficiently. Until now the GPM and LPGM have been used for radiological consequence assessment and emergency management. We studied the radiological safety and emergency

response of the VVER-1200 type nuclear power plant using the RASCAL 4.3 and HOTSPOT 3.1.2 codes for INES levels 5, 6, and 7 reactor accidents due to Station Black Out (SBO) concomitant with Loss of Coolant Accident (LOCA) for both dry and rainy seasons. The simulation was performed using GPM and LPGM for short and long-range, respectively. In this work, meteorological data was used for the model calculation at atmospheric dispersion of radionuclides in both time and space up to 48 hours and 40.2 km, respectively from the RNPP site. In this study, two times of the year, corresponds to dry and rainy seasons, around the RNPP site was considered for the measurement of the radioactive dispersion and the accidental consequence. The weather data of the Ishwardi area, Pabna district was collected from the www.worldweatheronline.com website.

PP-15: Real-time Radiation Monitoring at Outdoor of Mitford Hospital Campus and Estimation of Radiation Risk on Public

L. A. Tonu¹, M. S. Rahman^{2*}, Pretam K. Das¹, S. Yeasmin²

¹Department of Physics, Pabna University of Science and Technology, Pabna, Bangladesh

²Health Physics Division, Atomic Energy Centre, Shahbag, Dhaka-1000, Bangladesh

*Corresponding author, e-mail: msrahman1974@yahoo.com

The medical use of ionizing radiation has expanded worldwide. Radiation generating equipments and radioisotopes are frequently used in the hospital for diagnostics or treatment purposes to patients. Advanced technology has opened new prospect to diagnostics and therapeutic procedures to patients. Although the advanced technology has enhanced patient care, improper or unsafe handling of radiation technology may also cause potential health risks for both patients, workers and also public. So, real-time radiation dose rate monitoring at outdoor environment in hospital is important for detection of undue radiation hazard coming from medical use of ionizing radiation. The objective of the study is to monitor the real-time dose rate at outdoor environment of Mitford hospital and evaluation of radiation risk to public. The real-time radiation monitoring at outdoor environment of Mitford hospital was performed using digital portable radiation monitoring devices and those devices were placed at 1 meter above ground on tripod. 21 outdoor locations were selected for collection of the real-time radiation dose rate and data acquirement time for each monitoring point (MP) was 1.0 hour. The MPs were marked-out using Global Positioning System (GPS) device. The measured dose rates were ranged from 0.08 - 0.48 $\mu\text{Sv.h}^{-1}$ with an average of $0.244 \pm 0.079 \mu\text{Sv.h}^{-1}$. The annual effective doses to the public due to the natural as well as hospital radiation were ranged from 0.141- 0.841 mSv and the mean was found to be $0.428 \pm 0.139 \text{ mSv}$. The excess life-time cancer risk (ELCR) on public were ranged from 5.8×10^{-4} - 4.66×10^{-3} with an average of 1.86×10^{-3} . However, the annual effective doses to public were well below the prescribed limit of the International Commission on Radiological Protection (ICRP).

PP-16: Synthesis of Gallium (Ga) Doped CdO/p – Si Heterojunction and Evaluation of Junction parameters

AbdurRouf, M. K. R. Khan^{*}, M. Saifur Rahman, M. S. I. Sarker and M. Mozibur Rahman

Department of Physics, University of Rajshahi, Rajshahi 6205, Bangladesh

In this work, *CdO:Ga/p – Si* heterojunctions were fabricated by depositing Gallium (Ga) doped *CdO* (*CdO:Ga*) thin film on a *p*-type single crystal silicon wafer by spray pyrolysis technique. The characteristics of heterojunction and junction parameters were evaluated by Current-Voltage (*I – V*) and Capacitance-Voltage (*C – V*) study. The XRD study showed that the prepared *CdO:Ga* films on Si substrate are polycrystalline in nature and the crystal structure is identified as face-centered cubic (FCC). SEM images are found smooth and spherical shape grains of almost even sizes are distributed uniformly over the film surface for the film prepared on Si wafer. The room temperature PL study of *CdO:Ga* films

grown on $p-Si$ substrate showed emission peaks due to the band-to-band and defect states. From the Hall measurement, $CdO:Ga$ is found as n -type semiconductor with carrier concentration of the order of $\sim 10^{20} \text{ cm}^{-3}$. The Current-Voltage ($I-V$) characteristics confirmed the rectifying diode behavior of the $CdO:Ga/p-Si$ heterojunction. The magnitude of the ideality factor and the $C-V$ response of the fabricated heterostructure at different oscillation frequencies reveal the good diode characteristics.

PP-17: Surface Morphology of CaDoped $\text{Li}_{0.5}\text{Bi}_{0.5}\text{Fe}_{0.5}\text{Nb}_{0.5}\text{O}_3$ Perovskite

M. A. Rashid*, K. A. Rahman* and A.K.M. Akther Hossain**

*DSHE, Ministry of Education Bangladesh, Dhaka.

**Department of Physics, Bangladesh University of Engineering and Technology, Dhaka

In this research attempt has been made to study the grain boundary segregation in polycrystalline $\text{Li}_{0.5}\text{Bi}_{0.5}\text{Fe}_{0.5}\text{Nb}_{0.5}\text{O}_3$ (LBFNO) perovskite with different amount of Ca doping in A-site of ABO_3 perovskite. Standard solid state reaction technique followed by hand milling in Acetone medium was used to synthesize LBFNO with different sintering temperatures. Morphological analysis of sintered samples was made by Field Emission Scanning Electron Microscopy (FESEM). Moreover, Band Pass Filter was applied on digital SEM image for shading correction and smoothing the specified size by Gaussian filtering in Fourier Space to track the trend of grain boundary formation. Besides, we investigated how the Ca influences the segregation of grain boundary.

PP-18: Reduced Graphene Oxide Supported Cobalt Ferrite Nanoparticles: A Study of Synthesis Mechanism, Structural, Magnetic and Thermal Stability Characterization

Gobinda Chandra Mallick^a, M. Al-Mamun^{*b}, M. R. Rahman^a, M. Al-Fahat Hossain^a, Sheikh Manjura Hoque^b

^a Physics Discipline, Khulna University, Khulna-9208, Bangladesh.

^b Materials Science Division, Atomic Energy Centre Dhaka, Dhaka, Bangladesh

In present study, graphene oxide (GO) synthesized using the modified hummers' method was reduced using hydrazine hydrate to make it perform as a surface for the decoration of cobalt ferrite nanoparticles (CFN) produced via the co-precipitation route. CFN were successfully filled on the surface of reduced graphene oxide (RGO) through the hydrothermal method. The coexistence of RGO and CFN in the nanocomposite was confirmed by X-ray diffraction analysis (XRD), scanning electron microscopy (SEM), Fourier-transform infrared spectroscopy (FTIR). The XRD pattern of the nanocomposite exhibits the spinel cubic phase formation with the $Fd\bar{3}m$ space group with crystallite size 28.55 nm. SEM was used to corroborate the loading of CFN on the RGO nanosheet. FTIR results manifest the functional groups present in all the samples, while Raman study substantiates the reduction of GO. Thermogravimetric analysis (TGA) displays that the nanocomposite showed better thermal stability at high temperature than GO nanosheet. The soft magnetic nature is observed for RGO-CFN nanocomposite with a saturation magnetization of 24.11 emu/g at 300K, by means of a Physical Property Measurement System (PPMS). Such types of structural and magnetic behavior make the nanocomposite a good candidate in various application fields such as dye degradation, adsorption, photocatalytic activity, drug delivery etc.

PP-19: Structural, electrical and magnetic properties of Ce and Fe doped SrTiO_3

Tarique Hasan,¹ Arnab Saha,¹ M. N. I. Khan,² M. A. Basith,³ Muhammad Shahriar Bashar,⁴ H. N. Das,² R. Rashid², Tarique Hasan,¹ and Imtiaz Ahmed¹

¹Department of Electrical and Electronic Engineering, University of Dhaka, Dhaka-1000, Bangladesh ²Materials Science Division, Atomic Energy Centre, Dhaka-1000, Bangladesh

³Nanotechnology Research Laboratory, Department of Physics, Bangladesh University of Engineering and Technology, Dhaka-1000, Bangladesh

⁴Institute of Fuel Research and Development, BCSIR, Dhaka-1205, Bangladesh

E-mail: ni_khan77@yahoo.com, mtiaz@du.ac.bd

We used solid state reaction technique to synthesize Strontium titanate SrTiO₃ (STO), Ce doped Sr_{1-x}Ce_xTiO₃ and (Ce, Fe) co-doped Sr_{1-x}Ce_xTi_{1-y}Fe_yO₃ samples in powder form. The crystallization temperature of the samples was estimated to be ~1080° from differential scanning calorimetry. The Rietveld analysis of the powder X-ray diffraction pattern confirmed the cubic Pm-3m phase of synthesized samples. We observed grain size reduction in both Ce and (Ce, Fe) co-doped samples as compared to those of undoped STO; from scanning electron microscopy measurements. Chemical component identification and their relative atomic percentage estimations were done by energy dispersive X-ray spectroscopy. The complex impedance analysis revealed the effect of doping on frequency dependent dielectric constant and resistivity of the samples. The orders of magnitude enhancement in remnant magnetization and coercivity have been observed in (Ce, Fe) co-doped Sr_{0.97}Ce_{0.03}Ti_{0.90}Fe_{0.10}O₃ sample in vibrating sample magnetometer measurements. The ferromagnetic hysteresis in our (Ce, Fe) co-doped samples might have the potentials for interesting magnetic as well as multiferroic applications.

PP-20: Determination of thermo-optic coefficient, nonlinear absorption coefficient and nonlinear refraction coefficient in the thermal regime of L-tryptophan using Closed aperture CW Z-scan

S. A. Tarek¹, S. B. Faruque¹, S. M. Sharafuddin^{*1}, K. M. E. Hasan¹, A. K. M. M. Hossain¹, H. Ara¹, M. K. Biswas², Y. Haque¹

¹Nonlinear BioOptics Laboratory, Department of Physics, Shahjalal University of Science and Technology, Sylhet, Bangladesh

² Physics Department, Sunamgonj Government College, Sunamgonj, Bangladesh

^{*}Corresponding author: sharif-phy@sust.edu

The closed aperture (CA) continuous wave (CW) Z-scan of aromatic amino acid L-tryptophan was performed with red diode laser to investigate the variation of on axis nonlinear phase shift $\Delta\Phi_0$ with the change of optical field strength. In the studied range of incident optical fluence (I_0) varying from 150 MW/m² to 290 MW/m², $\Delta\Phi_0$ was found to vary nonlinearly. This nonlinear variation is explained by considering the effects of both linear and nonlinear absorptions of radiation on the thermo-optical refractive index. Using the quadratic fitting of $\Delta\Phi_0$ with I_0 we have found the thermo-optic coefficient of refractive index dn/dT , thermal coefficient of nonlinear refractive index n_2^T and the nonlinear absorption coefficient β in the observed power regime.

PP-21: Study on the iron-deficient non-stoichiometry driven electromagnetic and magnetoelectric properties of multiferroic composites

Sharifa Nasrin^{a, b) *}, Tabassum Haque Joyee^{a)}, A.K.M. Akther Hossain^{c)}, and Md. D. Rahaman^{a)}

^{a)} Department of Physics, University of Dhaka, Dhaka 1000, Bangladesh

^{b)} Directorate of Secondary and Higher Education (DSHE), Ministry of Education, Bangladesh

^{c)} Department of Physics, Bangladesh University Engineering and Technology (BUET), Bangladesh

Email: sharifa_labiba@yahoo.com

In this work, iron-deficient non-stoichiometry (IDNS) driven electromagnetic and magnetoelectric properties (1-y) [Ba_{0.90}Ca_{0.10}Zr_{0.10}Ti_{0.90}O₃] + (y) (Ni_{0.25}Cu_{0.13}Zn_{0.62}Fe_{2-x}O_{4-3x/2}) (x = 0.00-0.12; y = 0.2, 0.5)

multiferroic composites were investigated. The composites were developed via the solid-state sintering approach followed by sintering at 1200°C for 5h. The phase formation and the crystal structure of the individual phases and simultaneousness of the individual phases in the composites were confirmed by powder X-ray diffraction (XRD) and Fourier transform infrared spectroscopic (FTIR) analyses without any traceable secondary phase formation. The nonsystematic variation in lattice constant, crystallite size, and unit cell volume with IDNS was observed. The scanning electron microscopic (SEM) study ascertained the formation of grains which possessed polyhedral or irregular shapes and sizes with little agglomeration and porosity with IDNS. The dielectric constant was fitted by the modified Debye function and revealed that the low-frequency dielectric dispersive behavior followed Koop's and Maxwell-Wagner's model. The ac conductivity was fitted according to Jonscher's power law and governed by the hopping of small polarons amid the localized states. Nyquist plots were fitted using an equivalent circuit and ascertained that the conduction process was mainly attributed to the combined effect of grain and grain boundary contribution. The existence of a non-Debye type of relaxation was ascertained by complex electric modulus study. The permeability was declined with IDNS for $x = 0.0$ - 0.12 ; $y = 0.2$ while it was increased for $x = 0.04$, and after which decreased with IDNS for $y = 0.5$. The highest value ($a_{ME} \sim 0.17$ V/cm-Oe) of magnetoelectric coefficient was realized for $x = 0.0$; $y = 0.5$ composite due to the macro-elastic interplay mediated by strain between two phases.

PP-22: Comparison of perovskite nanorod's bandgap obtained via diverse methods for optoelectronic applications

Mohammad Tanvir Ahmed, Shariful Islam, Farid Ahmed

Department of Physics, Jahangirnagar University, Dhaka-1342, Bangladesh

Abstract Organic-inorganic perovskites (OIP) have become widely studied materials for their superior optoelectronic (OE) applications. Perovskite materials have become a major focus in OE technology because of their ease of manufacturing and low cost. In this research we synthesized $\text{CH}_3\text{NH}_3\text{PbI}_3$ perovskite nanorods (PNRs) as an efficient light absorber for OE applications via one step deposition. Equimolar mixture of hydroiodic acid (HI) and methylamine (MA) solution was continuously stirred for half an hour at 0°C temperature. The solution was then heated for around 20 minutes to evaporate the solvent, resulting in the formation of the methylamine iodide (MAI) crystal. Then, in dimethylformamide (DMF), 1.5M perovskite solution was prepared via dissolving equimolar MAI and PbI_2 . Finally, thin film containing PNRs was obtained via spin coating of the precursor solution at 1000 rpm for 30 sec and annealed at 80°C for 20 minutes. X-ray diffraction was performed to identify the crystal structure of the perovskite, revealing the cubic phase. Grains of PNRs were observed using Scanning electron microscope. UV-vis spectrometer and impedance analyzer were used to investigate the optical and electrical properties, respectively. Finally, a comparison of several bandgap measuring methods was carried out.

PP-23: Performance optimization of TCO-less back contact dye-sensitized solar cells utilizing indoline and porphyrin sensitizer based on cobalt electrolyte

Md. Zaman Molla*², Ajay Kumar Baranwal³, Shuzi Hayase³ and Shyam S. Pandey¹

¹Graduate School of Life Science and Systems Engineering, Kyushu Institute of Technology, 2-4 Hibikino, Wakamatsu, Kitakyushu, 808-0196, Japan

²Ahsanullah University of Science and Technology, Dhaka-1208, Bangladesh

³Info-Powered Energy System Research Center, University of Electro-Communications, Tokyo, Japan

E-mail address: zaman.molla.as@aust.edu, whyzaman@gmail.com

Transparent conductive oxide-less (TCO-less) back contact (BC) dye-sensitized solar cell (DSC) employing stainless steel (SS) metal mesh coated with nanoporous TiO_2 film as a flexible photoanode utilizing cobalt complex redox shuttle is being reported. A thin layer of titanium (Ti) metal on the SS metal mesh was proved to be effective to retard the back-electron transfer, which was ensured by the dark current measurements. It was assured by electrochemical impedance spectroscopy (EIS) that NP TiO_2 with 30 nm particle size demonstrated less charge transport resistance at TiO_2 -dye-electrolyte interface as compared to TiO_2 with the particle size of 15-20 nm. TCO-less BC-DSC using dye cocktail of indoline dyes D-205 and D-131 (1:1) with comparatively larger NP of TiO_2 of 30 nm as compared to smaller NP of TiO_2 of 15-20 nm demonstrated improved photoconversion efficiency (PCE) of 4.02 %. In order to enhance the PCE further, TCO-less BC-DSC with cobalt redox shuttle sensitized with porphyrin sensitizer (YD2-o-C8) with a larger optical area was explored. An optimum thickness of 10 μm of TiO_2 film was proved to be the best leading to an improved PCE of 5.26%.

PP-24: Design and investigation of step-index core polymer directional coupler for board-level optical circuitry

Fariha Tasnim¹, Md Omar Faruk Rase^{1*} and Takaaki Ishigure²

¹Physics Discipline, Khulna University, Khulna-9208, Bangladesh

²Faculty of Science and Technology, Keio University, Yokohama 223-8522, Japan

*Corresponding Author: ofr_ju@phy.ku.ac.bd

The optical circuits require a variety of devices, in which optical signal can transfer with high speed data transmission and release less energy as a Joule heating effect than the conventional electrical circuits. Meanwhile, polymer optical waveguides have been implemented in various optoelectronic devices and shown their potentials in a short-reach arena with low propagation loss. Hence, in this research, we demonstrate a directional coupler as a splitter realized with organic/inorganic hybrid polymer materials (core: NP-005 and Cladding: NP-211 correspond to refractive indices 1.575 and 1.567, respectively at 1550 nm) because of their low propagation loss, cost effective in manufacturing, and easy integration on printed circuit boards (PCBs). We introduce this polymer directional coupler as follows: two input and output straight cores are connected to two S-bend segments, and these two S-bend cores are connected to another two straight waveguides in the middle with a separation distance between them. The index profile of this coupler is a step-index (SI) type, and the core diameter should be controlled within 6 μm . We design and analyze this polymer coupler by utilizing the beam propagation method (BPM) at 1550 nm. The power efficiency of this SI directional coupler is approximately 68% at 1550 nm. We also investigate the insertion loss and polarization dependency for practical use.

PP-25: Effect of Gd substitution on the structural, dielectric and electric properties of Ni-Cu-Cd ferrite nanoparticles

M. Anwar Hossain^{1,2}, M. Belal Hossen^{2*}

¹Department of Physics, Chota Sarifpur Degree College, Lalmai, Cumilla, Bangladesh

²Department of Physics, Chittagong University of Engineering & Technology (CUET), Bangladesh

Gd substituted NiCuCd nanoferrites has been synthesized using sol-gel auto combustion technique. The XRD analysis ascertains single-phase cubic spinel structure of the samples free from impurity. Surface morphology and compositional analysis are characterized by Field Emission Scanning Electron Microscopy (FESEM) and the availability of the elements in the samples is confirmed Energy Dispersive X-ray (EDX) techniques. The lattice constant and grain size of this composition increases with Gd content. The dielectric measurement has been carried out at room temperature. The real part of dielectric constant (ϵ') initially decreases rapidly in the low frequency region but at very high frequencies it becomes independent of applied frequency. Due to the decrease of polarization, the dielectric loss tangent ($\tan\delta_E$) decreases with the increase of Gd content. The dielectric parameters, electric modulus,

impedance spectroscopy and ac conductivity (σ_{AC}) have been observed using impedance analyzer. The dynamics of the conduction process has been understood by the complex modulus spectra. The value of grain boundary resistance (R_{gb}) and grain resistance (R_g) has been calculated from the cole-cole plot drawn from impedance spectra. The value of σ_{AC} increases with AC applied field frequency which obeys the Jonschers power law.

PP-26: Synthesis and characterization of europium doped nickel zinc cobalt ferrite

Imran Sardar^a, Md. Nazrul Islam Khan^{b*}, Md. RashedurRahman^a, Md. Sohel Sikder^a

^aPhysics Discipline, Khulna University, Khulna-9208, Bangladesh

^bMaterials Science Division, Atomic Energy Centre, Dhaka 1000, Bangladesh

E-mail: ni_khan77@yahoo.com

The present work is focused on the influence of europium (rare earth) doped Ni-Zn-Co ferrites. The ferrite sample of the composition $Ni_{0.5}Zn_{0.3}Co_{0.2}Eu_xFe_{2-x}O_4$ (where $x = 0.00, 0.02, 0.04, 0.06, 0.08, 0.10$) was synthesized using conventional solid-state reaction method from the oxide powders of Ni, Zn, Co, Eu and Fe. Effects of ferrite contents on the structural, electrical, magnetic and dielectric properties were thoroughly investigated. The structural properties and phase identification were studied by using X-ray diffraction (XRD) and the analyses found spinel cubic structure for ferrite samples. XRD pattern of NZCEF has been introduced with $EuFeO_3$ secondary peak. The lattice parameter initially decreased slightly then increased with Eu concentrations (maximum at $x=0.08$). The porosity was found decreasing from 45.43% to 39.28% as the 'x' was increased from 0.02 to 0.10. FTIR analyses confirmed the metal-oxygen bonds in ferrite structures. The average grain size measured by SEM was found slightly increasing and maximum at $x=0.08$. VSM was used to calculate the M-H loop at room temperature. For $x=100\%$, the saturation magnetization was found to be maximum. The real part of relative permeability was maximum at $x=0.02$ and then decreased with additional content of x. The frequency dependent real part of relative permittivity (ϵ) was maximum for pure ferrite and decreased with europium. On the other hand, the resistivity (ρ) had the maximum values for $x=0.10$ and minimum for pure ferrite. From the observed magnetic, dielectric and electrical properties, the optimum content of composition for this material can be found which makes it a good candidate for potential applications in storage device, magnetic sensors and spintronic devices.

PP-27: Facile Method for Synthesizing ZnO Nanorod with Controllable Size

M. Sultana^{1,2}, Mohammad Jellur Rahman^{1*}, M. S. Bashar²

¹Department of Physics, Bangladesh University of Engineering and Technology, Bangladesh

²Institute of Fuel Research & Development, Bangladesh Council of Scientific and Industrial Research, Dhaka-1205, Bangladesh

*Corresponding author email: mjrahman@phy.buet.ac.bd

ZnO nanorods have been successfully synthesized by microwave assisted irradiation process using a customized domestic microwave. A simple one step microwave treated method has been used to optimize the synthesis time and the effects of different process parameters such as precursor reagents, synthesis time, precursor concentration, etc. have been studied. The morphological, structural and optical properties of the ZnO nanorods are studied using scanning electron microscope, powder X-ray diffraction and UV-Visible spectroscopy. The results show that all the above-mentioned process parameters influence to some extent the shape, size and properties of the nanorods. The diameter of the nanorods fall in the range of about 300 nm–500 nm and the length in the range of 1.5 μm –4 μm . Nanorods with smaller diameter has been synthesized using Zinc Nitrate precursor. Average diameter of the nanorods increases with precursor

concentration and synthesis time. An optimum condition for the customized system with basic precursor solution has been proposed.

PP-28: Study of structural and initial permeability of strontium and nickel co-doped barium titanate sintered at 1250°C

Mehedi Hasan*, A. K. M. Akther Hossain

Department of Physics, Bangladesh University of Engineering and Technology, Dhaka, Bangladesh

*Corresponding Author: mehedi.physics@gmail.com

ABO₃ type perovskite barium titanate is still one of the most important materials used in many applications ranging from electronics to medicine. Its ferroelectric properties are also useful in fabricating new memory storing devices. Doping on A-site and B-site of barium titanate and also co-doping have been done to improve its performance in targeted applications. In this study, co-doping of strontium and nickel on A-site of barium titanate has been done by conventional solid-state reaction technique at different concentration and then sintered at 1250°C for five hours in air. The effect of co-doping at different concentration on structural, initial permeability, relative quality factor and loss tangent have been studied.

PP-29: Structural and magnetic properties of Li-Cr-Zn ferrites

Rowshon Satara¹, M. Firoz Uddin¹, M. Zaman Molla³, Mahmudul Hasan¹, Faizus Salehin¹, S. Manjura Hoque², F. A. Khan¹ and M. Samir Ullah^{1*}

¹Department of Physics, Bangladesh University of Engineering and Technology, Dhaka-1000

²Materials Science Division, Atomic Energy Center, Dhaka-1000

³Department of Arts and Sciences, Ahsanullah University of Science and Technology, Dhaka-1208

Email: samirullah@phy.buet.ac.bd

The effects of Cr³⁺ substitution on the structural and magnetic properties of Li-Zn ferrites are observed in this study. The samples were prepared by the double sintering method and sintered at 1150°C. The crystal structure was studied by the X-ray diffraction (XRD) technique and it was found the single phase cubic spinel structure. The lattice parameter decreases with increasing of Cr contents which could be attributed to the difference in ionic radii. X-ray density, bulk density, porosity, crystallite size, bond length and hopping length were calculated for all the prepared samples. The variation of magnetization (M) with the applied magnetic field strength (H) for Li-Cr-Zn ferrites with different compositions was performed at room temperature and it is seen that the samples have shown typical soft magnetic hysteresis. From the study of M-H curve, it is found that the saturation magnetization decreases with the increase of Cr contents. The experimental and theoretical magnetic moments were evaluated for all the compositions. Frequency dependent magnetic permeability of the prepared samples was investigated to obtain the initial magnetic permeability (μ'_i) and relative quality factor (RQF) using an impedance analyzer. The resonant frequency shifts toward the higher frequency with Cr contents, which is expected according to Snoek's relation. Dielectric constant, dielectric loss, ac conductivity and resistivity were investigated as a function of frequency at room temperature. The complex impedance spectroscopy through Cole-Cole plot showed that the conduction process is dominated by both of effect of grain and grain boundary of the samples.

PP-30: Detailed Electrical Investigation on Highly Potential NCZA Ceramics for MLCI and Miniaturized Device Applications

M Rahim Ullah^{1*}, H M A R Maruf², N M Eman¹, N J Shirin^{2,3} and M Belal Hossen²

¹Department of Physics, University of Chittagong, Chattogram-4331, Bangladesh

²Department of Physics, Chittagong University of Engineering and Technology, Chattogram-4349, Bangladesh

³Department of Computer Science & Engineering, Premier University, Chattogram, Bangladesh

*Corresponding Author: rahimullah.physics.cu@gmail.com

The polycrystalline $\text{Ni}_{0.27}\text{Cu}_{0.10}\text{Zn}_{0.63}\text{Al}_x\text{Fe}_{2-x}\text{O}_4$ potential ceramics have been synthesized via conventional solid state reaction technique. The synthesized ceramics reveal cubic spinel structure with single phase via Rietveld refinements of XRD data. Lattice parameter, density and grain structure are observed to decrease with Al substitution. The electrical and dielectric properties of the synthesized samples have been studied at different sintering temperatures over the frequency range of 100 Hz to 100 MHz. The dielectric constant is found to decrease with frequency for all the compositions which shows the general behavior of ferrites. The synthesized specimen reveal multifunctional efficiency with low loss magnitudes. Electric modulus study confirms the non-Debye relaxation nature and complex impedance study obeys the Cole-Cole explanation. The increase of grain and grain boundary resistances makes the ceramics potential candidates for high frequency applications. The ac electrical conductivity investigation discloses hopping type conduction mechanism in the ceramics.

PP-31: Possible applications of multi-Josephson junction in superconductor as a quantum interferometer

H.M.A.R. Maruf^{1*}, Md. Abdullah Al Zaman², M.R. Islam³ and F.-U.-Z. Chowdhury¹

¹Department of Physics, Chittagong University of Engineering and Technology, Bangladesh

²Department of Textile Engineering, Northern University Bangladesh

³Department of Physics, University of Chittagong, Chattogram - 4331, Bangladesh

*corresponding author's e-mail: hasnat_maruf10@cu.ac.bd

The model of multi junction ac Josephson junction effect in superconductivity has been studied. Parallel combination of two or more than two Josephson junctions, called model of multi junction have been proposed for the last few years and explained many physical phenomena associated with the proposed model. In the optical physics, the coherence sources of light waves give the interference and diffraction phenomena. The coherence nature of Cooper pair waves (so-called quantum coherence) in Josephson junction gives the analogous effect. A comprehensive theoretical study has been performed for the evaluation of the amplitudes of the critical current in multi-Josephson junction. Numerical result shows the analogy between the optical phenomena and Josephson junction in superconductor. Finally, the possible applications as a quantum interferometer and quantum computation are also discussed.

PP-32: Analysis of beam contamination along the beam path by isotopes of ^{12}C beam and their role in charge changing cross section measurement by PHITS

Quazi Muhammad Rashed Nizam

Department of Physics, University of Chittagong, Chittagong-4331, Bangladesh

rnizam_83@yahoo.com, rnizam.physics@cu.ac.bd

In this study, we analyze the role of isotopes of projectiles for beam irradiation in accelerator facilities by using Monte Carlo calculation code, Particle and Heavy Ion Transport code System (PHITS). In this study, we simulate the transportation of ^{12}C beam through the beam materials along the beam path of Heavy Ion Medical Accelerator in Chiba (HIMAC), Japan. The carbon beam of different available energies in this facility has been transported along the path to target and analyze event by event interaction by PHITS. During traveling the materials along beam path, isotopes of projectiles are produced due to the interactions of beam with different materials like scatterer (Ta), Al, Air and polymethyl methacrylate (PMMA). We calculate the probability of production of these isotopes as mass changing cross section of the projectiles since actually these isotopes are produced by the removal of varieties number of neutron from the projectiles. We define the mass changing cross section mathematically from the formula of total charge changing cross section. We found the ^{11}C and ^{13}C are the significant isotopes with sufficient energy to contaminate the beam to the target in HIMAC. These isotopes play the important role of getting higher experimental result than calculation according to our analysis. It is important to isolate or distinguished these isotopes from their projectiles to get precise and accurate result with minimum error.

PP-33: Investigation of molecular transport through multipore into giant unilamellar vesicles using COMSOL simulation

¹Md. Asaduzzaman, ¹T. Rahman, ¹M.S. Ishtiaque, ¹M.I. Hossain, ²Md. A. S. Karal and ¹Md. K. Alam

¹Department of Physics, University of Barisal, Bangladesh.

²Department of Physics, Bangladesh University of Engineering and Technology, Bangladesh

E-mail: khoshed_du@yahoo.com

Now a days many applications such as gene transfection into cells, cancer chemotherapy, insert foreign proteins into cells and transdermal drug delivery can be possible if the molecules can transport through the nanopore in cell membrane with a tractable manner [1]. Antimicrobial peptides (AMPs) magainin 2, which was first isolated from the African clawed frog *Xenopus laevis*, has been extensively investigated [2]. Experimental study reported that magainin2 interacts directly with the lipid bilayer rather than with a specific protein target within the cell membrane [3]. (Hasan et al. 2018), observed the leakage of water-soluble fluorescent probes from the inner side to the outer side (buffer area) of GUVs through the pores [4]. However, kinetics of molecular transport through nanopores into GUVs is very important to unearth the details mechanisms of pore formation and nature of its effect on molecular transport has not been investigated in detail yet. Recently, theoretical study [5] investigated the molecular transport into the GUVs through a single nanopore for the various sizes of fluorescent probe using artificially designed GUVs and nanopore on the membrane based on the experimental parameters [6]. However, kinetics of molecular transport through multipore in the membrane of GUVs has not been clearly understood. In this simulation, we have designed a group of pores in the membrane of GUVs using computer-aided design software (AutoCAD) and performed simulation to see the kinetics of molecular transport, from the inside to the outside of GUV through the nanopores. Here we used various water-soluble fluorescent probes such as calcein, Texas-Red Dextran 3000 (TRD-3K), TRD-10K and TRD-40K. The size of the nanopore, GUVs and probes are considered based on experimental used data [2]. The diffusion constant observed by our simulation agrees reasonably consistent with experimental results.

References:

1. V. Jayasooriya, D. Nawarathna, 13th COMSOL Conference, Boston (2017)
2. Y. Tamba, M. Yamazaki, J Phys. Chem. B. 113: 4846-4852(2009)
3. Steve J. Ludtke, Ke He, William T. Heller, Thad A. Harroun, Lin Yang and Huey W. Huang, Biochemistry, 35, 13723-13728 (1996)
4. M. Hasan, MAS Karal, V. Levadnyy, M. Yamazaki. *Langmuir*, 34:3349–3362 (2018)
5. MAS Karal, Md. Kamrul Islam, Zaid Bin Mahbub, European Biophysics Journal, 49: 59-69 (2020)

6. Y. Tamba, M. Yamazaki, *J PhysChem B* 113:4846–4852 (2009)

PP-34: Synthesis of ZnO nanoparticles from waste materials

Tanvir Ahmed Chowdhury^{1,2}, Jahirul Islam Khandaker¹, Md. Abdul Gafur³

¹Department of Physics, Jahangirnagar University, Savar, Dhaka, Bangladesh

²Department of Textile Engineering, Daffodil International University, Dhaka, Bangladesh

³PP & PDC, Bangladesh Council of Scientific & Industrial Research, Dhaka, Bangladesh

The aim of this study was to prepare ZnO nanoparticles from waste materials. Zinc dross from galvanizing plant and zinc plate from spent zinc-carbon batteries were used as waste material to synthesize ZnO nanoparticles (NPs). Both of the materials were washed thoroughly to remove surface contamination. Then they were processed with HCl and NaOH followed by washing the precipitations for five times with distilled water. After that the washed precipitations were heated at 80°C for 12 hours. The produced NPs were examined with XRD. It was found that NPs produced from battery waste have the similar diffraction peaks as ZnONPs. On the other hand, NPs of zinc dross have some extra diffraction peaks along with ZnO NPs. It was also depicted that the crystallite size of NPs originated from two sources also varied from one another.

PP-35: Rietveld Analysis on the Structural Properties of Mn Substituted Ni-Cu-Cd Bulk Ferrites Synthesized from Nanocrystalline Powders

Mia Md Fakharuddin Ali Mazlobee¹, M. R. Shah¹ and M. Belal Hossen²

¹Military Institute of Science and Technology (MIST), Mirpur Cantonment, Dhaka-1216, Bangladesh.

²Department of Physics, Chittagong University of Engineering & Technology (CUET),
Chattogram-4349, Bangladesh

Email Id: mazlobi@yahoo.com¹ and belalcuet@gmail.com²

The concept of producing bulk ferrites from nano-powders is quite needful in electronic fields. With this objective, $\text{Ni}_{0.5-x}\text{Mn}_x\text{Cu}_{0.2}\text{Cd}_{0.3}\text{Fe}_2\text{O}_4$ ($x = 0.0, 0.1, 0.2, 0.3, 0.4$ and 0.5) bulk ferrites were produced from nano-crystalline powders applying the sol-gel auto-combustion technique and sintering temperature was 1200°C. The study has revealed certain influences of synthesis method and substitution of Mn ions on structural properties, density, and porosity. The Reitveld refinement method was applied to analyze XRD data. XRD patterns illustrate the presence of a single-phase cubic spinel ferrite structure. The crystallite sizes were within 30-57 nm. It is seen that lattice constant increases and x-rays density decrease with substitution of Mn content (x) that projects a clear indication of modification of spinel structure. The porosity shows mixed behavior of rising and fall. The projected cationic distribution explains the migration of cations and how it affects the behavior. It is also evident from Maximum Entropy Map analysis that the electron density varied with increasing Mn contents. The presence of strong covalent bonding was observed too. To the best of our knowledge, it is interesting to note that the Mn substituted Ni-Cu-Cd bulk ferrite shows appreciable changes in structural properties compared to other similar mixed spinel ferrites reported so far. The structural properties presented here certainly convey that the Ni-Cu-Cd bulk ferrite sintered from nano-powder would be a prospective identity in a wide variety of applications.

PP-36: Graphene oxide and Reduced graphene oxide reinforced hydroxyapatite based nano composites for biomedical application

Md. Ifat-Al-Karim¹, Md. Al Mamun², Md. Mahbulul Haque², Farzana Nahid¹

¹Physics Discipline, Khulna University, Khulna, Bangladesh²Materials Science Division, Atomic Energy Centre, Dhaka

Hydroxyapatite (HAP) is applied in medical applications for repair or replacement of bone tissues in body system. The constituent and structure of HAP is similar to the bone and teeth. Pure HAP has been synthesized by wet chemical precipitation method by using calcium nitrate $Ca(NO_3)_2 \cdot 4H_2O$ and diammoniumhydrogen phosphate $(NH_4)_2HPO_4$. However, HAP shows comparatively inferior mechanical properties than natural bone and as such, improvement of mechanical properties is necessary. One of the best candidate materials for the reinforcing phase to HAP is Graphene Oxide (GO) and Reduced Graphene Oxide (RGO), which exhibit excellent biocompatibility. Graphene Oxide have been synthesized by Tour method with modification. And the synthesized GO is reduced to Reduced Graphene Oxide (RGO). In this study, GO-HAP nano-composites have been synthesized by using In-situ method and RGO-HAP nanocomposites have been synthesized by vortex mixture method. GO-HAP and RGO-HAP bio-composites were fabricated with the objective to improve the mechanical, morphological and structural properties of the biomaterial and future biomedical uses. The X-ray diffraction (XRD) of GO-HAP and RGO-HAP nanocomposite indicates that the incorporation of a certain amount of GO and RGO does not affect the crystallinity and phase stability of HAP. Fourier transforms infrared spectroscopy (FTIR) confirms the presence of functional groups in HAP, GO, RGO and their composites. The morphology of the synthesized composites is investigated by FESEM, which predicts that the pore size of the composites is in the range of 100 nm, which is good for tissue ingrowth. Raman spectroscopy predicts that the amount of disorder of graphene layers increases due to the functionalization in GO-HAP and RGO-HAP composites. And also predicts that the bond strength of GO-HAP is greater than synthesized RGO-HAP. EDX analysis verifies the formation of nano-HAP particles on the GO and RGO flakes as the Ca/P ratio was close to standard 1.67 exists in natural bone tissue. UV-vis spectra show the strong interaction between graphene sheets and HAP nanoparticles. And also predicts lower chance of bonding between RGO and HAP nanoparticles. Eventually the prepared GO-HAP and RGO-HAP nanocomposites will be a good alternative option in the bone tissue engineering, bone regeneration or any other biomedical applications.

PP-37: Reduced graphene oxide supported cobalt ferrite nanoparticles: A study of synthesis mechanism, structural, magnetic and thermal stability characterization

Gobinda Chandra Mallick^a, M. Al-Mamun^{a,b}, M. R. Rahman^a, M. Al-Fahat Hossain^a, Sheikh Manjura Hoque^b

^a Physics Discipline, Khulna University, Khulna-9208, Bangladesh.

^b Materials Science Division, Atomic Energy Centre Dhaka, Dhaka, Bangladesh

In present study, graphene oxide (GO) synthesized using the modified hummers' method was reduced using hydrazine hydrate to make it perform as a surface for the decoration of cobalt ferrite nanoparticles (CFN) produced via the co-precipitation route. CFN were successfully filled on the surface of reduced graphene oxide (RGO) through the hydrothermal method. The coexistence of RGO and CFN in the nanocomposite was confirmed by X-ray diffraction analysis (XRD), scanning electron microscopy (SEM), Fourier-transform infrared spectroscopy (FTIR). The XRD pattern of the nanocomposite exhibits the spinel cubic phase formation with the Fd3m space group with crystallite size 28.55 nm. SEM was used to corroborate the loading of CFN on the RGO nanosheet. FTIR results manifest the functional groups present in all the samples, while Raman study substantiates the reduction of GO. Thermogravimetric analysis (TGA) displays that the nanocomposite showed better thermal stability at high temperature than GO nanosheet. The soft magnetic nature is observed for RGO-CFN nanocomposite with a saturation magnetization of 24.11 emu/g at 300K, by means of a Physical Property Measurement System (PPMS). Such types of structural and magnetic behavior make the nanocomposite a good candidate in various application fields such as dye degradation, adsorption, photocatalytic activity, drug delivery etc.

PP-38: Analysis of grain growth, densification and reduction of porosity, coercivity and functional properties of Mn substituted Ni-Cu-Zn nanocrystalline ferrites

Abdul Ahad^{*1,2} and A. K. M. Akther Hossain²

¹Department of Physics, Govt. Ispahani College, Keraniganj, Dhaka-1310, Bangladesh

²Department of Physics, Bangladesh University of Engineering & Technology, Bangladesh

Corresponding authorEmail: abdulahadlalpur@gmail.com

Nominal compositions of Mn Substituted $\text{Ni}_{0.50-x}\text{Mn}_x\text{Cu}_{0.15}\text{Zn}_{0.35}\text{Fe}_2\text{O}_4$ with $x = 0.00$ to 0.25 in terms of 0.05 have been synthesized by Sol gel Auto Combustion Technique. Analyzing the XRD pattern it is observed that there are several intensity peaks, the positions of the peaks comply with the cubic spinel structure where no traces of raw materials are obtained. Crystallite size is varied from $20\text{-}28\text{ nm}$ as well as average grain size is also varied from $69\text{-}126\text{ }\mu\text{m}$ with increasing Mn content. Bulk density increases and porosity decreases with increasing Mn content where a small amount of Mn ions acts as a slight accelerator of grain growth and also favor densification. The complex initial permeability graphs show that real part of initial permeability is increasing with the increase of Mn content in which maximum permeability ($\mu_i = 315$) exhibits for NiMnCuZn ferrite when $T_s = 1300^\circ\text{C}$, interestingly which is 6.5 times greater than that of parent composition. Temperature dependent permeability graphs show that permeability is increasing while Neel temperature is decreasing with increasing Mn content. The Magnetic Hysteresis loop shows that with increasing Mn content saturation magnetization is increasing while coercivity is decreasing exhibits the soft magnetic materials.

PP-39: Structural, electrical and magnetic properties inspection for rare-earth substituted magnetic dense ceramics synthesize from nanoferrites

M. Faishal Mahmood¹ and M. Belal Hossen^{2*}

Department of Physics, Chittagong University of Engineering and Technology, Bangladesh

Email: faishal.m.cuet@gmail.com¹ and belalcuet@gmail.com²

Powder specimens are not applicable in many electronic applications due to its lower density where dense ceramic is only solution. For that purpose, $\text{Ni}_{0.5}\text{Cu}_{0.2}\text{Cd}_{0.3}\text{La}_x\text{Fe}_{2-x}\text{O}_4$ bulk ceramics were prepared by sol-gel and sintered at 1200°C . In the aim of analyzing structural, magnetic, dielectric and electrical transport properties various characterizations were performed. For the structural analysis, firstly XRD and then Rietveld refinement was implemented which provide information about cation distribution, crystal structure, crystallite size and so on. Frequency dependence complex dielectric constant show pattern by following the usual nature of magnetic ceramics. The variation of dielectric loss tangent has been analyzed and it is depicted that it reduces remarkably with increasing La content. Electric modulus analysis of the studied samples provides the information about the dynamics of conduction mechanism of the ceramics. In addition of dielectric analysis, impedance spectroscopy measurements were performed for studying the impedance nature and the usual nature of grain and grain boundary resistive and capacitive contribution has been found in the characteristics of electrical impedance. The influence of La^{3+} substitution showed saturation in the stored magnetization with arisen frequency and showed a better-quality factor. It has been seen that the samples exhibit ferromagnetic behavior at room temperature obtained from the magnetic measurement done by PPMS. Strong correlation between dielectric loss tangent and the magnetic Q-factor at the optimum frequency range had been found for the investigate samples. The suitability of the compound for the technological applications was studied in this research by comparing all exceptional outcomes.

PP-40: Atomic-scale investigation of the formation of Al nanocluster in the Pulsed Laser Ablation Technique**Samiul Hossain Sajal¹, Nithika Datta¹ and Md EnamulHoque^{1*}**¹Department of Physics, Shahjalal University of Science and Technology Sylhet - 3114, BangladeshCorresponding Author: mjonyh-phy@sust.edu

The fabrication and synthesis of the metal nanoparticles and their oxides using the Pulsed Laser Ablation in Liquids (PLAL) are popular due to the stability of those particles in liquids. The physical process of the formation of nanoparticles with high energy lasers is usually described with models like plasma formation models. In this work, we have used molecular dynamics to describe the model of the formation of Aluminum Nanoparticles (ANPs) in the aqueous environment. The active forcefield (ReaxFF) has been applied to observe the ANPs formation in water. The physical system temperature has been reduced to 300 K from 5000 K to analyze the structural changes in molecules and the formation of ANPs. We have also discussed the required time of forming as in lack luster of ANPs, the modification, and the stability in the molecular structure at various phases of the experiment. In addition to that, we have found that the Graphene structures dominate the cluster formation.

PP-41: Hot Injection synthesized lead-free CsSnCl₃ nanocrystals: An experimental investigation**Yasir Fatha Abed, Md. Shahjahan Ali, Subrata Das, M. A. Basith**

Nanotechnology Research Laboratory, Department of Physics, Bangladesh University of Engineering and Technology, Dhaka-1000, Bangladesh

Email: yasirfatha.023@gmail.com

For decades, lead-free metal halide perovskites have attracted many researchers due to their distinctive optical and electrical characteristics and application as efficient light harvesters. In this current investigation, we have demonstrated a rapid synthesis technique of thermally stable cubic phase non-agglomerated cesium tin chloride (CsSnCl₃) nanocrystals (NCs) with an average crystal size of 300 nm via the hot-injection method. Employing the Rietveld refined powder XRD patterns, the space group was found as Pm3m, and no undesirable peak was observed, which confirmed the phase purity of the prepared NCs. The TGA and DSC analysis revealed the excellent thermal and crystallographic phase stability of as-synthesized NCs over a broad temperature range of 30 to 280 °C. No undesirable functional groups were observed as confirmed from the FTIR analysis. The surface chemistry analysis from the XPS spectroscopy validated the synthesis of pristine CsSnCl₃ nanocrystals as no peaks were found alongside the strong peaks correlating to the Cs, Sn, and Cl core levels. From UV-visible spectroscopic analysis, the direct band gap of CsSnCl₃ was determined to be ~2.98 eV which was further confirmed by the steady-state photoluminescence spectroscopy. Moreover, the synthesized NCs exhibited excellent absorption in the visible spectrum, which revealed its promising potential as an excellent solar absorber. The band-edge positions were determined by adopting the Mulliken electronegativity approach, which indicated the potential photocatalytic capability of the as-synthesized NCs. Later, we confirmed our predictions by performing the photo-degradation of rhodamine-B dye under both visible and UV-visible irradiation with the presence of CsSnCl₃ NCs, and up to 58% degradation was obtained under 180 minutes of solar irradiation. Our comprehensive investigation implies that the facile hot-injection method might be helpful for large-scale rapid synthesis of thermally stable cubic CsSnCl₃ NCs with potential photocatalytic capability.

PP-42: Study of the structural and magnetic properties of Gd doped CoFe₂O₄ nanoparticles synthesized via sol-gel route

M. S. I. Sarker^{a,*}, Marufa Yeasmin^a, S. Manjura Haque^b, M. M. Rahman^a, M. K. R. Khan^a

^aDepartment of Physics, University of Rajshahi, Rajshahi-6205, Bangladesh

^bMaterials Science Division, Atomic Energy Center, Dhaka-1000, Bangladesh

Correspondence E-mail: samiul-phy@ru.ac.bd

The structural and magnetic properties of sol-gel synthesized Gd-doped CoFe_2O_4 nanoparticles (NPs) have been studied. The x-ray diffraction (XRD) and FTIR spectroscopy along with the Raman spectra confirmed the formation of face centered cubic inverse spinel structure. TEM images showed the NPs are well-dispersed with average particle size 30 nm. Moreover, high resolution transmission electron microscopy (HRTEM) images confirmed the polycrystalline nature of the particles. Room temperature magnetic measurement showed the ferromagnetic nature of the NPs. The value of coercivity fluctuates from 353 Oe to 1060 Oe for different Gd content. The maximum coercivity, saturation magnetization, magnetic moment, magnetic anisotropy and remnant magnetization found for 0.03% Gd content are 1060.19 Oe, 77.53 emu/gm, 3.29 μ , 4.11×10^4 erg/cm³, 32.38 emu/gm, respectively. The high value of coercivity indicated that the larger values of interparticle interactions and crystalline anisotropy. Thus $\text{CoFe}_{2-x}\text{Gd}_x\text{O}_4$ magnetic NPs might be a potential candidate for data processing, automotive and telecommunications.

PP-43: Synthesis and Characterization of Co_3O_4 incorporated three-Dimensional MoS_2 nanostructure

Muhammad Hasive Ahmad^{1a*}, Rabeya Binta Alam, S.F. U. Farhad², Muhammad R. Islam^{1*}

¹Department of Physics, Bangladesh University of Engineering and Technology, Bangladesh,

²Industrial Physics Division, Bangladesh Council of Scientific & Industrial Research, Bangladesh

*corresponding Author: rakibul@phy.buet.ac.bd

In this study, a novel Co_3O_4 nanoparticle decorated MoS_2 nanoflower ($\text{MoS}_2/\text{Co}_3\text{O}_4$) has been fabricated via a facile hydrothermal method by taking a different concentration of Co_3O_4 (0 wt.%, 1 wt.%, 2 wt.%, 4 wt.%, and 6 wt.%). The Field Emission Scanning Electron Microscope (FESEM) images show a three-dimensional flower-like structure for MoS_2 and $\text{MoS}_2/\text{Co}_3\text{O}_4$. The different structural parameters of the nanomaterials were estimated from the XRD analysis, followed by the corresponding Rietveld refinement pattern, which confirms the phase purity of $\text{MoS}_2/\text{Co}_3\text{O}_4$. Transmission Electron Microscope (TEM) analysis revealed the inter-planar spacing of the nanostructures varied with the concentration of the Co_3O_4 nanoparticles and $\text{MoS}_2/\text{Co}_3\text{O}_4$ (4 wt.%) shows extended 0.633 nm inter-planar spacing. The 3D $\text{MoS}_2/\text{Co}_3\text{O}_4$ nanostructure with higher dislocation density synthesized from a simple and low-cost process can be used in the energy storage devices and as photo catalytic.

PP-44: Impact of particle size on the magnetic properties of highly crystalline Yb^{3+} substituted Ni-Zn nanoferrites

N. Jahan¹, M.N.I. Khan², F.-U.-Z. Chowdhury¹, M. R. Hasan², H. N. Das², M.M. Hossain¹ and M.M. Uddin^{1*}

¹Department of Physics, Chittagong University of Engineering and Technology (CUET), Bangladesh

²Materials Science Division, Atomic Energy Center, Dhaka 1000, Bangladesh

* mohi@cuet.ac.bd

Yb -substituted $\text{Ni}_{0.5}\text{Zn}_{0.5}\text{Yb}_x\text{Fe}_{2-x}\text{O}_4$ ($0 \leq x \leq 0.20$ in the step of 0.04) ferrites have been synthesized using sol-gel auto combustion method. The structural characterization of the compositions has been performed

by X-ray diffraction (XRD) analysis, field emission scanning electron microscopy (FESEM), quantum design physical properties measurement system (PPMS). That ensured the formation of single phase cubic spinel structure. Crystallite and average grain size are calculated and found to decrease with increasing Yb^{3+} contents. Saturation magnetization (M_s) and Bohr magnetic moment (μ_B) decrease while the coercivity increases with the increase in Yb^{3+} contents successfully explained by the Neel's collinear two sub-lattice model and critical size effect, respectively. Critical particle size has been estimated at 6.4 nm from the D_{XRD} vs. M_s , H_c plot, the transition point between single domain regime (below the critical size) and multi-domain regime (beyond the critical size). Curie temperature (T_c) reduces due to the weakening of A-O-B super exchange interaction and redistribution of cations, confirmed by the M-T graph. The compositions retain ferromagnetic ordered structure below T_c and above T_c , it becomes paramagnetic, making them plausible candidates for high temperature magnetic device applications. The relative quality factor (RQF) peak is obtained at a very high frequency ($\geq 10^8$ MHz), indicating the compositions could also be applicable for high frequency magnetic device applications.

PP-45: Dielectric, Modulus, Impedance Spectroscopy and Conductivity Properties of Mg-Substituted Cu-Zn-Al Nanoferrites with Structural Rietveld Refinement

S. K. Ahmed^a and M. B. Hossen^{b*}

^aSchool of Science and Engineering, University of Creative Technology Chittagong, Bangladesh.

^bDepartment of Physics, Chittagong University of Engineering and Technology, Bangladesh

*Corresponding author: kamal@uctc.edu.bd

Nanocrystalline ferrites are needed in many electronic applications instead of powder with grain in the nanometric range that is the most valuable objectives of the present research. In this research, $\text{Mg}_x\text{Cu}_{0.65-x}\text{Zn}_{0.35}\text{Fe}_{1.925}\text{Al}_{0.075}\text{O}_4$ ($0.0 \leq x \leq 0.5$ in the stages 0.1) nanoparticles were prepared annealed at 700 °C from notable Sol-gel synthesized techniques. It is revealed in many previous cases that suitable doping in ferrites showed improved characteristics like enhance resistivity and magnetization, reduce dielectric loss etc. Analyzing XRD data, the structure of every composition comply with the cubic spinel structure. By the implementation of XRD data, structures have been analyzed through Rietveld Refinement technique using Full prof suitable software. After getting good χ^2 -value different parameters have been determined. These include crystallite size, cation distribution and electron density. Moreover, bond structures are found by using the output of Rietveld Refinement procedure. It is depicted from electronic modulus study that dielectric loss tangent reduces exponentially with increasing frequency and remains constant at higher frequency. With the arisen frequency the electrical properties of grain and grain boundaries have been measured from the complex impedance study. In addition of Mg^{2+} content, both the resistance increases of grain and grain boundary. The σ_{ac} has been raised through the increasing frequency.

PP-46: Fabrication and Characterization of the Metallic Nanoparticles using Pulsed Laser Ablation Technique

Mustabi Mustafa Chowdhury and Md. Enamul Hoque*

Department of Physics, Shahjalal University of Science and Technology, Sylhet - 3114, Bangladesh

*Corresponding author: mjonhyh-phy@sust.edu

Laser ablation occurs when high fluence laser radiation interacts with materials. We have used this technique to produce nano colloids of metal oxides from the targeted metal slabs of Fe, Al, and Cu immersed in distilled water. A high-energy Nd:YAG laser having energy 300mW/pulse at wavelength 532nm is used for bombardment purposes. The UV-vis absorption spectrum of the prepared colloids is

used to determine the bandgap energies using Tauc formalism for further analysis. The environmental parameters of the experiment are also studied to obtain an efficient combination of the production.

PP-47: Effects of atomic number and pressure of different filling gases on soft X-ray yield from PF1000 plasma focus device

***M A Malek¹, L Akter², G S Rakib², M M Islam¹, M N Huda¹ and M K Islam³**

¹Physics Discipline, Khulna University, Khulna, Bangladesh

²Department of Nuclear Engineering, University of Dhaka, Dhaka, Bangladesh

³Plasma Physics Division, Atomic Energy Center, Dhaka, Bangladesh

*E-mail: malekphy@gmail.com

The effects of atomic number (Z_n) and operating pressure (P_0) of different filling gases on soft X-ray yield (Y_{sxr}) from PF1000 are studied through numerical experiments using the modified version of the Lee model code (RADPFV5.015b). In these numerical experiments, Hydrogen (H_2), Deuterium (D_2), Deuterium-Tritium ($D-T$), Helium (He), Nitrogen (N_2), Oxygen (O_2) and Argon (Ar) are used over the range of 4.0 – 0.1 Torr of P_0 as the filling gases. Optimum P_0 at which Y_{sxr} becomes maximum is obtained through numerical experiments for each gas. The number density (n_i), percentage of input energy into the pinch ($EINP$), speed factor (SF), maximum tube voltage (V_{max}), pinch temperature (T_{pinch}) and pinch column length (z_{max}) are computed at the optimum P_0 of each gas to realize the corresponding plasma behavior of the PF1000 device. The consequent effects of P_0 and Z_n on Y_{sxr} are then analyzed significantly. The results confirm that the heavier gas produces maximum Y_{sxr} at low P_0 , where T_{pinch} becomes high in the device compared to those for a lighter gas. It is observed that for heavier gas Ar , $Y_{sxr} = 28555.12$ J is found at $P_0 = 0.3$ Torr with $T_{pinch} = 3.2 \times 10^6$ K, whereas for lighter gas H_2 , $Y_{sxr} = 0.26$ J at $P_0 = 2.5$ Torr with $T_{pinch} = 1.15 \times 10^6$ K. The conclusion of the present numerical study is that in the case of soft X-ray production from PF1000, operating pressure for a particular gas would be adjusted carefully so that the maximum emission of soft X-ray is obtained.

PP-48: Design, Development and Simulation of a Nuclear Counting System using ATMEL Microcontroller

***M. N. Islam, M. S. Alam and M. A. S. Haque**

Institute of Electronics, Atomic Energy Research Establishment, Bangladesh Atomic Energy Commission, P.O. Box No. 3787, Dhaka, Bangladesh

E-mail: nislam_baec@yahoo.com

Design, Development and Simulation of a Nuclear Counting System using ATMEL Microcontroller has been presented in this paper. The Nuclear Counting System (NCS) consists of Nuclear Detector GM (ZP1324)/Scintillation NaI (TI) followed by Nuclear Detector Signal Channel (NDSC) Preamplifier-Amplifier-Shaper-Discriminator. The charge-sensitive preamplifier decay time constant (τ) is 10 μ s. The gain of amplifier used in this channel is 26. Shaping amplifier which is the combination of high pass and low pass filter with equal time constant ($\tau_1 = \tau_2 = \tau$) of 5 μ s to increase the signal-to-noise ratio. Single ended or integral discriminator function is to eliminate the system noise and pulse height discrimination. Atmel-AVR ATmega8L 8-bit Microcontroller is High-performance, Low-power with 8Kbytes In-System Programmable Flash as the Processor, LCD display (16 ch, 2-line), high voltage power supply (HVPS) for detector bias voltage and low voltage power supply (LVPS). An assembly language counting program based on BASCOM AVR IDE has been developed to control the operation of the designed NCS. The system has been designed and verified in Proteus 7.7 simulation platform.

PP-49: Data hiding using audio steganography considering less distortion of cover data for nuclear data

Md. Shamimul Islam*, Nayan Kumar Datta, Md. Mahbub Alam, Dr. Md. Dulal Hossain, Dr. Md. Shakil Ahmed

Institute of Computer Science, Atomic Energy Research Establishment, Bangladesh Atomic Energy Commission, Ganakbari, Savar, Dhaka-1349, Bangladesh

*shamimul32@gmail.com

In the modern era, we cannot imagine a single day without the internet and vast use of the internet of things (IoT). Due to the rapid growth of the internet and millions of smart devices, secure data communication becomes a challenging task for data sending and receiving sites in the wireless data communication field. So, when we consider a secured Digital Information exchange especially Nuclear related data exchange, it may require private, secure, invisible, and avoiding malicious communication. Audio Steganography is a mechanism in which a secret nuclear data message is being concealed audio cover file on the sender end and it is retrieved on the receiver end. In the proposed work, we focus on the implementation of audio steganography using the Least Significant Bit (LSB) algorithm technique. Then we evaluate the performance considering the file distortion, impairment, capacity. Our experimental study proved that how the LSB technique improves the robustness of the embedded audio stream. It also provides high-level security to the universal cyber data where the intruder is unable to distinguish between the original audio and the embedded audio streams.

PP-50: Theory of 3F4D Universe (Beyond SM of Particle Physics)

Yogesh V. Chavan

In this Theory, “Mass is Equivalent to Length of Imaginary Straight-Line Segment” and “Direction to Imaginary Line Segment is Intrinsic Property of that Particle which is Equivalent to its Intrinsic Spin”. With this concept, all fundamental particles, Fermions and Bosons are like Quanta String particles with definite direction. For e.g. Unidirectional Imaginary Straight Line with fixed length are Massive Spin $\frac{1}{2}$ Fermions; while Unidirectional Imaginary Quanta Curved Lines are Massless Spin 1 Bosons. Thus, it gives co-relation between Massless (Curved Imaginary Line) and spin = 1 properties of Boson as proved in QED theory. All Fundamental particles of Standard Model and Beyond Standard Model are arranged in one Simple Diagram in 3 Folds (Bottom Fold, Middle Upper and Lower Folds and Top Fold) projected in 4th Imaginary Dimension in order of decreased in Mass from TeV to approx. 0 eV respectively. This Theory is Beyond Standard Model because it predicts New Fundamental Particles viz. Dark Matter (Spin=0 Massive Boson) along with Gravitons (Spin=2 Massless Bosons); 4th Pair of Neutrinos, Vertical Massless Boson Particles and Tri-Axis Massive Boson (Spin=0) particle. Discovery of these particles will act as Solid Proof to this theory. With this 3F4D representation of the Universe at atomic and sub-atomic level, it solves lot of current problems of SM of Particle physics like Matter-Antimatter Asymmetry, Origin of mass of hadrons like protons, Origin of mass and L.H. nature for neutrinos, Wave-particle duality of particles etc. giving true insight of fundamental particles. With proving that, Dark matter is not a Quanta Particle, rather it is a Single Entity and spreads/ expands throughout the Universe in the form of “Web of Spider”, it shows space-time is not empty, but it is filled with Continuous lines of Dark Matter and we, materialistic Massive objects are floating/ sailing w.r.t. current of this vast ocean. Correlation of its Continuity with Time gives new definition to Time; “Time is neither Illusion nor 4th Dimension, but it is Intrinsic Property of Continuous Single Entity i.e. DM”. Space-Time is not Empty and is filled with Massive Dark Matter, hence, we have to add more terms to Newtonian Gravitational Equation to account for Gravitational Strength of Mass of Surrounding Dark Matter which represents Curvature of Space-Time in terms of Increase in its mass-density w.r.t. to Mass-Density of Flat Universe. Finally, using an Empirical Formula ($h=k*c*Q$; k =Boltzmann’s Constant=Mass in TeV Range) and Inverse relation of Mass-Density of DM with Age of the Universe ($H^2=Constant*G*Mass-Density$ of

DM); Unification of Gravity at TeV range is achieved with no need of “Gravitational Constant, G ”, hence, Planck’s Scale is not required.

PP-51: Elastic, electronic, bonding, optoelectronic and thermophysical properties of SnTaS₂: comprehensive insights from ab-initio calculations

M. I. Naher, M. Mahamudujjaman*, A. Tasnim, S. H. Naqib

Department of Physics, University of Rajshahi, Rajshahi 6205, Bangladesh

*Presenting author email: mahamudujjamanr@gmail.com

In this study, we report structural, elastic, bonding, optoelectronic and thermo-physical properties of layered superconductor SnTaS₂ by using DFT based CASTEP (Cambridge Serial Total Energy Package) code. Elastic constants, bonding properties, optical properties, different thermo-physical parameters and vibrational properties including phonon dispersion and DOS are explored for the first time. Elastic anisotropy factors show that SnTaS₂ possesses strong anisotropy. The metallic behavior of SnTaS₂ is predicted by the band structure and DOS diagram. Central force and metallic bonding dominate in the material under study. SnTaS₂ is fairly machinable and its theoretical hardness is low. Both, absorption coefficient and optical conductivity also confirm the metallic nature of the compound. The real part of refractive index has high value from 0 to ~ 5eV covering infrared to visible region. Therefore, the compound under investigation has intended optical characteristics for light emitting and optoelectronic display devices. All the optical parameters of SnTaS₂ show moderate anisotropy with respect to the polarization direction of the electric field.

PP-52: MAX Phase Materials: Prospect of MAX Phase Borides

M. A. Ali* M. M. Hossain, M. M. Uddin

¹Department of Physics, Chittagong University of Engineering and Technology (CUET), Bangladesh

*Corresponding author: ashrafphy31@cuet.ac.bd

MAX phase borides: the new platform for the MAX phase’s family which are found in two structures. The structure of 211 is similar to that of traditional MAX phase carbides. The structure of 212 phases is slightly different from 211 MAX phases. In the case of 212 phases, there is a 2D layer of B sandwiched between M layers in which an extra B atom exists as an X atom unlike from 211 phases. Within the 2D layer, two center-two electrons (2c- 2e) bond is formed that leads strong covalent B-B bond. We have performed DFT study of some 211 and 212 MAX phase borides and the obtained physical properties are compared with those of the corresponding 211 MAX phases. The mechanical properties and Vickers hardness of 212 MAX phases are higher than those of corresponding 211 MAX phases whereas the mentioned properties of 211 MAX phase borides are comparable with those of 211 MAX phase carbides. The thermal properties have also been investigated by calculating the Debye temperature, minimum thermal conductivity, Grüneisen parameter, and melting temperature of 211 and 212 MAX phase borides. Like mechanical properties, the thermal properties of 212 MAX phase borides are better than those of 211 MAX phases and the thermal properties of 211 borides are comparable with those of 211 MAX phase carbides.

PP-53: DFT based first principles calculation of lead-free CsSnCl₃ perovskite: A “GGA+U” approach

Md. Shahjahan Ali, Yasir Fatha Abed, Subrata Das, M. A. Basith

Nanotechnology Research Laboratory, Department of Physics, Bangladesh University of Engineering and Technology, Dhaka-1000, Bangladesh

E-mail: m.shahjahan.ali93@gmail.com

Lead-free metal halide perovskites have drawn great attention as light harvesters due to their promising optoelectronic and photovoltaic properties. Especially, Cesium (Cs) based halide perovskite exhibited high-power conversion efficiency and intriguing optoelectronic properties such as enhanced optical absorption, excellent charge-transport properties and broad chemical tunability. In this investigation, we have performed a density functional theory (DFT) based first-principles calculation of lead-free perovskite CsSnCl_3 considering the effect of on-site Coulomb and exchange interaction within the generalized gradient approximation (GGA) by implementing the GGA+U method. In many previously reported results, computationally more costly Heyd–Scuseria–Ernzerhof (HSE06) hybrid exchange-correlation function has been incorporated to carry-out the numerical simulation where 45.9% deviation has been observed from the experimentally obtained bandgap value. Employing the GGA+U method, we have achieved 90% accuracy of band gap estimation when $U_{\text{eff}} = U - J = 6 \text{ eV}$ is considered. In the benchmarked simulation environment, the estimation of the crystal structure and optical properties is in well agreement with the previously reported experimentally obtained result. The effective masses of electrons and holes are calculated from the curvature of the numerically obtained conduction band minima and valence band maxima. Based on our calculation from the benchmarked simulation environment and previously reported experimental findings, we have proposed a modification of the “D” value, which predicts the potential photocatalytic performance of a nanocrystal by considering the separation of photoexcited electron-hole pairs. Our theoretical calculations demonstrate that the DFT-based first-principles calculation incorporating the GGA+U method can predict the experimentally obtained result with 90% accuracy when $U_{\text{eff}} = 6 \text{ eV}$ is considered. We believe our comprehensive theoretical investigation might be helpful to conduct further study on analogous perovskite materials.

PP-54: Elastic, electronic, bonding, optoelectronic and thermophysical properties of SnTaS_2 : comprehensive insights from ab-initio calculations

M. I. Naher, M. Mahamudujjaman*, A. Tasnim, S. H. Naqib

Department of Physics, University of Rajshahi, Rajshahi 6205, Bangladesh

*Presenting author email: mahamudujjamanr@gmail.com

In this study, we report structural, elastic, bonding, optoelectronic and thermophysical properties of layered superconductor SnTaS_2 by using DFT based CASTEP (Cambridge Serial Total Energy Package) code. Elastic constants, bonding properties, optical properties, different thermophysical parameters and vibrational properties including phonon dispersion and phonon density of states are explored for the first time. Elastic anisotropy factors show that SnTaS_2 possesses strong anisotropy. The metallic behavior of SnTaS_2 is predicted by the electronic band structure and electronic energy density of states diagram. Central force and metallic bonding dominate in the material under study. SnTaS_2 is fairly machinable and its theoretical hardness is low. Both, absorption coefficient and optical conductivity also confirm the metallic nature of the compound. The real part of refractive index has high value from 0 to $\sim 5 \text{ eV}$ covering infrared to visible region. All the optical parameters of SnTaS_2 show moderate anisotropy with respect to the polarization direction of the electric field.

PP-55: Structural, elastic and optoelectronic properties of CaZn_2X_2 (X = N, P, As) semiconductors: density functional theory-based investigations

Md. Sajidul Islam*, Md. Mahamudujjaman, S. H. Naqib

Department of Physics, University of Rajshahi, Rajshahi-6205, Bangladesh

*Presenting author email: sajidul.ru.phy@gmail.com

We present herein a detailed first principles DFT calculations to study the structural, elastic and optoelectronic properties of ternary semiconductors CaZn_2X_2 ($\text{X} = \text{N}, \text{P}, \text{As}$) using density functional theory. The unit cell of all the compounds was optimized using generalized gradient approximation (GGA) and local density approximation (LDA). The obtained lattice parameters are in good agreement with the experimental data and other theoretical findings. With the optimized unit cell geometries of CaZn_2X_2 ($\text{X} = \text{N}, \text{P}, \text{As}$), the elastic constants were calculated using the GGA. From the computation, we obtain six independent elastic constants, i.e., c_{11} , c_{12} , c_{13} , c_{14} , c_{33} and c_{44} . These elastic constants satisfy the mechanical stability criteria. The electronic band structures show that CaZn_2N_2 show a direct band gap while CaZn_2P_2 and CaZn_2As_2 compounds show indirect band gap.

PP-56: Insights into the physical properties of aCaCuO_3 and SrCuO_3 semi-metals: A DFT study

M. Monira*, M.N.H. Liton, M.A. Helal and M. Kamruzzaman

Department of Physics, Begum Rokeya University, Rangpur, Rangpur-5400, Bangladesh

*corresponding author: mniramarjanum@gmail.com

The first-principles calculations based on density functional theory have been implemented to elucidate the mechanical, electronic, and optical properties of ACuO_3 ($\text{A} = \text{Ca}, \text{Sr}$) perovskite compounds. The calculated elastic constants of ACuO_3 fulfill the required mechanical stability condition. The elastic parameters show that ACuO_3 possesses good machinability, ductility, relatively high Vickers hardness, mixed ionic and covalent character and high melting temperature. In addition, ACuO_3 is highly anisotropic, and the relatively low value of Young modulus makes a promising thermal barrier coating (TCB) material. Mulliken bond analysis also supports the bonding nature predicted by the elastic parameters. The electronic band structure and density of states (DOS) confirm the semi-metallic behavior of these present compounds. The high DOS value at the Fermi level implies subsequent good electrical conductivity. Different optical properties such as dielectric constant, optical absorption, reflectivity, photoconductivity, refractive index and dielectric loss function of these two compounds show interesting features. The high reflectivity in the infrared-visible spectral range makes ACuO_3 a good choice for coating material to prevent solar heating. ACuO_3 possesses high refractive index in the infrared to visible range while they become a good absorber in the ultraviolet energy region. The metallic feature of ACuO_3 is reconfirmed from the optical analysis.

PP-57: Realization of the role of donor (F) impurity on the electronic structure and optical properties of ZnO : A first principles study

M. N. H. Liton^{a*}, M. K. R. Khan^b

^aDepartment of Physics, Begum Rokeya University, Rangpur-5400, Bangladesh

^bDepartment of Physics, University of Rajshahi, Rajshahi-6205, Bangladesh

*Corresponding author: E-mail: liton_mnhru@yahoo.com

We perform first principles calculations based on density functional theory to investigate the effect of F doping on the electronic and optical properties of ZnO . Electronic band structure study confirms the degenerate semiconducting nature with n-type conductivity in pristine ZnO and as well in F-doped ZnO . The increase of band gap in F: ZnO is attributed to the well-known Burstein-Moss effect which is in accord with experimental results. Furthermore, it is elucidated that incorporating F into ZnO introduced impurity bands below the conduction band (CB), subsequently, the Fermi level shifted towards CB. The

shifting of Fermi level into CB fallouts the improvement of electrical conductivity and carrier concentrations of the doped system. Different optical properties such as dielectric constant, optical absorption, reflectivity, photoconductivity, refractive index and dielectric loss function have also been studied as a function of photon energy. The absorption spectra of F:ZnO approved that the blue shift occurs at the absorption edge. This result implies that the optical band gap has increased which complies with the electronic study. These findings suggested that F doped ZnO system could be a potential candidate for short wavelength optoelectronic and photo-electrochemical applications.

PP-58: Wigner Rotation in Different Space Time

Md. Tarek Hossain

Department of Physics, American International University-Bangladesh

E-mail: tarek.phy@aiub.edu

We have introduced the Wigner rotation in two different ways. The formula of Wigner rotation has been derived in flat space in two different ways. The numerical values of Wigner rotation have been calculated for different cases. The graph of the Wigner rotation with respect to different velocities has been plotted. Rapidity is a hyperbolic angle that differentiates two frames of reference in relative motion. We have observed that the rapidity space provides a geometric approach to the Wigner rotation and the Thomas precession. We have also derived the formula of Wigner rotation in hyperbolic space. The numerical values of Wigner rotation in hyperbolic space have also been calculated. A graph of Wigner rotation versus boost angle for different boost velocities has been plotted. We have presented different types of Black holes such as Miniature Black hole, Stellar Black hole, Intermediate-mass Black hole, Supermassive Black hole, Schwarzschild Black hole, Kerr Black hole and Reissner-Nordstrom Black hole. We have derived the line element in Schwarzschild Black hole and the line elements of different Black holes have been represented. The formula of Wigner rotation in the outer space of Schwarzschild Black hole has been derived. We have also calculated the numerical values of Wigner rotation in the outer space of Schwarzschild Black hole. The graph of the Wigner rotation with respect to different velocities of a moving object has been plotted.

PP-59: Analysis of the HTS inductor design for optimum energy storage in SMES

M. R. Islam and Jahangir Alam* and M A A Zaman

*Corresponding author email: Jahangir.phy@cu.ac.bd

Superconducting magnet coils are the major component parts of energy storage in SMES (Superconducting Magnetic Energy Storage). To maximize the storage energy, the coil must be designed to have the maximum inductance for a given length of conductor as its operating current. This report will discuss the design optimization for a superconducting solenoid made of silver sheathed first generation high-TC superconductor (1G HTS) BSCCO-2223 tape conductor and consider various practical issues regarding the choice for a prototype. We have performed the inductance calculation for specific design and shown the effects of variation of parameters related to it. Numerical results suggest that the optimum inductance value (L) depends on the geometrical parameters i.e., size ratios and height of pancake layers (H) and so on. Finally, storage energy calculation with specific design and necessary explanations has been included.

PP-60: A computational molecular design of new potential molecules for D/A type OLED and investigating TADF properties for high luminescence: A DFT study

Banasree Sarkar Mou, Ahsan Ullah, Dr NaziaChawdhury*

Department of Physics, Shahjalal University of Science and Technology, Sylhet, Bangladesh

*E-Mail: nc-phy@sust.edu

A plethora of attention is being attracted on Organic Light Emitting Diodes (OLEDs) in recent years employing Thermally Activated Delayed Fluorescence (TADF) emitters which is rare metal-free, environmentally safe and highly efficient with an Internal Quantum Efficiency (IQE) of nearly 100%. Herein, we propose a theoretical design strategy for Donor–Acceptor (D\A)-type small molecules as they facilitate permit the small energy gap (ΔE_{ST}) between singlet–triplet states, hence reduced exchange energy (J) between electron-donating and accepting subunits for efficient Reverse Intersystem Crossing (RISC) which is a prerequisite for successful TADF. Our approach involves molecular design between 2,4-diphenyl-1,3,5-triazine acceptor and 9,10-dihydroacridine donor moieties connected by a rigid fluorine linker which shows less singlet–triplet splitting energy than the molecule where the same donor and acceptor are attached with a flexible 1-2 phenylene bridge, resulting in the former one as a better candidate for TADF prior to further experimental studies. For a more comprehensive understanding, we also investigate ionization potentials (IA), electron affinities (EA), oscillator strengths, reorganization energies and charge transport properties of the two molecules in order to differentiate their efficiencies.

PP-61: Thermophysical and optoelectronic properties of Nb₂P₅: density functional theory-based insights

M. I. Naher* and S. H. Naqib

Department of Physics, University of Rajshahi, Rajshahi 6205, Bangladesh

*Presenting author email: irinju26@gmail.com

Binary metallic phosphide, Nb₂P₅, is a promising system for technological applications. A number of thermophysical properties, together with bonding characteristics and optical properties, have been explored in this study for the first time. Nb₂P₅ is found to be a mechanically and dynamically stable elastically anisotropic compound with weakly brittle character. The bondings between the atoms are dominated by covalent and ionic contributions with small signature of metallic feature. The compound possesses high level of machinability. Nb₂P₅ is a moderately hard compound. The band structure and density of states calculations disclose metallic feature with a large electronic density of states at the Fermi level. Calculated values of different thermal properties indicate that Nb₂P₅ has the potential to be used as a thermal barrier coating material. The energy dependent optical parameters show close agreement with the underlying electronic band structure. The optical absorption and reflectivity spectra and the static index of refraction of Nb₂P₅ show that the compound holds promise to be used in optoelectronic device sector. Unlike notable anisotropy found in elastic and mechanical properties, the optical constants are found to be largely isotropic.

PP-62: Simulation Study of Macrobending and Microbending Losses of a Single Mode Step Index Optical Fiber

P. Roy* and H. R. Khan

*Physics Discipline, Khulna University, Khulna-9208

Corresponding author's e-mail: preangka.666@gmail.com

Optical fiber forms the basis of local, national and international network. It is used mostly as a means to transmit light between the two ends of the fiber and wide usage in fiber-optic communications, where they permit transmission over longer distances than copper cables. But the fiber itself has many chances to attenuate the transmitting signal. Macrobending and microbending losses are the important sources of signal loss. Therefore, it is essential to optimize these losses of the transmitting signal. We perform a simulation study of the macrobending and microbending losses of a single mode step index optical fiber.

The study has been done by using the software “Understanding Fiber Optics on a PC”. From this study, it has been found that the minimum macrobending and microbending losses are obtained at an operating wavelength of $1.3\ \mu\text{m}$, core radius of $4.0\ \mu\text{m}$, relative refractive index difference of 0.35%. Using these parameters, a fiber is capable to curve of 7 cm bend radius without any signal loss. This result may be an important consideration for designing of a good optical fiber.

PP-63: Density functional theory-based *ab-initio* insights into the physical properties of Mo_3P

Md. Sohel Rana*, Razu Ahmed, Sajidul Islam, Md. Mahamudujjaman, S. H. Naqib

Department of Physics, University of Rajshahi, Rajshahi-6205, Bangladesh

*Presenting author email: sohelrana017732@gmail.com

Tri-molybdenum phosphide (Mo_3P) is a tetragonal low- T_c superconducting compound. In this work, we have studied the structural, elastic, mechanical, thermal, electronic, and optical properties of Mo_3P in detail via first-principles method using the density functional theory (DFT). The unit cell of the compound was optimized. The six independent elastic constants (C_{11} , C_{12} , C_{13} , C_{33} , C_{44} , and C_{66}) are calculated which satisfy all the elastic and mechanical stability criteria. Mo_3P possesses very low level of elastic anisotropy, reasonably good machinability, ductile nature and relatively high Vickers hardness with a low Debye temperature and high melting temperature. The electronic band structure shows that Mo_3P has no band gap and exhibits conventional metallic behavior. The chemical bonding is interpreted by calculating the electronic energy density of states, electron density distribution, elastic parameters and Mulliken bond population analysis. All the energy dependent optical parameters exhibit clear metallic behavior and are in complete accord with the underlying bulk electronic density of states calculations.

PP-64: Study on shielding effectiveness of a conceptual active radiation shield constructed with multi-wall carbon nanotube added YBCO-123 superconducting material

Md. Abdullah Al Zaman^{1*}, H. M. A. R. Maruf², Md. Rafiqul Islam³

¹Department of Textile Engineering, Northern University Bangladesh Dhaka-1213, Bangladesh

²Department of Physics, Chittagong University of Engineering and Technology, Bangladesh

³Department of Physics, University of Chittagong Chattogram-4331, Bangladesh

*Corresponding author's E-Mail: abdullah.alzaman@nub.ac.bd

It is well known that the astronauts will be exposed to galactic cosmic rays (GCR) and solar particle events (SPE) during long-termed space missions. As a result of their exposure to space radiation, the crew members will undergo both immediate and delayed effects. So, the effective shielding is necessary and there are two types of countermeasures namely active and passive shielding. Superconducting magnetic shield is considered a visionary and one of the most promising active shielding methods. After briefly discussing the active and passive methods, this paper presents a conceptual superconducting magnetic shield constructed with multi-wall carbon nanotube added YBCO-123 (Yttrium barium copper oxide) superconducting material. Theoretically, the proposed shield can deflect the lighter particles of up to 2400 MeV/n while for higher Z particles this cut-off energy is about 560 MeV/n. Some distinct limitations of this study are also discussed.

PP-65: Ternary Scandium based Antiperovskite Sc_3GaX ($X=\text{B}, \text{N}$): DFT Study

IstiaqAhmed¹, F. Parvin¹, A.K.M. A. Islam^{1,2}

¹Department of Physics, Rajshahi University, Rajshahi-6205, Bangladesh

²International Islamic University Chittagong, Kumira-4318, Chittagong, Bangladesh

We present an investigation on structural, mechanical, electrical, thermal and optical properties of the cubic inverse perovskite Sc_3GaX ($X=\text{B}, \text{N}$) by first-principles density functional theory (DFT). The optimized lattice parameters, three independent elastic constants, bulk moduli, shear moduli, Young's moduli, Pugh's ratio, Poisson's ratio are estimated and discussed. Changes in the mechanical properties are noticed when B is replaced by N. The electronic properties such as band structure and partial density of states of Sc_3GaX ($X=\text{B}, \text{N}$) at zero pressure are studied. The band structure shows considerable hybridization of Sc- d states with the p -states of B/N. Thermal properties such as Debye temperature, specific heats, thermal expansion coefficient have also been studied in the pressure range 0 to 50 GPa and the temperature range 0 to 1000 K. Optical functions are calculated and the prominent features discussed. The high reflectivity of 95-80% in the IR region and 50-55% above this region up to 8 eV would predict these to be good coating materials.

PP-66: Dust-Acoustic Shock Waves in Nonthermal Dusty Plasmas with Two Population Ions

K. N. Mukta^{1*}, I. Tasnim², M. M. Masud³, and A. A. Mamun⁴

¹Department of Physics, Faculty of Science and Technology, American International University Bangladesh

²Department of Physics, Begum Rokeya University, Rangpur

³Department of Physics, Bangladesh University of Engineering & Technology (BUET), Dhaka

⁴Department of Physics, Jahangirnagar University, Savar, Dhaka

A rigorous theoretical investigation has been made on dust-acoustic (DA) shock structures in an unmagnetized dusty plasma system whose constituents are negatively charged cold mobile dust fluid, electrons following Boltzmann distribution, and positively charged ions of two distinct temperatures following nonextensive (q) and nonthermal distributions, respectively. In this study, the Burgers' equation has been derived by employing reductive perturbation technique which is valid for small but finite amplitude limit. It is observed that both the nonextensive and nonthermal ions of two distinct temperatures and dust kinematic viscosity significantly modify the basic properties (amplitudes, width, and polarities) of the DA shock waves (DASHWs). The effects of lower (higher) temperature ions following nonextensive (nonthermal) and dust kinematic viscosity on DASHWs are examined both analytically and numerically. The implications of these results to some astrophysical environments and space plasmas (e.g. stellar polytropes, peculiar velocity distributions of galaxies, collisionless thermal plasma, etc.), and laboratory dusty plasma systems are briefly mentioned.

PP-67: Strategy of improving photovoltage and efficiency of FeS_2 based heterojunction solar cell through absorber, buffer and window layers optimization with SCAPS-1D software

M. Kamruzzaman^{*}, R. Afrose, M. N. H. Liton, M. A. Helal and M. Aktary

Department of Physics, Begum Rokeya University, Rangpur, Rangpur-5400, Bangladesh

^{*}Corresponding author: kzaman.phy11@gmail.com

In this work, first time we propose glass/FTO/ZnO:Al/CdS/ FeS_2 /MoS₂ solar cell architecture where MoS₂ layer is used to make heterojunction $\text{FeS}_2(\text{n})/\text{MoS}_2(\text{p})$ solar cell along with buffer layer CdS. The photovoltage and the efficiency of iron pyrite (FeS_2) based solar cell has been improved through the component layers optimization. The CdS and MoS₂ layers were studied as electron transporting (ET) and holetransporting (HT) materials for fabricating and improving low-cost, durable and efficient solar cell.

The thickness of the absorber layer FeS_2 and HTM- MoS_2 layers gave distinct photovoltaic properties to designing the proposed solar cell device. The results show that MoS_2 layer could considerably improve open circuit voltage and short circuit current density hence power conversion efficiency. Importantly, the absorber and buffer layers thickness affect the cell's output parameters and efficiency were extensively simulated. For a optimizing of FeS_2 , MoS_2 , CdS and ZnO:Al layers with a thickness of 1.40, 0.80, 0.10 and 0.20 μm multijunctionsolar cell showed, $\eta=36.60\%$, $J_{\text{sc}}=50.20 \text{ mA/cm}^2$, $V_{\text{oc}}=0.842 \text{ V}$ and $\text{FF}=86.56\%$ without any defect, series and shunt resistances. However, the efficiency is reduced with increasing of series resistance and the operating temperature. This study shows that large thickness of FeS_2 and MoS_2 layers with low band gap favor the optimization and model equations can be used to predict high efficient solar cell which may lead the way to direction for laboratory experiment.

PP-68: Study of Thermal and DC Electrical Properties of Plasma Polymerized 1,2-Diaminocyclohexane Thin Films

Md. Mahmud Hasan^{a,*}, Mohammad Jellur Rahman^a, Md. Saddam Sheikh^a, Md. Juel Sarder^a, Md. Masud Reza^a, and A. H. Bhuiyan^{a,b}

^aDepartment of Physics, Bangladesh University of Engineering and Technology (BUET), Bangladesh

^bUniversity of Information Technology and Sciences (UITS), Baridhara, Dhaka-1212, Bangladesh

*Correspondence: hasan.sust.phy@gmail.com

Plasma polymerized 1,2-diaminocyclohexene (PPDACH) thin films of varying thicknesses have been synthesized onto ultrasonically cleaned glass substrates using a parallel plate capacitively coupled low-pressure RF ($f = 13.56 \text{ MHz}$) plasma system. The thermal and electrical transport properties of the as-deposited thin films were analyzed by TG/DTA and DC electrical measurements, respectively. The thermal analysis of the PPDACH thin films in N_2 environment confirmed that the thin films are thermally stable up to about 165°C . The J - V characteristics revealed that the dependence of J on V is Ohmic in the lower voltage region and in the higher voltage region it is non-Ohmic. Space charge limited conduction (SCLC) mechanism is found to be operative in the PPDACH thin films. The values of activation energy (ΔE) in the low temperature region is observed to be almost the same ($\sim 0.12 \text{ eV}$), whereas in the higher temperature region it increases from $0.24 - 0.44 \text{ eV}$ and $0.19 - 0.55 \text{ eV}$ at 10 V and 60 V , respectively.

PP-69: Optical and structural properties of spin coated $\text{Cu}^2\text{NiSnS}_4$ (CNTS) thin film: effect of thiourea concentration

M.M. Rashid^{1,*}, S. Islam², F. Ahmed², M.S. Bashar³, A.T.M.K. Jamil¹, S.J. Ahmed¹

¹Department of Physics, Dhaka University of Engineering & Technology, Gazipur, Bangladesh

²Department of Physics, Jahangirnagar University, Savar, Dhaka, Bangladesh

³Institute of Fuel and Research Development, Bangladesh Council for Scientific and Industrial Research, Dhanmondi, Dhaka, Bangladesh

E-mail: mamun92@duet.ac.bd

Copper nickel tin sulfide (CNTS) thin films have been fabricated on glass substrates by using spin coating technique. The spin coated solutions were prepared with different molar concentrations of thiourea while the concentrations of copper chloride dihydrate, nickel chloride hexahydrate and tin chloride dihydrate were kept fixed. The optical and structural properties of the grown CNTS thin films have been studied using XRD and UV-Vis spectra. The absorbance and transmittance spectra were recorded in the wavelength range of $(350 - 1100) \text{ nm}$ to analyze the optical properties. The optical energy band gap for allowed direct transition was $(2.56 - 2.86) \text{ eV}$ with a high absorption coefficient of the order of 10^5 cm^{-1} in the visible region and it is suitable for solar cell applications. Our prepared CNTS film confirmed a cubic crystalline structure which was studied by XRD. The results of microstructural properties such as crystallite size, dislocation density, microstrain, d-spacing and lattice parameter were also investigated.

PP-70: Structural, Morphological, and Optical Properties of CuO Thin Films Synthesized by Dip-coating Technique for Gas Sensing Applications

A. M. M. Musa^{a*}, M. A. Gafur^b, S. U. F. Farhad^{a,c}, and A. T. M. K. Jamil^a

^aDepartment of Physics, Dhaka University of Engineering & Technology, Gazipur-1707, Bangladesh

^bPilot Plant and Process Development Centre, Bangladesh Council of Scientific and Industrial Research, Dhaka-1205, Bangladesh

^cCentral Analytical and Research Facilities (CARF), Bangladesh Council of Scientific and Industrial Research, Dhaka-1205, Bangladesh

*Corresponding author, E-mail address: musamonsur80@gmail.com

Copper oxide (CuO) thin films have been deposited onto clean glass substrates by sol-gel dip-coating technique with different withdrawal speeds at molar concentration, 0.35 M. The thickness of the film, t decreases with the increase of dip-coating withdrawal speed which is influenced the structural, morphological, and optical properties of CuO films. The XRD spectra reveal that the CuO thin films are polycrystalline in nature having a monoclinic crystal structure with preferential orientations along the (111) and $(\bar{1}\bar{1}1)$ planes. These films are free from impurity phases further confirmed by Raman spectroscopic analysis. The crystalline size is increased from 15.41 to 21.83 nm with increasing t while the lattice parameters remain almost constant. The surface morphology of the films is observed to be uniform, continuous, and defect less with uniformly distributed nanosized grain over the smooth background. The grain size is increased with increasing t which is asserted in XRD results. The optical parameters of the films like direct (E_{gd}) and indirect (E_{gi}) band gaps, refractive index, extinction coefficient, dielectric constant, optical conductivity, etc. are investigated from ultraviolet-visible spectroscopic measurements. Low transmittance and high absorbance are observed in the visible region for the film deposited at a lower withdrawal speed of 0.73 mm/s. The E_{gd} and E_{gi} values are found to decrease from 1.52 to 1.47 and 1.42 to 1.21 eV, respectively with increasing t due to the improvement of crystalline size as well as grain size. Among these studies, the sample accumulated by withdrawal speed 0.73 mm/s exhibit the higher crystallinity with lower micro strain, lower dislocation density, lower band gap with maximum gas sensing response of carbondioxide (CO₂) vapor in the air indicating the good quality thin film, which suggests that the dip-coated CuO thin film can be offered great potential for CO₂ gas sensing applications as well as optoelectronic devices.

PP-71 Analysis of Purification of Charged Giant Vesicles in a Buffer using their Size Distribution

Marzuk Ahmed and Mohammad Abu Sayem Karal

Department of Physics, Bangladesh University of Engineering and Technology, Dhaka-1000, Bangladesh

Email: marzuk38ku@outlook.com

We have analyzed the purification of charged giant unilamellar vesicles (GUVs) prepared in a buffer containing various concentrations of salt using their size distribution. The membranes of GUVs were synthesized by a mixture of dioleoylphosphocholine (DOPC) and dioleoylphosphatidylglycerol (DOPG) lipids. The DOPG mole fractions (X) in the membranes of GUVs were 0.10, 0.25, 0.40, 0.55, 0.70, 0.90 in a physiological buffer containing 162 mM salt. In addition, for a fixed value of X the concentrations of salt (C) in the buffer were 12, 62, 112, 162, 212, 312, 362 mM. The size distribution histograms of experimentally investigated unpurified and purified GUVs were fitted with the lognormal distribution and obtained the multiplication factor γ for mean (μ) and η for standard deviation (σ) of the lognormal distribution. The key parameters γ and η were responsible for changing the average size and size distribution of unpurified GUVs to purified ones. The theoretically fitting equation of experimentally

obtained X and C dependent values of γ and η provided the calibration equation for estimating the average size of purified GUVs theoretically for any values of X and C . The estimated size of purified GUVs increased with the increase of electrostatic effect (i.e., increase of vesicle surface charge density or decrease of salt concentration in buffer). The estimated size of purified GUVs varied with X and C , which supported the previous report qualitatively. These investigations might be helpful in the field of cell/chemical biology for understanding the process of purification of vesicles/cells investigated by any other techniques.

PP-72: An overview of global fusion energy r&d trends and current perspectives of Bangladesh

Md Mahbub Alam^{1,*}, Md Maidul Islam², Md Abdur Rob Sheikh²

¹ICS, AERE, Bangladesh Atomic Energy Commission, Dhaka, Bangladesh

²NSSSD, Bangladesh Atomic Energy Regulatory Authority, Dhaka, Bangladesh

*Corresponding author's email: mahbub.baec@gmail.com

World energy demand to sustainability receives much interest in research and development communities since last few decades. Since world energy demand cannot be satisfied much longer with fossil fuels [1] and fossil fuels have significant environmental impacts; large-scale and sustainable energy generation satisfying environmental requirement has to be developed. Nuclear energy, in particular fusion energy can become a promising option to replace fossil fuels as the world's primary energy source. It could utilize abundance sea water as fuel, produce no CO₂ or any other harmful chemicals into the environment and radioactive waste are very low. In fact, fuel reserves, environmental impact, and safety are definitely remarkable of fusion energy.

Now fusion energy is moving towards commercially-viable fusion power. Around the world, both public and private sectors are speeding up to grasp a commercially viable fusion energy system. One major step to achieve this goal in a short period of time is the ITER project, a 35-nations collaborative megaproject [2]. On the other hand, the EUROfusion proposed a DEMOnstration power plant, DEMO that will be the successor of ITER. The main objectives of DEMO is the production of electricity from the commercial power plants [3]. Beside the ITER and DEMO projects, the U.S. fusion community is conducting fusion R&D from multiple directions. The UK has been playing a pioneer role in continuing experiment with fusion since 1960. Several countries in EU take initiatives to develop fusion technology. Australia, Canada, China, Japan, Korea and India also invested huge amount both from the public and private sectors to make the fusion power commercially available. Figure 1 and 2 show the worldwide fusion energy R&D facilities for moving towards commercially-viable fusion power. Hence it is the right time for us to move forward in that direction.

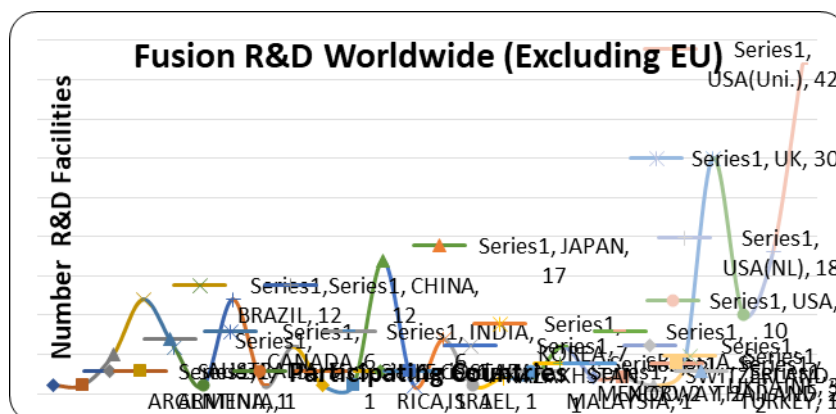


Fig-1: The fusion R&D facilities worldwide excluding European Union

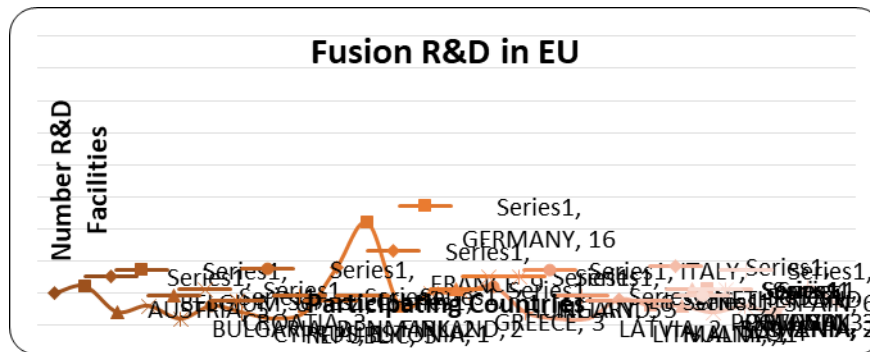


Fig-2: The fusion R&D facilities in European Union

1. N. Armaroli and V. Balzani, "The Future of Energy Supply: Challenges and Opportunities," *Angewandte Chemie International Edition*, vol. 46, no. 1-2, pp. 52–66, Nov. 2006.
2. <https://www.iaea.org/newscenter/news/fusion-energy-in-the-21st-century-status-and-the-way-forward>
3. <https://nucleus.iaea.org/sites/fusionportal/Pages/DEMO-Concepts.aspx>

PP-73: Challenges and approaches to develop and maintain a strong nuclear knowledge base for the country started construction of its first nuclear power reactor

Md Mahbub Alam^{1,*}, Nayan Kumar Datta¹, Md. Shakil Ahmed¹

¹ICS, AERE, Bangladesh Atomic Energy Commission, Dhaka, Bangladesh

*Corresponding author's email: mahbub.baec@gmail.com

Today more than 10% of the world's electricity has been generating from about 450 nuclear power reactors operating in 31 countries. More than 50 power reactors are currently being constructed in 15 different countries. Among them Bangladesh, United Arab Emirates, Belarus, and Turkey started construction of their first nuclear power reactor [1]. Additionally, about 30 countries are considering, and planning to start the construction of their first nuclear power reactor and more than 20 countries have expressed their interest to construct their first nuclear power reactor [2]. Countries that introducing nuclear power for the first time, have been facing almost similar key challenges. Building and maintain a knowledge base skilled workforce is one of the most important as well as consistent challenge. A strong nuclear knowledge management system that can be used for collecting, transferring, sharing, maintaining, preserving and utilizing knowledge and expertise can mitigate this milestone.

Developing and maintaining nuclear knowledge management for the country started construction of its first nuclear power reactor, carries yet diverse challenges. In this context, the newcomer countries have the scope to gain knowledge and capabilities for the development of the nuclear knowledge base system, while vendors and other collaborator countries typically handover of the technical knowledge. This would be helpful to the working scientists and engineers to become knowledge providers that mitigate the knowledge gaps or knowledge loss. Another key challenge is to build up leadership for developing and maintaining knowledge management processes. A balanced combination of a top-down and bottom-up approaches is a key success to that direction. The data and record management, and overall management of knowledge over the technology lifecycle are also considerable agenda to develop a knowledge management system that ensure extremely widen accessibility and timely availability of data.

1. <https://www.world-nuclear.org/information-library/current-and-future-generation/nuclear-power-in-the-world-today.aspx>
2. <https://www.world-nuclear.org/information-library/country-profiles/others/emerging-nuclear-energy-countries.aspx>

PP-74: Precautions to reduce uncertainty during sample preparation for analysis

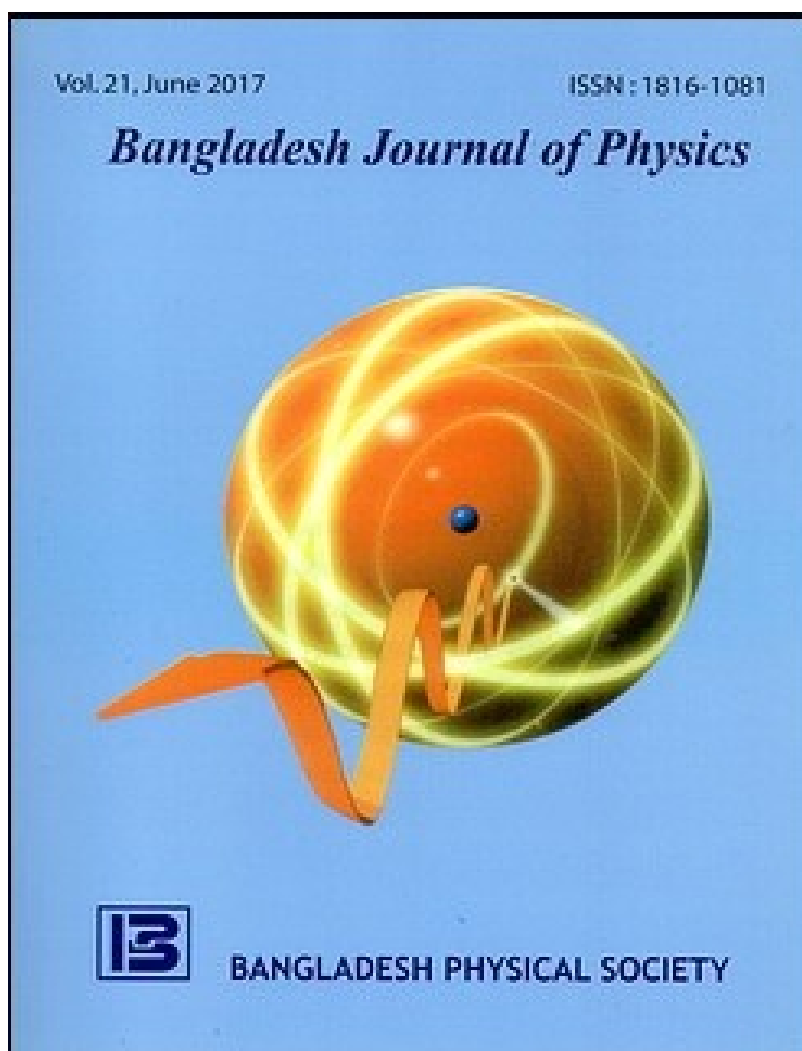
M. A. Maksud, A.K.M. Atique Ullah, N. E. Alam, S. R. Khan, M. M. Hosen, L. N. Lutfu, T. R. Choudhury, S. B. Quraishi

Chemistry Division, Atomic Energy Center, Dhaka

It is important to calculate the uncertainty of any analysis. Because the acceptability of any analysis depends on the uncertainty of its measurements. So, before the analysis of the sample, the sample preparation should be done carefully to reduce the uncertainty of measurements. For example, caution needs to be taken while preparation of the solid samples that need to be liquified for analysis using AAS (Atomic Absorption Spectrophotometer) and ICP-MS (Inductively Coupled Plasma Mass Spectrometer). Care should be taken regarding the moisture content of the sample, weight (upto 3 decimal places) of the sample, calibration and level of the weighing machine. A closed vessel microwave digestion system is preferable to a hotplate or furnace to reduce the uncertainty. In the event of using the hotplate or furnace, one should be careful so that the sample does not spill out. The temperature should be kept under the boiling point of the target element in all cases. Besides, care should be taken so that the maximum amount of the sample is transferred from the digestion glassware or vessel to the vial. In case the volume of the sample changes, it is necessary to note it down. If filter paper is used, then the size should be adjusted according to the funnel and deionized water must be used before filtering the sample. Weight by weight and weight by volume values of the prepared sample should be noted too. Overall, the deviation of the values in each step should be noted down. Thus, these steps and the precaution of the analyst will reduce the value of the total uncertainty calculation and the result of the analysis will be within the tolerance.

Call for Research Manuscript

Bangladesh Journal of Physics invites research papers for upcoming issue



Focus and Scope

ISSN: 1816-1081

Bangladesh Journal of Physics is an international peer-reviewed journal encompassing the contemporary interest of the researchers in the field of Science, Engineering and Technology. The scope of this is to include review, theoretical, experimental etc. papers on different subjects on physical science, including nanomaterials, thin films, composites, magnetic materials, superconductors, condensed matter, electronic, optoelectronic, sensor, devices, nuclear physics, particle physics, high energy physics, computational, mathematical etc.